HAW HAMBURG

Homework

Redesign - Lockheed L-1011 TriStar

Author: Adrian Eusebiu Cojocaru Gall

Supervisor: Prof. Dr.-Ing. Dieter Scholz, MSME

Submission date: 2025-07-11

Aircraft Design SS2025

Faculty of Engineering and Computer Science
Department of Automotive and Aerospace Engineering

Abstract

Objective – As part of the "Aircraft Design" course at Hamburg University of Applied Sciences (HAW) during the summer semester 2025, and under the supervision of Prof. Dr.-Ing. Dieter Scholz, this project presents the **redesign of an old commercial aircraft**. The aircraft is the "Lockheed L-1011 TriStar", a three engine wide-body airliner dimensioned to fulfill FAR-25 certification requirements and is optimized for medium to long-haul missions.

Approach – The design process followed a structured methodology using Excel-based tools developed by Prof. Scholz and previous student cohorts. Starting from a set of top-level aircraft requirements (TLARs), the aircraft configuration includes the fuselage, cabin, wing, empennage, landing gear, and high-lift devices which were developed using analytical methods introduced in the course. Performance characteristics such as aerodynamic coefficients, mass estimations, and center of gravity locations were iteratively refined. A cost analysis was also performed, including an estimation of Direct Operating Costs (DOC). The resulting aircraft geometry was modeled in 3D using OpenVSP.

Results – The proposed aircraft meets the predefined mission requirements with a strong base compared with other similar and existing airplanes. The results show good alignment with comparable aircraft in its class, confirming that the applied methods lead to a coherent and realistic conceptual design.

Table of contents

List of Figures

List of Tables

List of symbols

a	Speed of sound (Schallgeschwindigkeit)
b	Wingspan (Spannweite)
c	Specific fuel consumption or chord (Spezifischer Kraftstoffverbrauch oder Profiltiefe)
C_D	Drag coefficient (Widerstandsbeiwert)
C_f	Skin friction drag coefficient (Reibwiderstandsbeiwert)
C_L	Lift coefficient (Auftriebsbeiwert)
C_{D0}	Zero-lift drag coefficient (Null-Auftriebs-Luftwiderstandsbeiwert)
d	Diameter (Durchmesser)
e	Oswald efficiency factor (Oswald-Faktor)
g	Acceleration due to gravity (Erdbeschleunigung)
h	Altitude (Flughöhe)
i_W	Angle of incidence (Einstellwinkel)
k	Constant (Konstante)
L	Lift force (Auftrieb)
L/D	Lift-to-drag ratio (Gleitzahl)
m	Mass (Masse)
M	Mach number or pitching moment (Machzahl oder Moment um die Querachse)
M_{ff}	Mission fuel fraction
m/S_W	Wing loading (Flächenbelastung)
n	Load factor or number (Lastvielfaches oder Anzahl)
R	Range (Reichweite)

r	Radius (Radius)
Re	Reynolds number (Reynolds-Zahl)
s	Distance (Strecke)
S	Area (Fläche)
t	Thickness (Profildicke)
t/c	Relative thickness (relative Profildicke)
T	Thrust (Schub)
T/mg	Thrust-to-weight ratio (Schub-Gewichtsverhältnis)
V	Velocity (Geschwindigkeit)
x	Distance from a reference point along the fuselage (parallel to cabin floor, toward aft)
y	Distance from symmetry plane toward the wingspan (lateral axis)
Δy	Leading-edge sharpness parameter (leading-edge sharpness parameter)
z	Distance from a reference point perpendicular to the x–y plane, upward

Greek symbols

α	Angle of attack (Anstellwinkel)
δ	Control surface deflection angle (Ausschlagwinkel einer Steuerfläche)
ε	Twist (Schränkung)
η	Relative span (relative Spannweite)
γ	Flight path angle (positive: climb) or isentropic exponent (Bahnneigungswinkel oder Isentropenexponent)
Γ	Dihedral angle (V-Winkel)
λ	Taper ratio (Zuspitzung)
μ	Bypass ratio (Nebenstromverhältnis)

ϕ	Tail angle (Heckwinkel)
ϕ_{te}	Trailing edge angle (Hinterkantenwinkel)
ψ	Bank angle (Kippwinkel)
ρ	Density (Dichte)
σ	Relative air density (relative Luftdichte)
τ	Relative thickness ratio (Verhältnis relative Profildicke)
θ	Sweep angle (Pfeilung)
ν	Kinematic viscosity (kinematische Viskosität)
φ	Sweep angle (alternate symbol for Pfeilung)

Indices

$()_{APP}$	Approach
$()_{BC}$	Business class
$()_{FC}$	First class
$()_{cargo}$	Cargo
$()_{CG}$	Center of gravity
$()_{CR}$	Cruise
$()_{cushion}$	Seat height
$()_{E,inst}$	Engine
$()_{eff}$	Effective value
$()_{SYS}$	Equipment
$()_{F}$	Fuselage

$()_F$	Fuel (context-dependent)
$()_{HL}$	Hinge line
$()_i$	Inner
$()_{INF}$	Inflation
$()_K$	Kink
( )L	Landing
$()_t$	tip
$()_r$	root
$()_{LEMAC}$	Leading Edge of Mean Aerodynamic Chord
$()_{LFL}$	Landing Field Length (required)
$()_{LG,M}$	Main landing gear
$()_{LG,N}$	Nose landing gear
$()_{LG}$	Landing gear
$()_{MAC}$	Mean Aerodynamic Chord
$()_{MAX}$	Maximum value
$()_{ML}$	Maximum landing mass
$()_{TO}$	Maximum take-off mass
$()_N$	Nacelle
$()_O$	Outer
$()_{OE}$	Operating empty mass
$()_{PAX}$	Passenger (PAX)

$()_{PL}$	Payload
$()_{SA}$	Seats abreast
$()_{SEAT}$	Seat
$()_{thr}$	Reverse thrust
$()_{APP}$	Take-off Field Length (required)
$()_{V}$	Vertical tailplane
$()_{H}$	Horizontal tailplane
$()_{W}$	Wing
$()_{WET}$	Wetted surface or wetted
$()_{EXP}$	Exposed surface

List of abbreviations

A/C	Aircraft
AC	Aerodynamic Center or Advisory Circular
ACR	Aircraft Classification Rating
ACN	Aircraft Classification Number
AEA	Association of European Airlines
BPR	Bypass Ratio (Nebenstromverhältnis)
CG	Center of Gravity (Schwerpunkt)
DOC	Direct Operating Costs (Direkte Betriebskosten)
FG	Fuselage Group (Rumpfgruppe)
FAR	Federal Aviation Regulations
HLW	Horizontal Tailplane (Höhenleitwerk)

ICAO	International Civil Aviation Organization
LCN	Load Classification Number
JAR	Joint Aviation Requirements
LER	Leading-Edge Radius (Nasenradius)
MAC	Mean Aerodynamic Chord (Mittlere aerodynamische Flügeltiefe)
NACA	National Advisory Committee for Aeronautics
PCR	Pavement Classification Rating
PCN	Pavement Classification Number
PreSTo	Aircraft Preliminary Sizing Tool
SFC	Specific Fuel Consumption (Spezifischer Kraftstoffverbrauch)
SLW	Vertical Tailplane (Seitenleitwerk)
THS	Trimmable Horizontal Stabilizer (Trimmbare Höhenflosse)
TLARs	Top-Level Air Requirements
TRW	Engine (Triebwerk)
WG	Wing Group (Flügelgruppe)

1 Introduction and initial data

The task consists of the redesigning of an aircraft analyzing all the parameters and data given for the specific airplane selected. A three-view drawing combined with requirements and calculations of the fuselage as well as cabin layouts are necessary to ensure that the aircraft accomplish all restrictions and objectives for an optimal redesign.

This work is entirely based on Prof. Scholz's lecture materials. This comprises all lecture notes and projects. The design methodologies outlined in the lecture notes are listed in the bibliography, however the following draft is based only on Scholz's teaching materials. All chapters of the current lecture notes are freely accessible at:

http://LectureNotes.AircraftDesign.org

The selected aircraft is the **Lockheed L-1011 TriStar.** The initial parameters needed are a key step to start iterating and selecting the exact configuration to make the final results more precise.

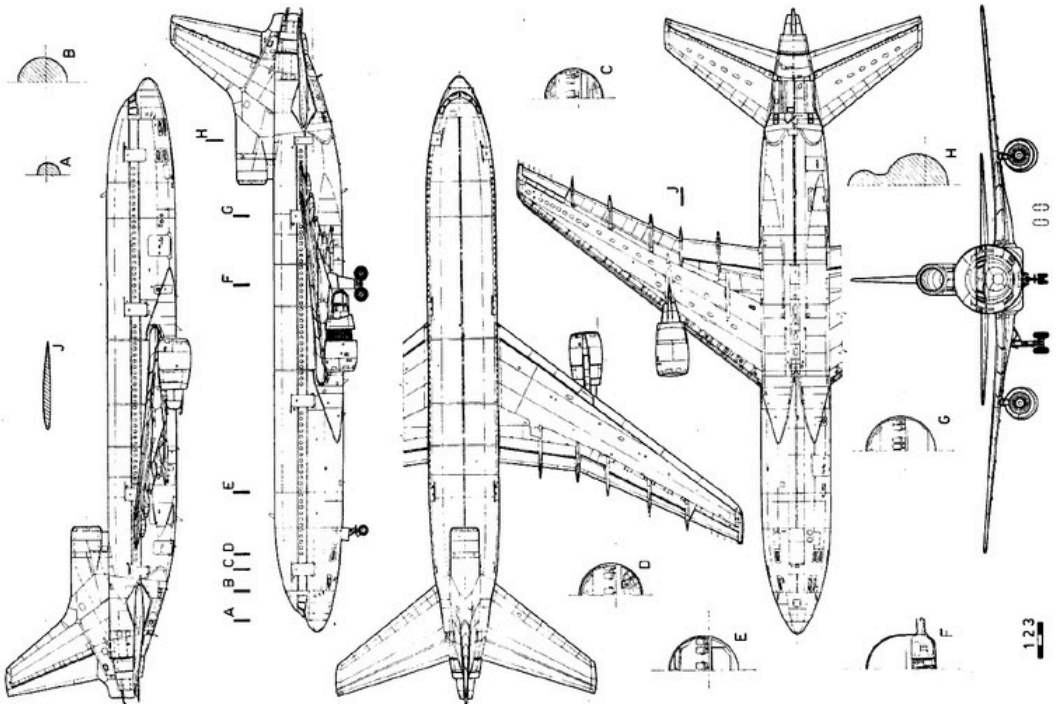

Figure 1.1: *Image of the Lockheed L-1011 TriStar*

1.1 Planned initial requirements

As explained before, there is some preparatory work needed before based on the collection of data which is found within the research of the planned designs of the aircraft as these parameters are not going to be modified, creating the base for our task.

The aircraft is certified according to FAR 25 and therefore, the initial parameters are the following:

- Range at maximum payload R
- Number of passengers n_{pax}
- Take-off field length s_{TO}
- Landing field length s_L

The different parameters have been collected in the next table, showing the different sources that helped on the development of the task.

Table 1.1: *Initial requirements for the Lockheed L-1011 TriStar*

Parameters	Airlines inform	Elsevier	Blog	Selected value for design
R	7000 km	4685 km	8932 km	8676 km
n_{pax}	400	400	384	195 pax
s_{TO}	3300 m	3292 m	2834 m	3292 m
s_L	1 800 m	1768 m	1850 m	1768 m

The data provided by the different sources was taken within the maximum limits of the aircraft, selecting the L-1011-100 type configuration with maximum payload and fuel capacity, maximum passengers and take-off/landing distances. Therefore, in order to have better configurations and after careful consideration, the selected values are taken into account disregarding on some parameters the maximum capacities of the aircraft.

Another important factor is the antiquity of the aircraft, the L-1011-100 TriStar was mainly used in the decades of 1970-1980, and information as the density of fuel, engines analysis and mass per passenger has changed and improved to be more

detailed and flexible to all type of flights, explaining the different values selected and the difference between each source.

Another important data is collected in the next table, summarizing all the parameters needed for the next step.

- Maximum take-off weight (m_{TO})
- Maximum landing weight (m_{L})
- Operating empty weight (m_{OE})
- Maximum payload (m_{PL})
- Maximum zero fuel weight (m_{ZF})
- Mach number (M_{CR})
- Fuel weight (m_{F}) for maximum take-off weight
- Wing area (S_{W})

Table 1.2: *Other requirements for the Lockheed L-1011 TriStar*

Parameters	Airlines inform	Elsevier	Blog	Selected value for design
m_{TO}	211380 kg	211374 kg	211375 kg	211375 kg
m_{L}	166920 kg	166922 kg	166920 kg	166920 kg
m_{OE}	111670 kg	111795 kg	110723 kg	111795 kg
m_{PL}	41600 kg	33355 kg	34427 kg	33355 kg
m_{ZF}	153310 kg	145150 kg	145150 kg	145150 kg
m_{F}	80080 kg	80000 kg	79360 kg	80080 kg
S_{W}	320 m^2	321.5 m^2	321.1 m^2	320 m^2
s_{LFL}	1800 m	1768 m	1850 m	1768 m
s_{TO}	3300 m	3292 m	2834 m	3292 m

Taking all the information collected and consulting different sources, the payload-range diagram can be created to have a simple view on how the aircraft perform.

Different points are selected taking into account the maximum take-off weight (m_{TO}), payload (m_{PL}), operational empty mass (m_{OE}) and fuel mass (m_F) on the different points:

$$m_F = m_{TO} - m_{OE} - m_{PL} \quad (1.1)$$

For points 1 and 2:

$m_F = 211375 - 111795 - 33355 = 66225\ kg$

From Aircraft Investigation blog [3] the range with maximum payload is:

$R = 4106\ NM$ (7605 km)

$m_F = 211375 - 111795 - 33355 = 66225\ kg$

For point 3, an intermediate selection of fuel and payload is determined taking a range for maximum fuel from Elsevier [4] :

$R = 4685\ NM$ (8676 km)

$m_F = 211375 - 111795 - 19138 = 80442\ kg$

For point 4:

According to Aircraft Investigation blog [3] the tank limit is:

$m_F = 80080\ kg$

Table 1.3: *Data collected for the payload-range diagram*

Point	Payload	Fuel	Range
1	33355 kg	66225 kg	0 NM
2	33355 kg	66225 kg	4106 NM
3	19138 kg	80442 kg	4685 NM
4	0 kg	80080 kg	5370 NM

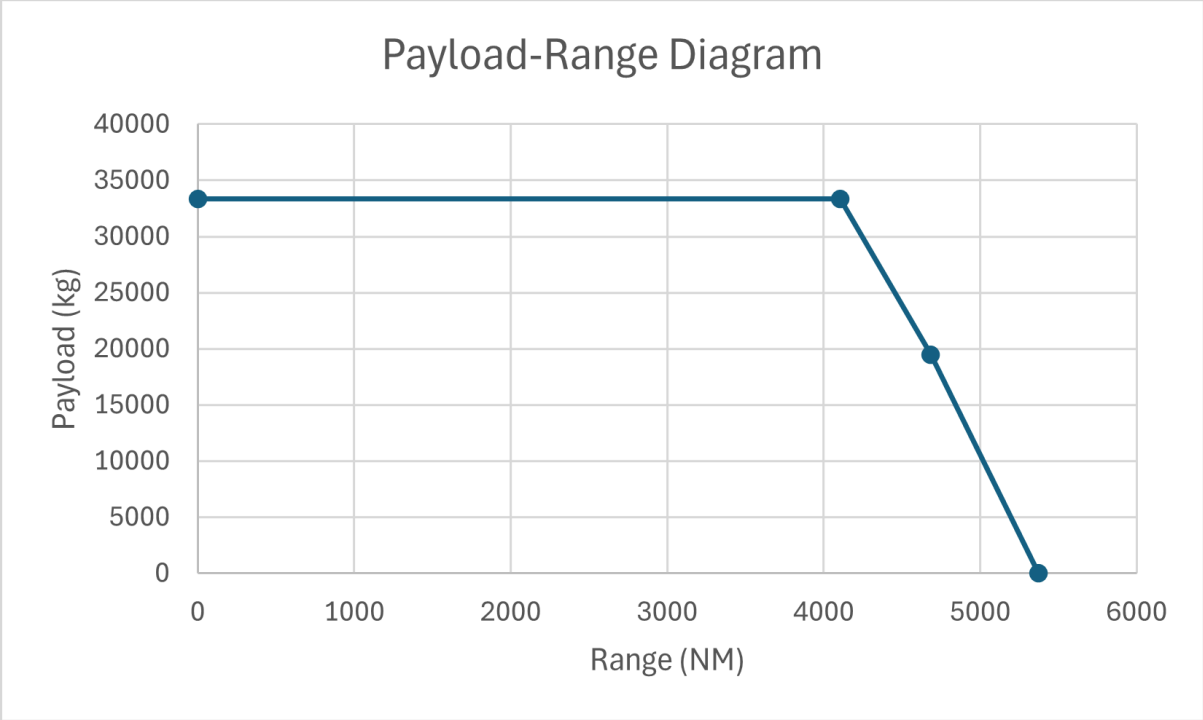

Figure 1.2: *Graphic of the Payload-Range Diagram of the aircraft*

2 Preliminary sizing

To optimize the design, the presizing of the aircraft is carried out step-by-step using "PreSTo-Classic" (PreSTo - Aircraft Preliminary Sizing Tool) tool with the information collected in the preparatory work determined.

https://www.fzt.haw-hamburg.de/pers/Scholz/PreSTo.html

The results obtained with the tool will be compared with the ones given by the different sources, with the objective of obtaining a difference of less than 1% between each value.

2.1 Lift coefficients and wing loading

According to the method of Loftin found on the lecture notes of Scholz [1] , for a given aircraft with jet engines the approach speed is:

$$V_{APP} = k_{APP} \cdot \sqrt{s_{LFL}} \tag{2.1}$$

V_{APP}: Approach speed

k_{APP}: Safety factor constant, with a settled value of $1.70\sqrt{m/s^2}$

s_{LFL}: Landing distance taken from [Table 1.2]

$$V_{APP} = 71,6\ m/s = 139,1\ kt$$

Following Roskam I, the maximum lift coefficients for the aircraft are determined:

type of aircraft	$C_{L,max}$	$C_{L,max,TO}$	$C_{L,max,L}$
business jet	1.4 – 1.8	1.6 – 2.2	1.6 – 2.6
jet transport	1.2 – 1.8	1.6 – 2.2	1.8 – 2.8
single engine propeller driven	1.3 – 1.9	1.3 – 1.9	1.6 – 2.3
twin engine propeller driven	1.2 – 1.8	1.4 – 2.0	1.6 – 2.5
fighter	1.2 – 1.8	1.4 – 2.0	1.6 – 2.6
supersonic cruise	1.2 – 2.8	1.6 – 2.0	1.8 – 2.2

Figure 2.1: *Maximum lift coefficients based on Roskam I, as cited in Scholz [3]*

The L-1011-100 TriStar is a jet transport aircraft, and the maximum landing coefficient selected is verifying the best value $CL_{L,max,L} = 2,75$.

The coefficient for take-off:

$$CL_{L,max,TO} = 0,8 \cdot CL_{L,max,L} \tag{2.2}$$

$CL_{L,max,TO} = 2,2$

The wing loading at maximum landing weight results on the following relationship taking constants and expressions at ground with standard atmosphere:

$$\frac{m_L}{S_W} = k_L \cdot \sigma \cdot CL_{L,max,L} \cdot s_{LFl} \tag{2.3}$$

$k_L = 0,107\ kg/m^3$(landing constant)

$\sigma = 1$ (relation between the actual density and density at sea level)

The wing loading given by the maximum landing mass is, following **Equation 2.3**:

$\frac{m_L}{S_W} = 520\ kg/m^2$

In order to meet the requirements, the aircraft shall not exceed the wing loading given by the maximum take-off mass.

$$\frac{m_{TO}}{S_W} = \frac{m_l/S_W}{m_L/m_{TO}} \tag{2.4}$$

Which, taken the information of [Table 1.2] and regarding the **Equation 2.3**:

$\frac{m_{TO}}{S_W} = 659\ kg/m^2$

Finally, to check if the data chosen is correct, the ratios between maximum landing and take-off masses ($\frac{m_L}{m_{TO}}$) can be calculated and compared with Roskam I:

type of aircraft	$\frac{m_{ML}}{m_{MTO,min}}$	$\frac{m_{ML}}{m_{MTO,av}}$	$\frac{m_{ML}}{m_{MTO,max}}$
business jet	0.69	0.88	0.96
short range jet transport	0.9	0.93	0.97
medium range jet transport	0.76	0.88	0.95
long range jet transport	0.65	0.78	0.95
ultra long range jet transport	0.65	0.71	0.73
fighter	0.57	-	1
supersonic cruise	0.63	0.75	0.88

Figure 2.2: *Ratios between masses based on Roskam I, cited in Scholz [3]*

For this case, the ratio is $\frac{m_L}{m_{TO}}$=0,79 which taking into account that the average is being considered explains that the aircraft is a medium-long range jet, capable of surpassing 5500 km with the proper configuration according to Loftin.

design range classification	**design range (NM)**	**design range (km)**	m_{ML} / m_{MTO}
short range	up to 1000	up to 2000	0.93
medium range	1000 – 3000	2000 – 5500	0.89
long range	3000 – 8000	5500 – 15000	0.78
ultra long range	more than 8000	more than 15000	0.71

Figure 2.3: *Classification of ranges given by Loftin 1980, cited in Scholz [3]*

2.2 Thrust-to-weight ratio

Another important factor considered designing an aircraft is the thrust-to-weight ratio which cannot be higher than the limit value:

$$\frac{T_{TO}/(m_{TO}\cdot g)}{m_{TO}/S_W} = \frac{k_{TO}}{s_{LFL}\cdot\sigma\cdot CL_{L,max,TO}} \tag{2.5}$$

$k_{TO} = 2,34\ m^3/kg$ (take-off constant following Loftin 1980)

m_{TO}/S_W (wing loading from **Equation 2.4**)

$g = 9,81\ m/s^2$ (Earth acceleration)

Knowing all the values, the thrust-to-weight ratio is $T_{TO}/(m_{TO} \cdot g) = 0,222$.

2.3 Glide ratio in second segment, missed approach and cruise flight

Stated by JAR 25.121 it is required that twin-engine aircraft still achieve a climb gradient of at least 2.4% in the second segment with one engine inoperative.

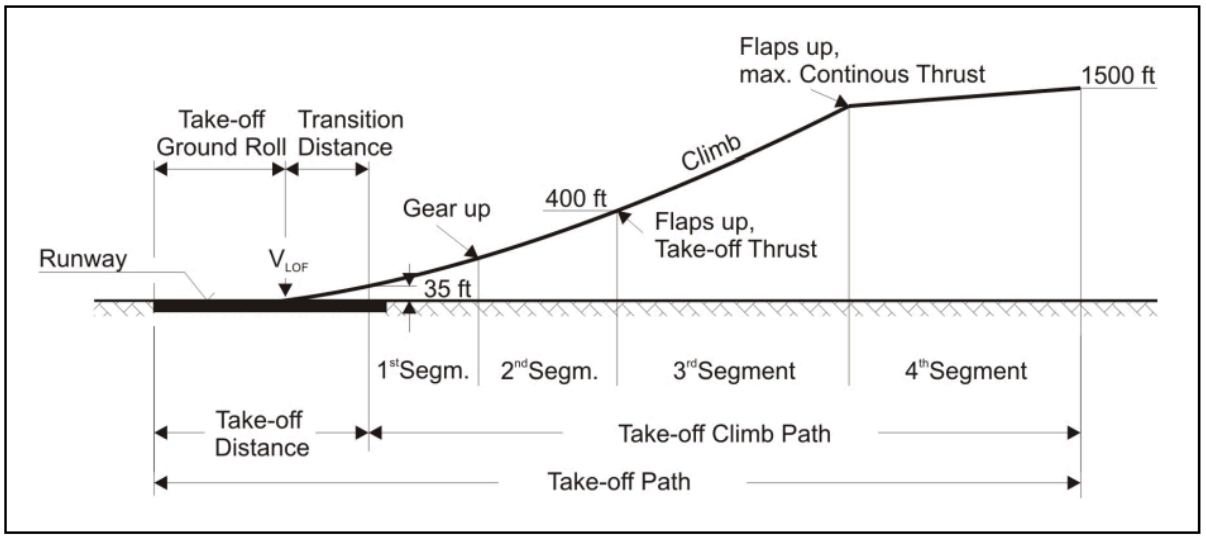

Figure 2.4: *Take-off path by Brüning 1993, cited in Scholz [1]*

The climb angle together with the efficiency factor are key to balance the drag and weight effects in order to improve the manoeuvrability of the aircraft.

$$sin\gamma = \left(\frac{climb\ gradient}{100}\right) \tag{2.6}$$

$$E = \frac{L}{D} = \frac{CL}{CD} \tag{2.7}$$

$$\frac{CL}{CD} = \frac{CL}{CD_{POLAR} + \frac{CL^2}{\pi \cdot A \cdot e}} \tag{2.8}$$

$$CD_{POLAR} = CD_0 + \Delta CD_{flap} + \Delta CD_{flat} + \Delta CD_{gear} \tag{2.9}$$

γ: Climb angle

E: Lift to drag ratio

A: Aspect ratio

e: Oswald efficiency factor

Regarding the formulas and taking into account that the aircraft has three engines, $sin\gamma$ = 0,027 rad, confirming it with **Figure 2.5**.

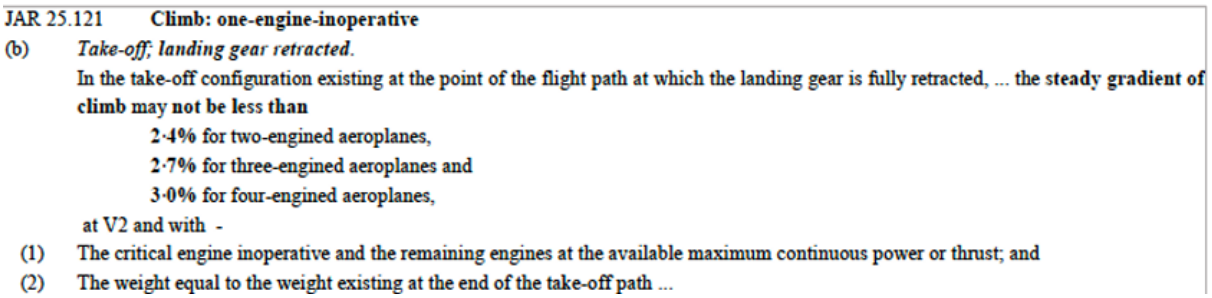

JAR 25.121 **Climb: one-engine-inoperative**

(b) ***Take-off; landing gear retracted.***

In the take-off configuration existing at the point of the flight path at which the landing gear is fully retracted, ... the steady gradient of climb may not be less than

2·4% for two-engined aeroplanes,

2·7% for three-engined aeroplanes and

3·0% for four-engined aeroplanes,

at V2 and with -

(1) The critical engine inoperative and the remaining engines at the available maximum continuous power or thrust; and

(2) The weight equal to the weight existing at the end of the take-off path ...

Figure 2.5: *Climb gradient regarding JAR 25.121 by Scholz [1]*

e	0.7 due to extended flaps and slats
$C_{D,0}$	0.02
$\Delta C_{D,flap}$	for $C_L = 1.3$: flaps 15° => $\Delta C_{D,flap} = 0.01$
	for $C_L = 1.5$: flaps 25° => $\Delta C_{D,flap} = 0.02$
	for $C_L = 1.7$: flaps 35° => $\Delta C_{D,flap} = 0.03$
$\Delta C_{D,slat}$	negligible
$\Delta C_{D,gear}$	0.015 in case landing gear is extended.

Figure 2.6: *Data provided by Loftin 1980 of passenger aircraft, cited in Scholz [3]*

$$A = \frac{b^2}{S_W} \tag{2.10}$$

b: Aircraft span.

For this airplane, the aspect ratio is $A = 6,97$.

$$CL = \frac{CL_{L,max,TO}}{1,44} \tag{2.11}$$

According to **Equation 2.11**:

CL =1,53.

2.3.1 Glide ratio for second segment and take-off:

Following **Figure 2.6**, **Equation 2.8** is given as follows.

Second segment:

$E = \frac{L}{D} = 7,94.$

$e = 0,7.$

$CD_0 = 0,02.$

$\Delta CD_{flap} = 0,02.$

$\Delta CD_{slat} = \Delta CD_{gear} = 0$ (in second segment).

Take-off:

$E = \frac{L}{D} = 7,37.$

$\Delta CD_{gear} = 0,015.$

The thrust-to-weight ratio can also be calculated in the different configurations:

$$\frac{T_{TO}}{m_{TO} \cdot g} = \left(\frac{n_E}{n_E - 1}\right) \cdot \left(\frac{1}{E_{TO}} + sin\gamma\right) \quad (2.12)$$

n_E: number of engines.

For the take-off configuration, $\frac{T_{TO}}{m_{TO} \cdot g}$=0,239

The thrust in take-off will be $T_{TO} = 499725,91\ N$

2.3.2 Glide ratio for missed approach segment

$$CL = \frac{CL_{L,max,L}}{1{,}69} \tag{2.13}$$

$CL = 1,63.$

Resulting from Figure 2.6:

$E = \frac{L}{D} = 7,64.$

$e = 0,7.$

$CD_0 = 0,02.$

$\Delta CD_{flap} = 0,02.$

$\Delta CD_{flat} = 0.$

$\Delta CD_{gear} = 0,015$ (landing gear extended regarding FAR Part 25).

Thrust-to-weight ratio:

$$\frac{T_{TO}}{m_{TO} \cdot g} = \left(\frac{n_E}{n_E - 1}\right) \cdot \left(\frac{1}{E} + sin\gamma\right) \cdot \frac{m_L}{m_{TO}} \tag{2.14}$$

$\frac{T_{TO}}{m_{TO} \cdot g}$=0,184

According to FAR Part 25:

CS 25.121	Climb: one-engine-inoperative
(d)	**Discontinued Approach.** ... the **steady gradient** may **not be less than**
	2·1% for two-engined aeroplanes,
	2·4% for three-engined aeroplanes and
	2·7% for four-engined aeroplanes, with -
(1)	**The critical engine inoperative**, the remaining engines at the available take-off power or thrust;
(2)	The maximum landing weight; and
(3)	A climb speed established in connection with normal landing procedures (these are 1·3 VS), but not exceeding 1·5 VS.
(4)	Landing gear retracted. *
*	(4) is only contained in CS-25 not in den FAR Part 25 !!!

Figure 2.7: *Climb gradient regarding FAR 25 by Scholz [1]*

$sin\gamma$ = 0,024 rad

2.3.3 Glide ratio for cruise flight:

The thrust-to-weight ratio at take-off is determined by the following relation:

$$\frac{T_{TO}}{m_{TO} \cdot g} = \frac{1}{\frac{T_{CR}}{T_{TO}} \cdot (L/D)} \tag{2.15}$$

$\frac{T_{CR}}{T_{TO}}$: Ratio of cruise thrust.

For the ratio of cruise thrust to take-off thrust, **Equation 2.16** is used for normal Mach number ($M \approx 0,8$):

$$\frac{T_{TO}}{T_{CR}} = (0.0013 \cdot \mu - 0.0397) \cdot \frac{1}{km} \cdot h_{CR} - 0.0248 \cdot \mu + 0.7125 \tag{2.16}$$

μ: bypass ratio.

h_{CR}: cruise altitude.

The engine by-pass ratio and the specific fuel consumptions (SFC) are the following ones according to DataHammami [5], as the L-1011-100 TriStar uses three Rolls Royce jet motors (RB211-524B4-02).

$\mu = 5:1$.

$SFC = 1,7 \cdot 10^{-5}\ kg/N/s$.

The maximum lift to drag ratio in cruise flight, according to Raymer 1899, can be approximated by:

$$\left(\frac{L}{D}\right)_{max} = k_e \cdot \sqrt{\frac{A}{S_{WET}/S_W}} \tag{2.17}$$

k_e: Empirical factor imposed by Raymer 1899.

S_{WET}/S_W: relation of a small wetted area of the aircraft relative to the wing area.

According to Raymer 1899, the relation is the following one:

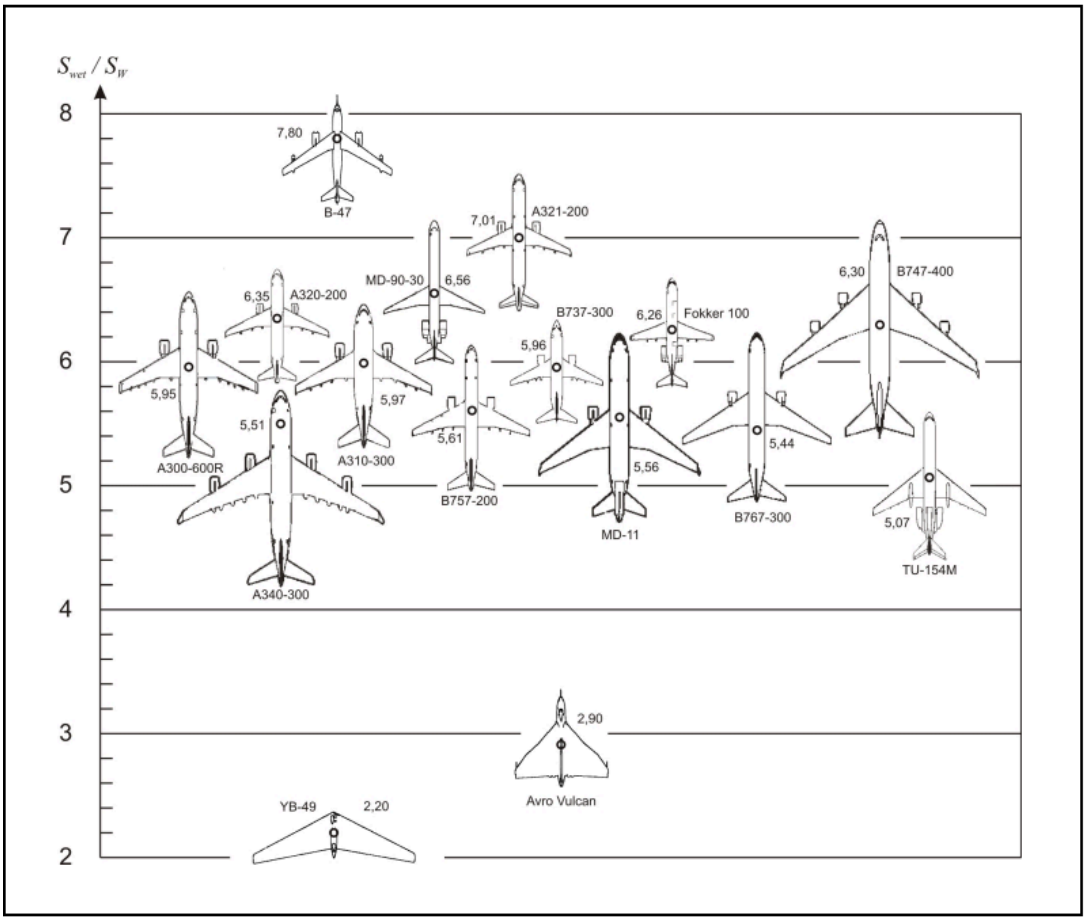

Figure 2.8: *Relation of S_{WET}/S_W according to Raymer 1899, cited in Scholz [1]*

Which, for this aircraft, a value of $S_{WET}/S_W = 5,7$ and $k_e = 15$ is settled.

$(\frac{L}{D})_{max} = 16,59$

The corresponding lift coefficient is:

$$CL_{md} = \frac{\pi \cdot A \cdot e}{2 \cdot (L/D)_{max}} \tag{2.18}$$

CL_{md}=0,56

$$CL = \frac{\frac{\pi \cdot A \cdot e}{2 \cdot (L/D)_{max}}}{(V/V_{md})^2} \tag{2.19}$$

V/V_{md}: Ratio between velocity of the aircraft and the velocity for minimum drag, which regarding Scholz [1] can be settled to a value of 1,12 taking into account the cruise flight condition and that usually varies from 1 to 1,316.

Also a value of $e = 0,85$ is considered according to Loftin 80 for steel-engined aircrafts.

$CL = 0,447$ (in cruise flight)

The final lift to drag ratio:

$$E = \frac{2 \cdot (L/D)_{max}}{\frac{1}{(\frac{CL}{CL_{md}})} + (\frac{CL}{CL_{md}})} \qquad (2.20)$$

$E = 16,17$

2.4 Matching chart

A matching chart is a design tool used in aircraft design to study the feasibility of a proposed aircraft configuration by comparing critical performance constraints: take-off, missed approach, second segment, landing and cruise.
The chart plots the thrust-to-weight ratio ($\frac{T_{TO}}{m_{TO} \cdot g}$) on the vertical axis versus the wing loading ($\frac{m_{TO}}{S_W}$) on the horizontal axis. Each curve on the chart represents a performance requirement derived from regulations (e.g., FAR/CS-25).
The aim of this project is to optimize the design point where the smallest thrust-to-weight ratio and the maximum wing loading are achieved as all the parameters declared before have a crucial effect on the performance of the aircraft.

According to PreSTo Classic, **Table 1.3** will give the last information needed for the matching chart, as it also helps verifying the numbers calculated on the preliminary sizing of the L-1011-100 TriSTar.

Table 2.1: *Data collected according to PreSTo Classic*

Altitude	Cruise	Cruise	Cruise	Cruise	2nd Segment	Missed appr.	Cruise
$h\ [km]$	$\frac{T_{TO}}{T_{CR}}$	$\frac{T_{TO}}{m_{TO} \cdot g}$	$p(h)\ [Pa]$	$\frac{m_{TO}}{S_W}\ [kg/m^2]$	$\frac{T_{TO}}{m_{TO} \cdot g}$	$\frac{T_{TO}}{m_{TO} \cdot g}$	$\frac{T_{TO}}{m_{TO} \cdot g}$
0	0.589	0.105	101325	2282	0.222	0.199	0.11
1	0.555	0.111	89873	2024	0.222	0.199	0.12
2	0.522	0.118	79493	1790	0.222	0.199	0.12
3	0.489	0.126	70105	1579	0.222	0.199	0.13
4	0.456	0.135	61636	1388	0.222	0.199	0.14
5	0.423	0.146	54015	1216	0.222	0.199	0.15
6	0.389	0.159	47176	1062	0.222	0.199	0.16
7	0.356	0.174	41036	925	0.222	0.199	0.17
8	0.323	0.192	35595	802	0.222	0.199	0.19
9	0.291	0.213	30737	692	0.222	0.199	0.21
10	0.260	0.238	26431	595	0.222	0.199	0.23
11	0.223	0.277	22627	510	0.222	0.199	0.28
12	0.190	0.325	19316	435	0.222	0.199	0.34
13	0.152	0.394	16498	372	0.222	0.199	0.44
14	0.124	0.500	14091	317	0.222	0.199	0.58
15	0.091	0.683	12035	271	0.222	0.199	0.68

The final matching chart has been created, aiming to determine the thrust-to-weight ratio on cruise configuration.

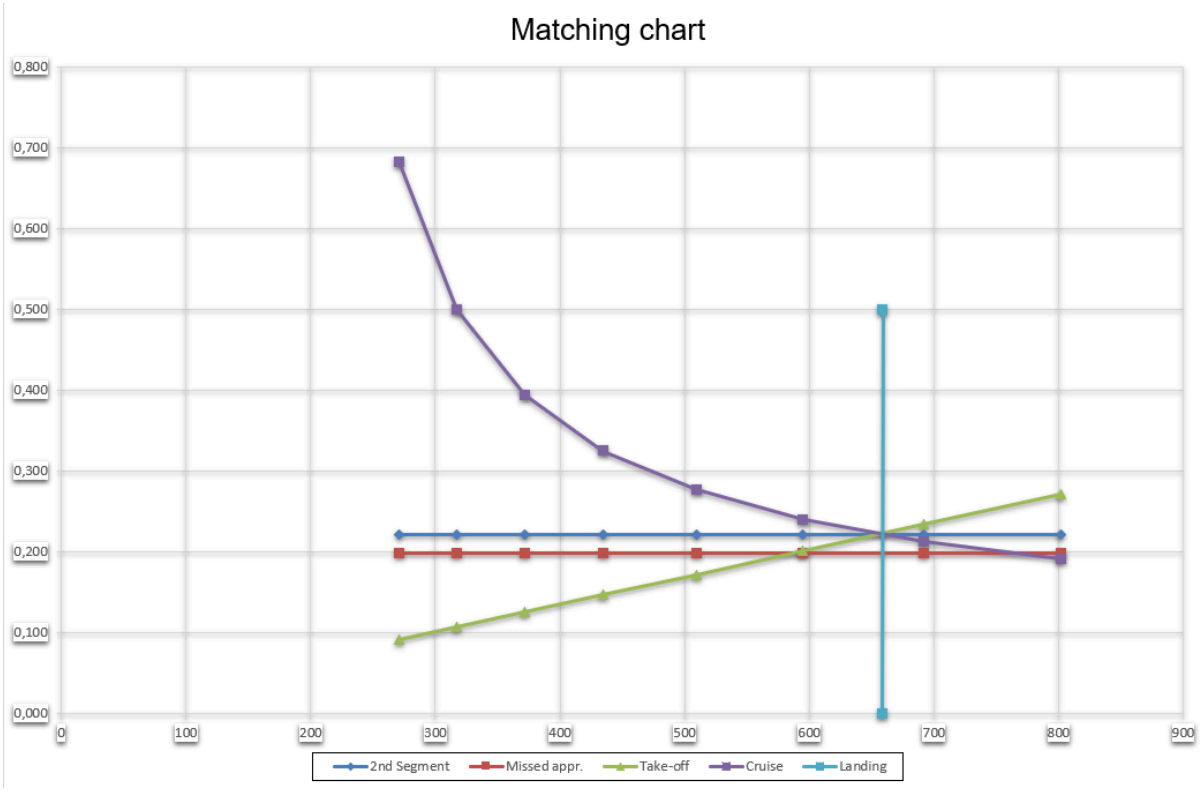

Figure 2.9: *Matching chart of the L-1011-100 TriStar*

Extracting the data from the graphic:

$$\frac{T_{TO}}{m_{TO} \cdot g} = 0,223$$

$$\frac{m_{TO}}{S_W} = 659\ kg/m^2$$

Using the **Equation 2.15** the ratio of cruise thrust is determined.

$$\frac{T_{CR}}{T_{TO}} = 0,277$$

Accordingly with **Equation 2.16**:

$$h_{CR} = 9369\ m$$

Using Table 1.3 the data calculated can be confirmed as correct, with values such as thrust-to-weight ratio and wing loading (for the different segments of the flight) appearing between 9 and 10 km of flying cruise altitude.

Finally in order to verify the results, a table comparing the data of the different phases of the flight calculated and computed on PreSTo Classic and the ones selected with different sources on **Table 1.2** has been created in order to clarify if the difference between each is less than 1%, giving accuracy to the work created.

Table 2.2: *Comparison of key data between PreSTo Classic and sources*

Data extracted	PreSTo Classic	Sources selection	Δ% Difference
m_{TO}	213140 kg	211375 kg	1%
m_L	168381 kg	166920 kg	1%
m_{OE}	112751 kg	111795 kg	1%
m_F	80889 kg	80080 kg	1%
S_W	324 m^2	320 m^2	1%
T_{TO}	499725, 91 N	495585,37 N	1%
$\frac{m_L}{m_{TO}}$	0,79	0,79	0%

As it can be seen, the usage of a program like PreSTo Classic is pretty useful to define the main important factors to size the aircraft, such as the maximum weights, take-off thrust or maximum loading. Aswell as in this step, the program can also be useful to size the fuselage of the aircraft, to know how the payloads are distributed.

3 Fuselage design

As mentioned before, in this section the fuselage of the aircraft will be defined and modified in order to meet the cabin layout requirements while ensuring balance with aerostructural and operational constraints. The sizing and repositioning of cabin elements such as lavatories, galleys, and seating rows have been performed using the Excel-based "PreSTo-Cabin" design tool.

https://www.fzt.haw-hamburg.de/pers/Scholz/PreSTo.html

This tool facilitates the precise recalculation of fuselage length, station positions, and cargo hold adaptation by accounting for all relevant cabin dimensions and regulatory constraints, including those defined by FAR-25. The goal is to define the fuselage explaining how the payload, including pax and their carry-on luggage are distributed and ensure compliance with certification standards during the modified configuration.

3.1 Configuration of classes

Regarding the previous work, the important data collected for this part is:

$n_{PAX} = 200;$

$R = 8676620\ m;$

$m_{TO} = 213140\ kg;$

Based on the technical profile manual for the L-1011 TriStar [6], airlines that used the aircraft usually added two different classes, first class and economy class, being the last one settled to 9.
However, in order to maintain balance on the payload distribution and to keep the possibility of having a high density class sitting, the number of seats per row in economy class is reduced to $n_{SA,YC,ROW} = 8$, and in case of first class seatings the number can be calculated with a formula using average finesses ratio.

$$n_{SA} = 0,45 \cdot \sqrt{n_{PAX}} \tag{3.1}$$

$n_{SA,FC,ROW} = 6,36 \approx 6$: number of seats per row

The next figure shows how the seats are distributed per row, distributing them on left, middle and right seats.

First class seats, right aisle	$n_{seats,right,FC}$	2	[-]
First class seats, middle aisle	$n_{seats,mid,FC}$	2	[-]
First class seats, left aisle	$n_{seats,left,FC}$	2	[-]
Check : First class seats abreast	$n_{SA,FC}$	6	[-]
Economy class seats, right aisle	$n_{seats,right,YC}$	2	[-]
Economy class seats, middle aisle	$n_{seats,mid,YC}$	4	[-]
Economy class seats, left aisle	$n_{seats,left,YC}$	2	[-]
Check : Economy class seats abreast	$n_{SA,YC}$	8	[-]

Figure 3.1: *Seat distribution per row according to PreSTo Cabin*

3.2 Seat and aisle dimensions

According to RAYMER 89 the sizes inside the cabin are defined in the next figure.

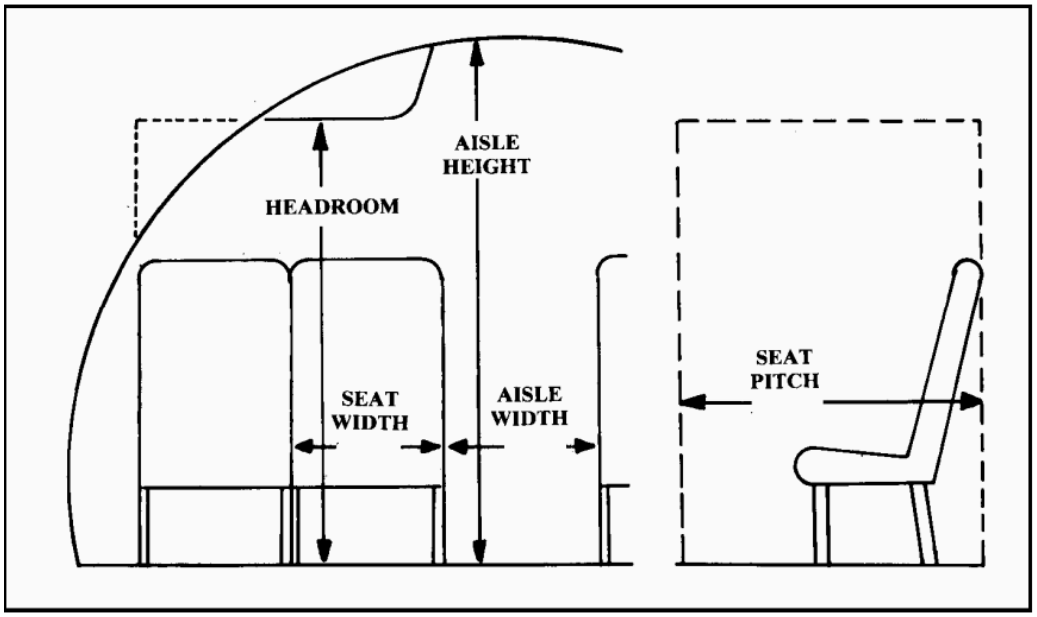

Figure 3.2: *Cabin and seat dimensions by RAYMER 89, cited in Scholz [1]*

	First class	Economy	High density/ small aircraft
Seat pitch (in.)	38–40	34–36	30–32
Seat width (in.)	20–28	17–22	16–18
Headroom (in.)	>65	>65	–
Aisle width (in.)	20–28	18–20	≥12
Aisle height (in.)	>76	>76	>60
Passengers per cabin staff (international-domestic)	16–20	31–36	≤50
Passengers per lavatory (40″ × 40″)	10–20	40–60	40–60
Galley volume per passenger (ft^3/pass)	5–8	1–2	0–1

Figure 3.3: *Typical cabin and seat dimensions by RAYMER 89, cited in Scholz [1]*

A table is created with all the information about the seat sizes on first and economy class.

Table 3.1: *Seat dimensions*

Data	Economy class (YC)	First class (FC)
$n_{SA\ IN\ TOTAL}$	176	24
Cushion width $w_{cushion}$	0,56 m	0,71 m
Cushion height position $\Delta y_{cushion}$	0,42 m	0,42 m
Cushion thickness $t_{cushion}$	0,14 m	0,14 m
Armrest width $w_{armrest}$	0,05 m	0,08 m
Armrest height position, top $h_{armrest,\ top}$	0,56 m	0,56 m
Armrest height position, bottom $h_{armrest,\ bottom}$	0,18 m	0,18 m
Backrest height $h_{backrest}$	0,59 m	0,59 m
Seat length l_{seat}	0,61 m	0,71 m
Seat pitch p	0,91 m	0,97 m

The values computed are equal or bigger than in typical cabin configurations of different airlines and similar aircrafts as the McDonnell Douglas DC-10, Airbus 300 or Boeing B767, where the width is usually $w_{cushion} = 0,53\ m$ for first class seats and a pitch of $p = 0,94\ m$ according to SeatGuru [7], as the main plan is to fit all seats in the cabin.

Finally according to **Figure 3.2**, the aircraft will have two aisles (according to JAR 25.817) with a width of $w_{aisle} = 0,53\ m$ ($w_{aisle,FC} = 0,62\ m$ as it has to be bigger) and a height of $h_{aisle} = 2,41\ m$, being the minimum sizes $w_{aisle} = 0,51\ m$ and $h_{aisle} = 2,41\ m$ according to JAR 25.185.

JAR 25.815 **Width of aisle**

The passenger aisle width at any point between seats must equal or exceed the values in the following table:

Passenger seating capacity	Minimum passenger aisle width (inches)	
	Less than 25 inches from floor	25 inches and more from floor
10 or less	12 *	15
11 to 19	12	20
20 or more	15	20
	* A narrower width not less than 9 inches may be approved when substantiated by tests found necessary by the authority.	

Figure 3.4: *Width of the aisle according to JAR 25.81, cited in Scholz [1]*

3.3 Cross sections

According to ROSKAM III the fuselage of the L-1011 has a cabin height $h_{f,i} = 177\ inch = 4,49\ m$ and a cabin width $w_{f,i} = 223\ in = 5,66\ m$, with a ratio of $(h/w)_{cabin} = 0,79$.

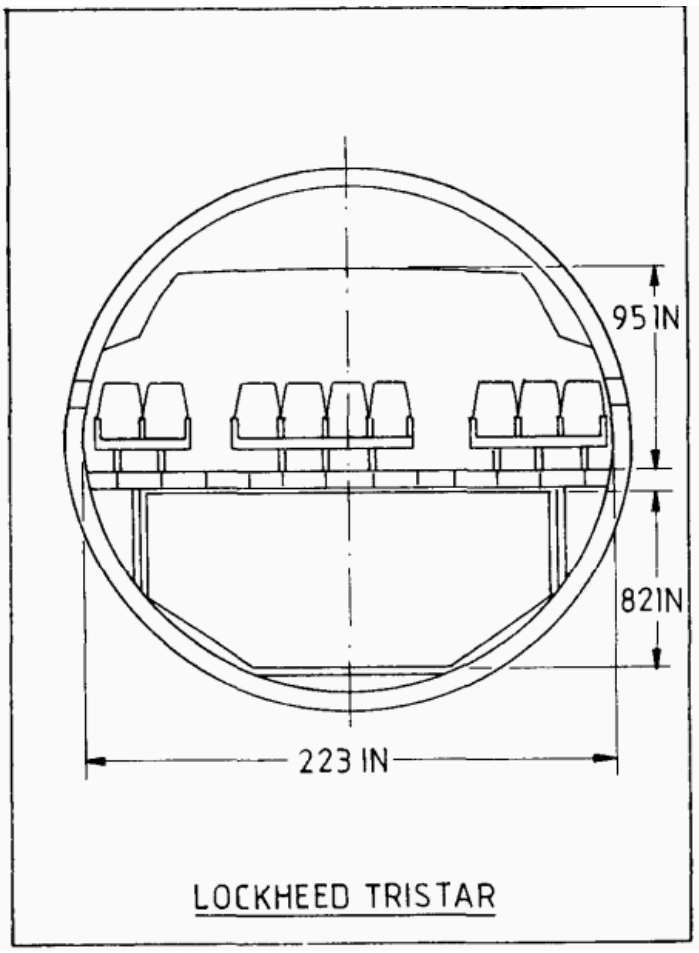

Figure 3.5: *Fuselage cross section according to ROSKAM III,, cited in Scholz [1]*

Using the PreSTo Cabin simulator, the next data is computed for the cabin.

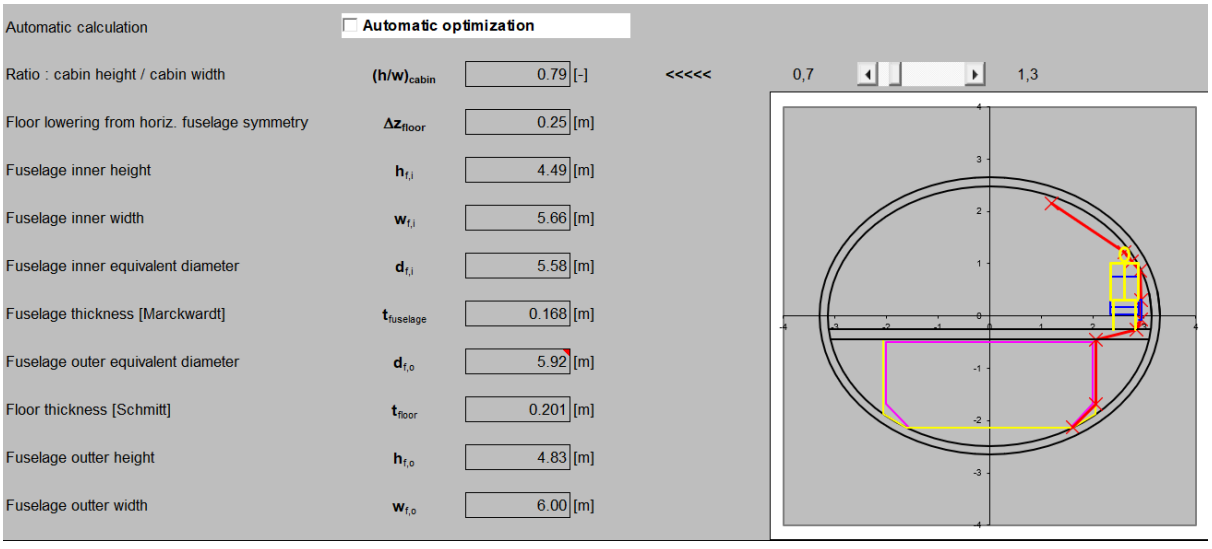

Figure 3.6: *Fuselage cross section according to PreSTo Cabin*

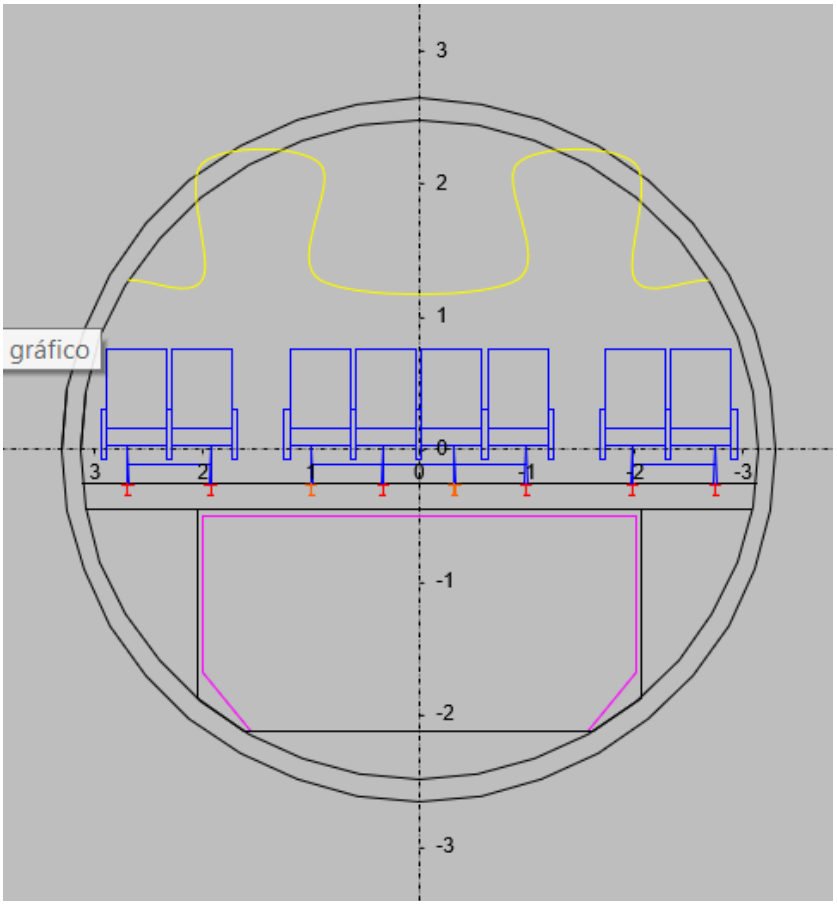

Figure 3.7: *Fuselage cross section of economic class of PreSTo Cabin*

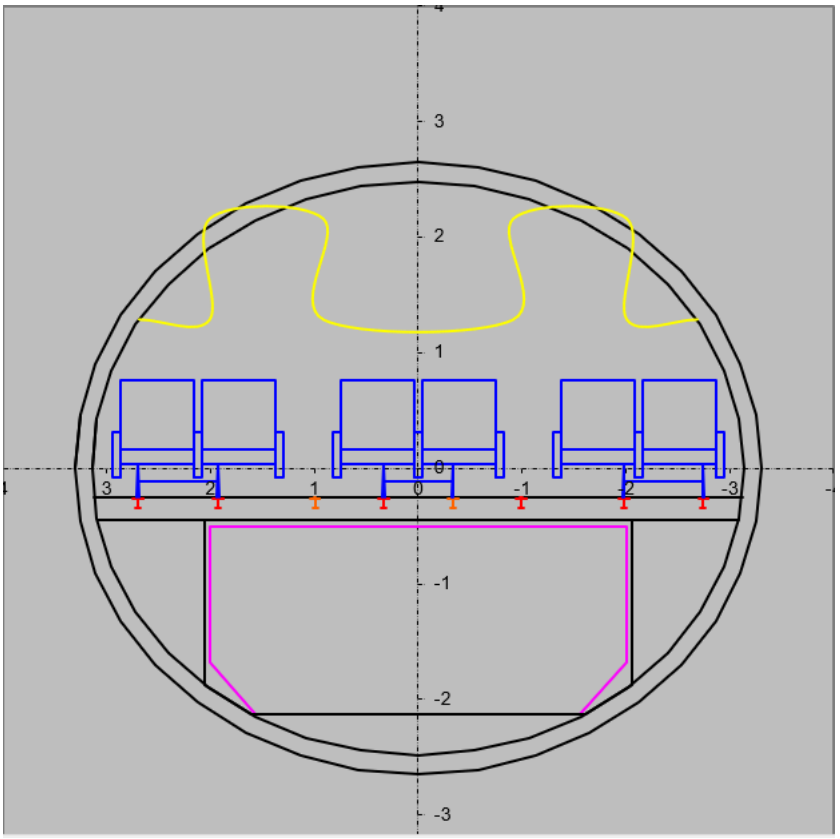

Figure 3.8: *Fuselage cross section of first class of PreSTo Cabin*

Based on the simulations, the number of rails and their size is computed as it stands.

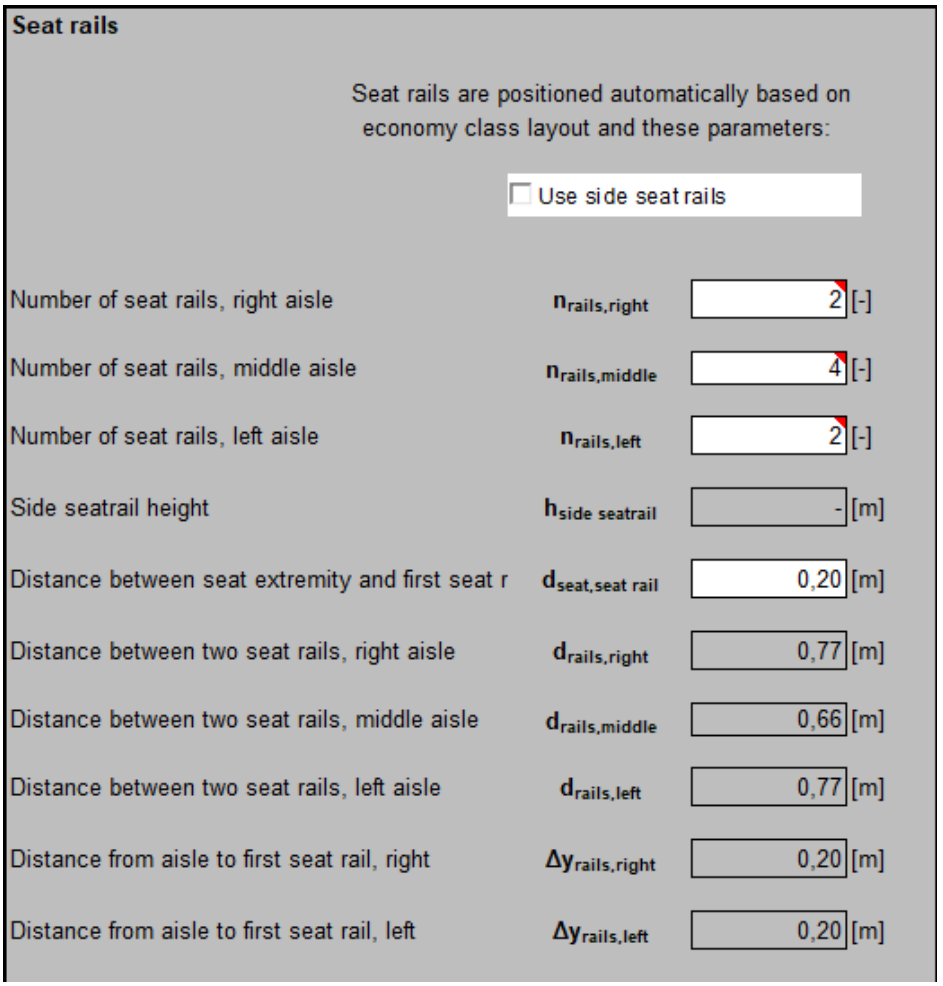

Figure 3.9: *Seat rails distribution and dimensions of PreSTo Cabin*

3.3 Cabin floor plan

Inside the typical airline's cabin configurations the design of basic equipment for the crew and passengers is essential, as it's the last part needed to fill the aircraft. Therefore, the galleys and lavatories are going to be defined as well as the number of emergency exits.

3.3.1 Galley definition

Using the formula provided by MARCKWARDT 98A, cited in Scholz [1]:

$$s_{GALLEY} = k_{GALLEY} \cdot \frac{n_{PAX}}{1000} + \frac{1}{2}\ (m^2\ ) \tag{3.2}$$

k_{GALLEY}: factor to estimate floor space for galleys, for typical flights of the L-1011 TriStar the number selected is 41.

Routes	k_{GALLEY} [m²]
Südatlantik, Fernost, Südafrika	41
Nordatlantik, Nahost	32
Europa	23
Innerdeutsch und Nachbarschaft	16

Figure 3.10: *Factor galley estimation depending in on the route, cited in Scholz [1]*

$$s_{GALLEY} = 8,7\ m^2$$

Following L-1011's technical profile document [6], the number of galleys used was splitted on 1 for first class and 2 for economy class. In the case of this project, the same number will be used, adding one galley on the front and two on the back.

Table 3.2: *Galley dimensions for different classes selected*

Data provided to PreSTo Cabin	First class	Economy class
n_{galley}	1	2
l_{galley} (length)	1,4 m^2	2,3 m^2
w_{galley} (width)	1,4 m^2	1,5 m^2

Checking the size of the galleys selected, the surface must not be lower than the one calculated with **Equation 3.2** as it's the minimum size needed.

$$s_{GALLEY} = l_{galley} \cdot w_{galley} \cdot n_{galley} \tag{3.3}$$

Accordingly, the surface is surpassing the limit:

$$s_{GALLEY} = 8,86\ m^2$$

3.3.2 Lavatories definition

Using the same methodology as before, the number of lavatories typically used by the airlines was 8, but as the number of pax taken has been reduced, the following data will be used according to SCHMITT 89.

		SR Kurzstrecke SR ≤ 3000 nm	MR Mittelstrecke 3000 nm < MR < 5500 nm		LR Langstrecke LR ≥ 5500 nm		
		YC	FC	YC	FC	BC	YC
Sitze	Sitze in %	100	8 - 10	90 - 92	5 - 7	18 - 20	73 - 77
	Sitzabstand [inch]	32	40	32	60	38	32
	Sitzlehnenneigung [inch]	5	7.5	5	15	7	5
	Sitzbreite (2er Bank)	40	48	40	53	50	40
Kabinenpersonal pro Pax		1 / 45	1 / 8	1 / 35	1 / 8	1 / 20	1 / 35
Toiletten pro Pax		1 / 60	1 / 14	1 / 45	1 / 14	1 / 25	1 / 45
Galley / Trolleys [Tabletts / Pax]		1.7	9	2.3	9	7	2.7
Mantelstauraum [inch / Pax]		Nein	1.5	Nein	1.5	1.5	Nein

Figure 3.11: *Cabin equipment used based according to SCHMITT 89, cited in Scholz [1]*

Knowing that the aircraft can carry up to 24 first class and 176 economy class passengers, the number of lavatories for an aircraft of 4685 NM of range is found.

$$n_{lav} = n_{pax,FC}/14 \tag{3.4}$$

$n_{lav} \approx 1$

$$n_{lav} = n_{pax,YC}/45 \tag{3.5}$$

$n_{lav} \approx 4$

Lavatories			
Number of lavatories, first class	$n_{lavatories,FC}$	1	[-]
Number of lavatories, economy class	$n_{lavatories,YC}$	4	[-]
Lavatory length	$l_{lavatory}$	1,2	[m]
Lavatory width	$w_{lavatory}$	1	[m]

Figure 3.12: *Number and sizes of lavatories computed on PreSTo Cabin*

According to MARCKWARDT 98a, the usual area of a lavatory is 1,20 m^2 , value that coincides with the one computed.

$$S_{lavatory} = l_{lavatory} \cdot w_{lavatory} \tag{3.4}$$

3.3.3 Exits definition

The number of emergency exits placed on the aircraft depends on the number of passengers the aircraft carry as the size will change to fit the number of people exiting through these doors.

Type of exit and Location	PAX allowed	Size (b*h)
Type A (Floor-level exit)	110	1,07m*1,83m
Type B (Floor-level exit)	75	0,81m*1,83m
Type C (Floor-level exit)	55	0,76m*1,22m
Type I (Floor-level exit)	45	0,61m*1,22m
Type II (Floor-level or over-wing exit)	40	0,51m*1,12m
Type III (Rectangular opening)	35	0,51m*0,91m
Type IV (Located over the wing)	9	0,48m*0,66m

Figure 3.13: *Exit types and sizes computed on PreSTo Cabin*

Using **Figure 3.13,** 2 Type A (floor-level) exits have been selected with an additional Type III (for aircraft configurations greater than 179 seats an extra emergency exit needs to be installed in both parts of the fuselage), allowing the exit for 255 passengers.

3.4 Aircraft dimensions

In this section the aircraft dimensions will be specified in order to fit all the requirements and equipment added taking into account the proper sizes of the aircraft. In order to achieve accurate results and as proof of more reliable data, the sizes chosen have been compared with similar aircraft fuselages, such as the McDonnell Douglas DC-10 and McDonnell Douglas MD-11.

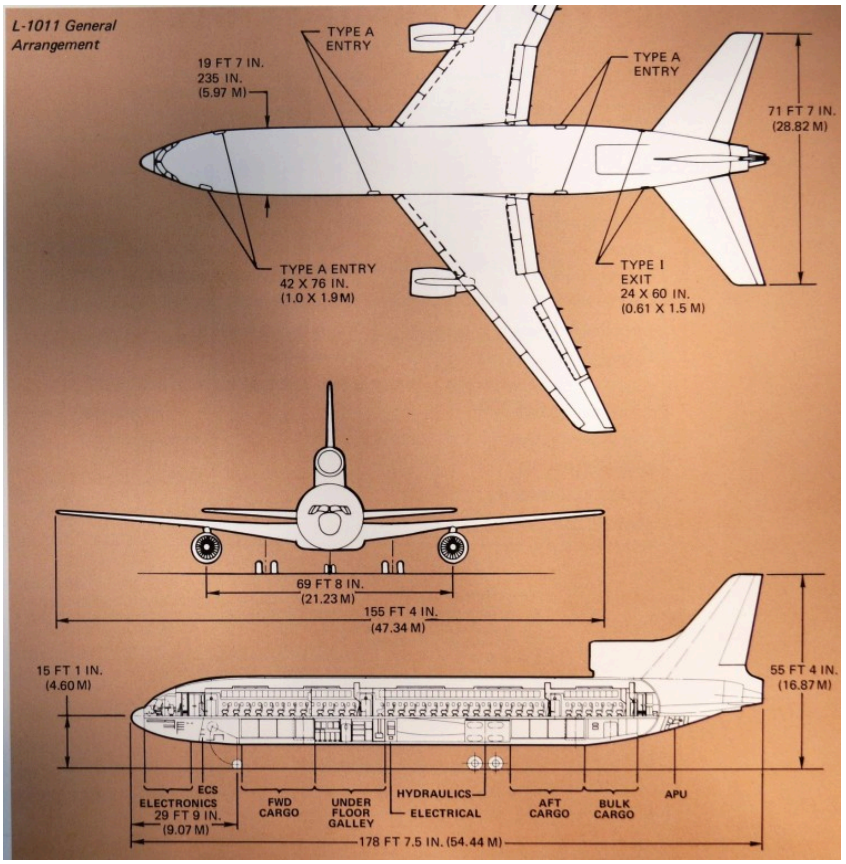

Figure 3.14: *L-1011 TriStar fuselage dimensions following Airline reporter [8]*

After careful analysis of the different dimensions and comparatives, the total length of the fuselage computed on PreSTo Cabin has followed the formulas provided by Scholz [1]

$$l_{cabin} = k_{cabin} \cdot \frac{n_{PAX}}{n_{SA}} \tag{3.6}$$

k_{cabin}: statistical constant provided by Scholz [1], with a value selected of $1,1\ m$

$l_{cabin} = 34,60\ m$

The total fuselage following Schmitt 98, cited in Scholz [1]:

$$l_f = l_{cabin} + 1,6 \cdot d_{f,E} + 4m \tag{3.7}$$

$d_{f,E}$: External diameter of the fuselage, following **Figure 3.5** using PreSTo Cabin the value has been settled to 5,92 m, which verifying the technical profile it's inside the correct range as the number used was 6,0 m

$l_f = 48,1\ m$

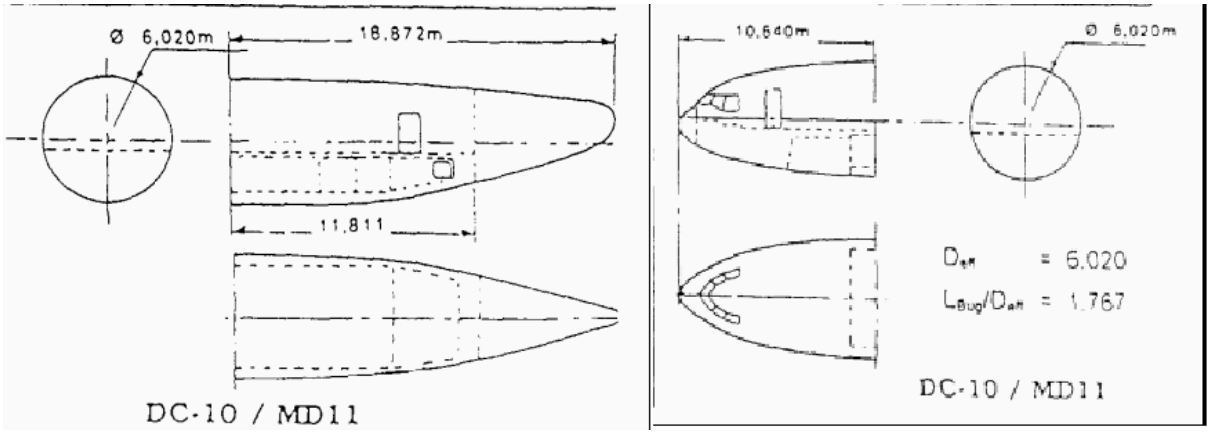

Figure 3.15: *Examples nose and tail sizes by SCHMITT 98, cited in Scholz [1]*

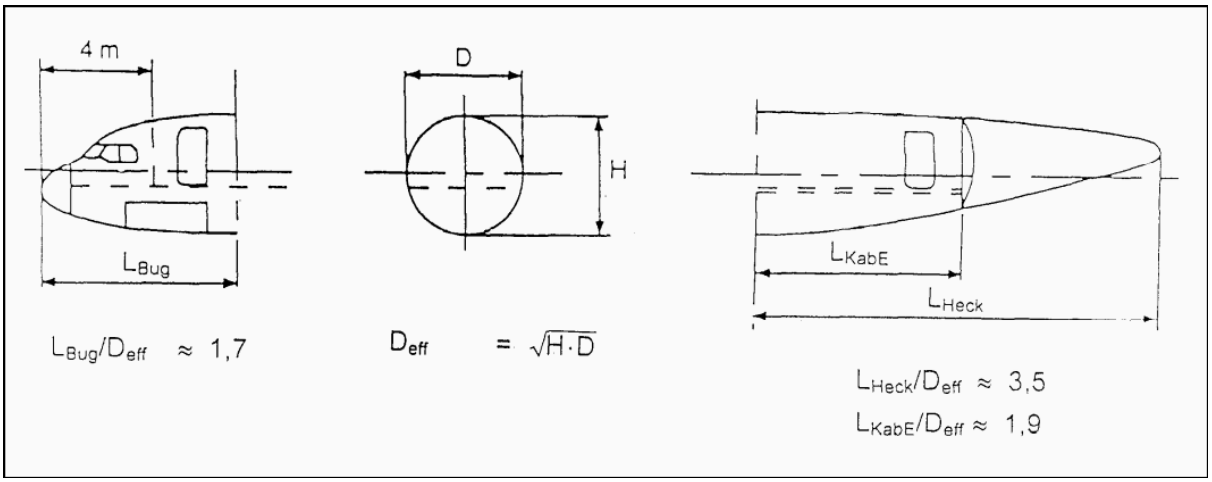

Figure 3.16: *Bug and heck calculations by Scholz [1]*

As explained before, similar models of aircrafts have been chosen to determine the dimensions of the aircraft.

The bug and heck have also been calculated using this method, as **Figure 3.16** is showing, the bug and heck length results are provided with the **Equation 3.8** and **Equation 3.9**.

$$l_{bug} = d_{eff} \cdot 1,7 \tag{3.8}$$

$$l_{heck} = d_{eff} \cdot 3,5 \tag{3.9}$$

d_{eff}: Effective external diameter, with a value of 5,04 m following **Figure 3.15.**
$l_{bug} = 8,568\ m.$

$l_{heck} = 17,64\ m.$

In order to compute these values on the PreSTo Cabin, different relations have been computed, such as the nose/tail length to diameter ratio or the bug offset, among others.

Nose length to diameter ratio	l_{nose}/d_f	1,45	[-]	>>>>>	Nose length	l_{nose}	8,56 [m]
Nose offset	Δx_{nose}	0,00	[m]				
Tail length to diameter ratio	l_{tail}/d_f	2,98	[-]	>>>>>	Tail length	l_{tail}	17,63 [m]
Tail offset to diameter ratio	$\Delta x_{tail}/df$	1,20		>>>>>	Tail offset	Δx_{tail}	7,10 [m]

Figure 3.17: *PreSTo Cabin fuselage dimensioning.*

As it can be seen, the model presented is very similar to other aircrafts presented before, which have similar structure and were created for similar purposes as for the L-1011 TriStar.

The required cabin space is the sum of all the areas of the equipment and installations together.

$$S_{aisle} = 2 \cdot (w_{aisle} \cdot l_{cabin}) \tag{3.10}$$

$S_{aisle,FC} = 42,904\ m^2$

$S_{aisle,YC} = 50,986\ m^2$

$$S_{seat} = w_{cushion} \cdot h_{backrest} + w_{cushion} \cdot I_{seat} \tag{3.11}$$

$S_{seat,FC} = 0,923\ m^2$

$S_{seat,YC} = 0,672\ m^2$

$$S_{TOTAL\ SEAT} = S_{seat,FC} + S_{seat,YC} \tag{3.12}$$

$S_{TOTAL\ SEAT} = 140,424\ m^2$

$$S_{req} = S_{galley} + 5 \cdot S_{lavatory} + S_{TOTAL\ SEAT} + S_{aisle,FC} + S_{aisle,YC} \tag{3.13}$$

$S_{req} = 249,174\ m^2$

From **Figure 3.5**:

$$S_{cabin} = l_{cabin} \cdot d_{f,I} \tag{3.14}$$

$d_{f,I}$: Internal diameter of the fuselage

$S_{cabin} = 193,068\ m^2$

$S_{cabin} \geq S_{req}$

The cabin area is bigger than the space of the elements that the airlines can configure, explaining that there is sufficient space to meet cabin requirements.

The rear cone angle is calculated using the external diameter and the length of the heck (tail).

$$\psi_{heck} = tan^{-1}(\frac{d_{f,E}}{l_{heck}}) \tag{3.15}$$

$\psi_{heck} = 18,55$ º.

3.5 Cargo volume

In this final section regarding the fuselage design, the cargo section will be defined, completing the final layouting.

The mass of passengers, carry on bags and cargo is calculated first, regarding **Table 1.3**:

$$m_{pax} = \frac{m_{pax}}{n_{pax}} \cdot n_{pax} \tag{3.16}$$

$$m_{baggage} = \frac{m_{baggage}}{n_{pax}} \cdot n_{pax} \tag{3.17}$$

$$m_{cargo} = m_{pl} - m_{pax} - m_{baggage} \tag{3.18}$$

$\frac{m_{pax}}{n_{pax}}$: ratio of mass per number of passengers, according to Roskam I is 79, 4 kg.

$\frac{m_{baggage}}{n_{pax}}$: ratio of baggage per number of passengers, 13, 6 kg according to Roskam I.

$m_{pax} = 15880\ kg.$

$m_{baggage} = 2720\ kg.$

$m_{cargo} = 538\ kg.$

For the cargo density, values of $\rho_{cargo} = 160\ kg/m^3$ and $\rho_{baggage} = 170\ kg/m^3$ are used by Torenbeek 88, cited in Scholz [1].

Then, the cargo volume is:

$$V_{cargo} = \frac{m_{cargo}}{\rho_{cargo}} \tag{3.19}$$

$V_{cargo} = 3,3625\ m^3$.

$$V_{baggage} = \frac{m_{baggage}}{\rho_{baggage}} \tag{3.20}$$

$V_{baggage} = 16\ m^3$.

The available cargo volume is also calculated:

$$V_{cargo\ compartment} = l_f \cdot S_{cc} \cdot k_{cc} \tag{3.21}$$

S_{CC}: Cross section of the cargo compartment.

k_{CC}: Proportion of fuselage length used for cargo, 0,40 according to PreSTo Cabin.

$$S_{cc} = w_{ld,top} \cdot h_{ld} - \left(\frac{w_{ld,top} - w_{ld,bottom}}{2}\right)^2 \tag{3.22}$$

$w_{ld,top}$: width of the top lower deck.

$w_{ld,bottom}$: width of the bottom lower deck.

h_{ld}: height of the lower deck.

According to PreSTo Cabin, $S_{CC} = 6,69\ m^2$.

$V_{cargo\ compartment} = 128,72\ m^3$.

$$V_{overhead\ stowage} = \frac{V_{overhead\ stowage}}{n_{pax}} \cdot n_{pax} \tag{3.23}$$

$\frac{V_{overhead\ stowage}}{n_{pax}}$: ratio of baggage store overhead the passengers per number of pax.

Usually a value of $0,05\ m^3$ is used as passengers take their baggage into the cabin with them.

$V_{overhead\ stowage} = 10\ m^3$.

In order to check the volume used, **Equation 3.24** is used as the cargo compartment volume has to be equal or bigger to the sum of baggage and cargo taking apart the overhead baggage.

$$V_{cargo\ compartment} \geq (V_{baggage} + V_{cargo}) - V_{overhead\ stowage} \tag{3.24}$$

$128,72\ m^2 \geq 9,3625\ m^3$.

The cargo volume is more than enough.

Following the technical profile[6], LD3 containers are installed on the aircraft as the airlines use this configuration.

3.6 Waterline

Following JAR 25.807 cited in Scholz [1], during an emergency ditching the door sills must remain above the waterline. Cto be established. If an emergency ditching occurs right after takeoff, the aircraft will likely still be near its maximum takeoff weight.

The maximal mass for water ditching can be split sequentially, the elevation of the waterline needs ed in three parts, the bug, heck and fuselage.

Following the data calculated in the last segments applied to PreSTo Cabin:

$$m_{wd-nose} = I_{nose} \cdot w_{fo} \cdot \frac{h_{fo}}{4} \cdot \left(\frac{\pi}{2} + arcsen(\Delta) + (\Delta) \cdot cos(\Delta_1)\right) \cdot 333,3 \quad (3.25)$$

The maximal mass for water ditching on the nose is $m_{wd-nose}$, where $\Delta = \frac{-\Delta z_{floor}}{h_{fo} \cdot 2}$ and $\Delta_1 = arcsen(\Delta)$.

$$m_{wd-tail} = I_{tail} \cdot w_{fo} \cdot \frac{h_{fo}}{4} \cdot \left(\frac{\pi}{2} + arcsen(\Delta) + (\Delta) \cdot cos(\Delta_1)\right) \cdot 333,3 \quad (3.26)$$

$m_{wd-tail}$: Maximal mass for water ditching on the tail.

$$m_{wf} = w_{fo} \cdot \frac{h_{fo}}{4} \cdot \left(\frac{\pi}{2} + arcsen(\Delta) + (\Delta) \cdot cos(\Delta_1)\right) \cdot 10^3 \cdot (l_{cabin} - \Delta x_{nose} - \Delta x_{tail}) \quad (3.27)$$

m_{wd-f}: Maximal mass for water ditching on the fuselage

$m_{wd-nose} = 28132\ kg.$

$m_{wd-tail} = 57930\ kg.$

$m_{wf} = 241667\ kg.$

The total sum of the mass calculations gives a value of 327729 kg, bigger than the maximum take-off mass (m_{TO}) indicating that the door steps are above the water line in case of an emergency case.

The sizes are defined below:

$$d_{fuselage} = \frac{d_{f,E} - d_{f,I}}{2} \tag{3.28}$$

$d_{fuselage} = 0,17\ m$: fuselage diameter.

$$h_d = d_{f,E} - d_{fuselage} - h_{aisle} \tag{3.29}$$

$h_d = 3,34\ m$: door height.

$h_{aisle} = 2,41\ m$: aisle height according to PreSTo Cabin.

$$\varphi = 2 \cdot arccos\left(1 - \frac{h_d}{r}\right) \tag{3.30}$$

$\varphi = 194,75$ º: opening angle.

$r = 2,96\ m$: radius of the external cabin.

$$s = 2 \cdot r \cdot sin(2\varphi) \tag{3.31}$$

$s = 2,915\ m^2$: circular arc section length.

$$S_{section} = \frac{h_d}{2 \cdot s} \cdot (3 \cdot h_d^{\ 2} + 4 \cdot s^2) \tag{3.32}$$

$S_{section} = 38,65\ m^2$: circular arc section surface.

3.7 Cabin layout

To finish this section, the scale drawing of the cabin layout is computed using PreSTo Cabin, the green and blue small squares in the middle are the seats for first and economy class, respectively. The cockpit is marked on the left side of the image, and

the galleys (green) and lavatories (white) are placed on the front and rear part of the aircraft (corners).

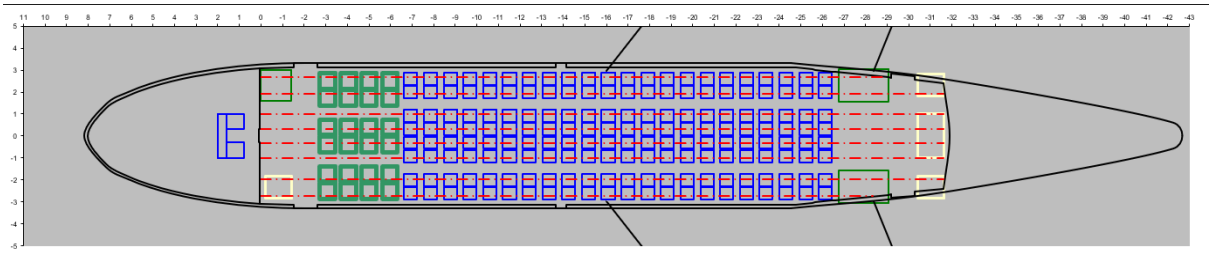

Figure 3.18: *PreSTo Cabin 2D modelling layouting.*

Using the information provided on **Figure 3.10**, the number of cabin crew personnel has been settled to 3 for first class and 5 for economy class in order to fulfill all passenger requirements.

3.8 Summary

Table 3.3 resumes all the important information clarified in this section.

Table 3.3: *Important data calculated for the fuselage design*

Data demanded	Data computed
Number of seats per row ($n_{SA,ROW}$)	6 for FC, 8 for YC
Number of aisles (n_{aisle})	2
Number of cabin crew members (n_{crew})	8
Fuselage diameter ($d_{f,E}$)	5,92 m^2
Fuselage length (l_f)	50,7 m
Length of the cabin (l_{cabin})	31,61 m
Length of the bow section (l_{bug})	8,568 m
Length of the stern section (l_{heck})	17,64 m
Rear cone angle (ψ_{heck})	18,55 º

4 Wing definition

After the fuselage analysis the wing and its high lift incorporations can be defined and organised, using from now on the "PreSTo" version 3.4.2 tool in order to create plots and compute key data in order to accomplish all the demands of the double trapezoidal type wing that the aircraft carry.

https://www.fzt.haw-hamburg.de/pers/Scholz/PreSTo.html

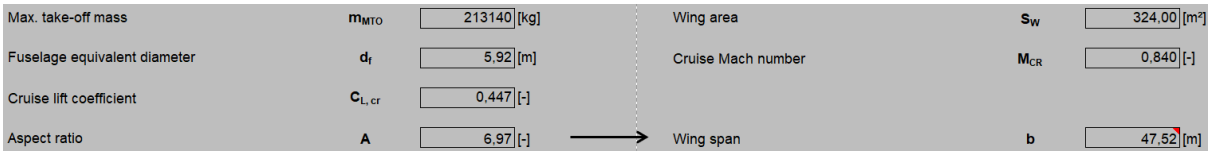

Figure 4.1: *PreSTo data collected from previous sections.*

4.1 Quarter chord sweep angle and relative thickness

After contrasting with different sources, such as Elsevier [4] or the technical profile manual [6] the quarter chord sweep angle (angle between the aircraft's lateral axis and the line connecting the 25% chord points along the span of the wing) has been settled to 35 º which is a reasonable value as long range jets are used to have values of minimum 30-33º.
This number is important as it usually is where the aerodynamic center is located in order to study the stability of the design.

A plot is created with the PreSTo tool, showing location of the designed sweep angle on the Mach number that Figure **4.1** shows together with a line showing Raymer suggestions for the selection of the angle.

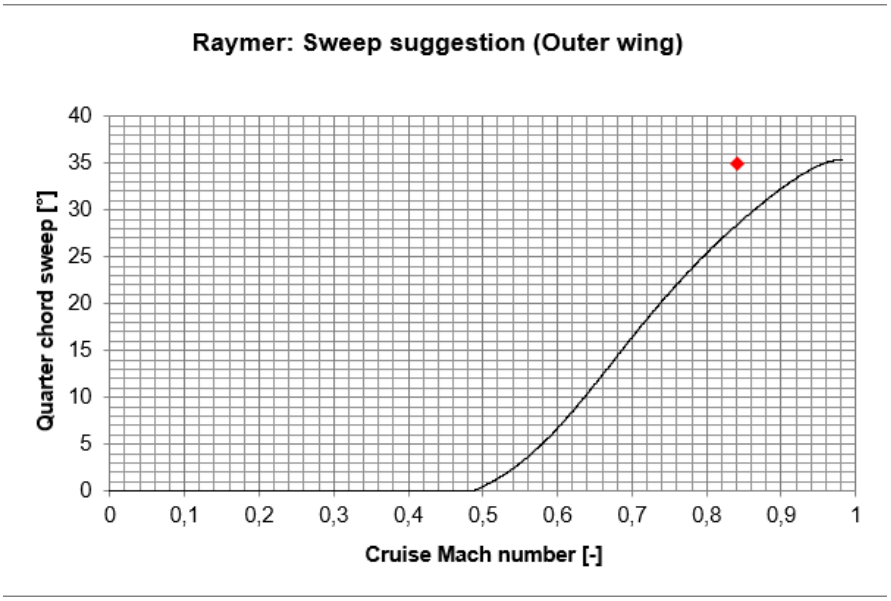

Figure 4.2: *Plot comparing the quarter chord angle and the Mach number for cruise.*

As it can be seen, the number selected is close to the line, but bigger as the aircraft has different dimensions than the usual Airbus and Boeing models, as an example.

In order to calculate the relative thickness of the aircraft (thickness of the aircraft divided it's chord), the value chosen has been selected using the information of Elsevier [4], providing a number of 0, 107.

According to **Figure 4.3** the value chosen is very close to one computed using non-linear regression at the sweep angle determined before.

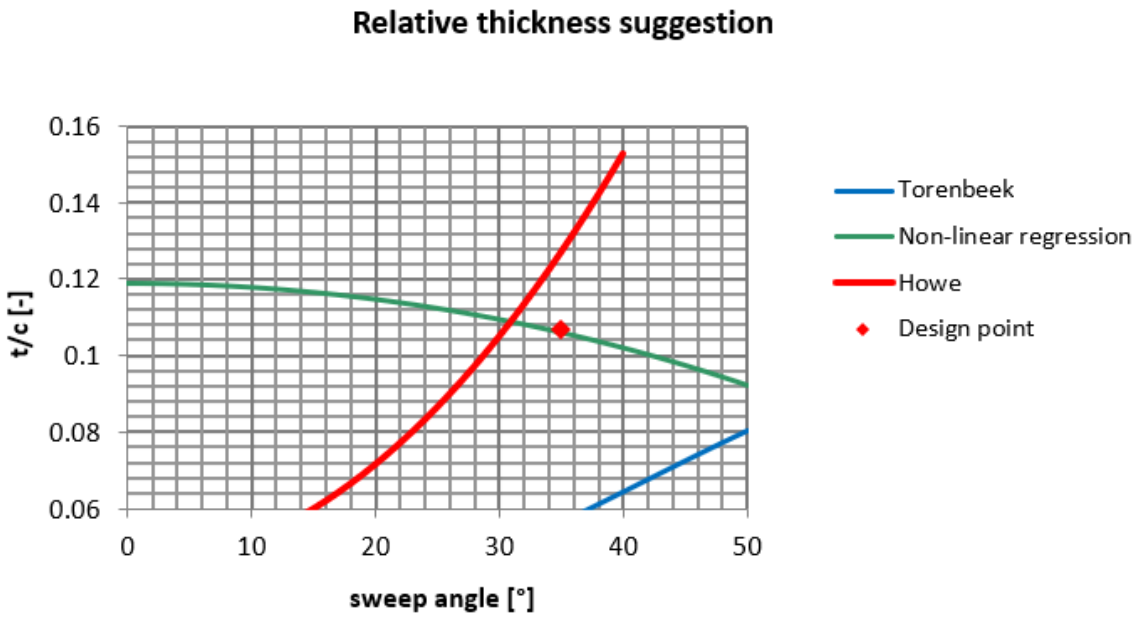

Figure 4.3: *Plot comparing the thickness ratio and quarter chord sweep angle.*

It will be assumed that the aircraft has a double trapezoidal area, separating the root to kink area (inner surface) and kink to tip (outer surface).

Using the formulas provided by Scholz [1] it is possible to calculate the root, tip and kink thickness ratios assuming that the inner and outer relative thickness are 0,975 and 1, respectively.

$$\tau = t_i \cdot t_o \tag{4.1}$$

t_i: inner relative thickness.

t_o: outer relative thickness.

The relative thickness ratio is $\tau = 0,975$.

$$\left(\frac{t}{c}\right)_r = \frac{4}{3 \cdot \tau + 1} \cdot \frac{t}{c} \tag{4.2}$$

$$\left(\frac{t}{c}\right)_t = \left(\frac{t}{c}\right)_r \cdot \frac{t}{c} \tag{4.3}$$

$$\left(\frac{t}{c}\right)_k = \left(\frac{t}{c}\right)_r \cdot t_i \tag{4.3}$$

$\frac{t}{c}$: relative thickness .

The values calculated are $\left(\frac{t}{c}\right)_r = 0,109, \left(\frac{t}{c}\right)_t = \left(\frac{t}{c}\right)_k = 0,106$.

4.2 Surface area

The surface is defined in this section, defining both of the different parts of the wing.

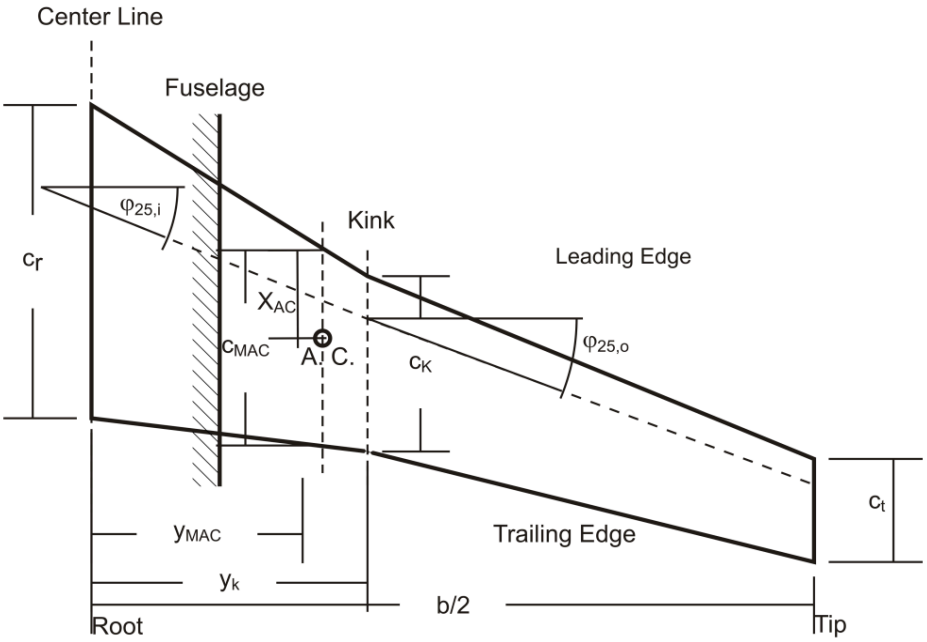

Figure 4.4: *Geometry of the wing provided by Scholz [1].*

Stating different kink ratios for different aircrafts, a value of 0,368 has been selected using as an example aircrafts as the MD-11 or the B767 which have similar values of wing area.

Using the data provided by Elsevier [4], the wing taper ratio has been settled to 0,259 which will be computed on PreSTo to define the tapering and dimensions of the L-1011 wing.

Kink semi-span:

$$Y_k = \eta_k \cdot \frac{b}{2} \tag{4.4}$$

η_k: kink taper ratio.

b: wing span.

Inner taper ratio:

$$\lambda_i = \frac{c_t}{c_r} \tag{4.5}$$

c_t: tip chord.

c_r: root chord.

$$\lambda_o = \frac{\lambda}{\lambda_i} \tag{4.6}$$

λ: wing taper ratio.

Inside fuselage area:

$$S_f = d_{f,E} \cdot c_r \tag{4.7}$$

Inner wing area:

$$S_i = (c_k + c_r) \cdot (Y_k - \frac{b}{2}) \tag{4.8}$$

Outer wing area:

$$S_f = (c_k + c_t) \cdot (\frac{b}{2} - Y_k) \tag{4.9}$$

Knowing how the different data is related, and knowing that the wing is defined by two trapezoids, **Equation 4.10** can help define the inner taper ratio, a crucial value that is used to calculate the formulas determined before.

$$c_k = c_r - (c_r - c_t) \cdot \eta_k \tag{4.10}$$

$$c_t = \lambda \cdot c_r \tag{4.11}$$

Being $c_t = 0,259 \cdot c_r$, resulting on a relation substituting the **equation 4.7** and the kink taper ratio to the **equation 4.6**:

$$c_k = c_r - (c_r - \lambda \cdot c_r) \cdot \eta_k \tag{4.12}$$

Finally, $c_k = c_r \cdot (0,632 + 0,095) = 0,727 \cdot c_r$ which, with **Equation 4.5**, explains the relation between the kink and root resulting on the inner taper ratio, with a value of $\lambda_i = 0,727$.

$$c_k = \frac{S_W}{Y_k \cdot (\frac{1}{\lambda_i} - \lambda_o) + \frac{d_{f,E}}{2} \cdot (\frac{1}{\lambda_i} - 1) + \frac{d_{f,E}}{2} \cdot (1 + \lambda_o)} \tag{4.13}$$

$$c_r = c_k / \lambda_i \tag{4.14}$$

Aspect ratio inner trapezoid:

$$A_i = \frac{(2 \cdot Y_k - d_{f,E})^2}{S_i} \tag{4.15}$$

Aspect ratio outer trapezoid:

$$A_o = \frac{(b - 2 \cdot Y_k)^2}{S_o} \tag{4.16}$$

All the formulas provided by Scholz [1] and PreSTo have been computed to draw the wing, as **Figure 4.5** and **Figure 4.6** show.

Root chord	c_r	10,55	[m]
Kink chord	c_k	7,67	[m]
Tip chord	c_t	2,73	[m]
Kink semi-span	Y_k	8,74	[m]
Aspect ratio inner trapezoid	A_i	1,27	[-]
Aspect ratio outer trapezoid	A_o	5,78	[-]
Inside fuselage area	S_f	62,41	[m²]
Inner trapezoid area	S_i	105,41	[m²]
Outer trapezoid area	S_o	156,18	[m²]

Figure 4.5: *Wing geometry results calculated on PreSTo*

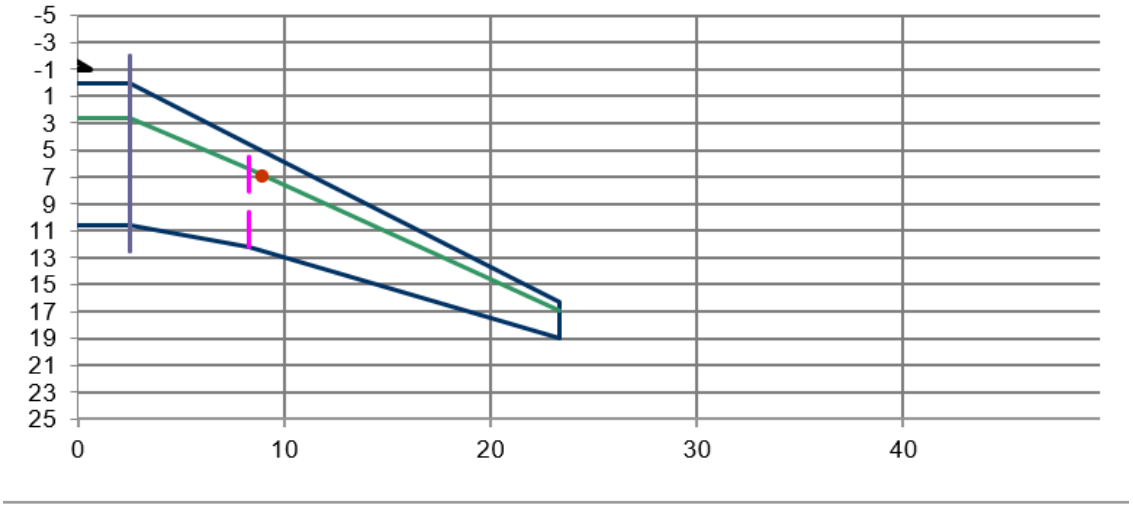

Figure 4.6: *Wing draw created with PreSTo*

4.3 Airfoil profile

Knowing the aircraft's thickness, an airfoil can be chosen as it sets other important data such as the maximum lift coefficient, the pitching moment coefficient, maximum camber and the distribution of thickness from root to tip of the wing.

The L-1011 is an old model and most of the airfoils dated on PreSTo were created after the aircraft's design. In order to find a similar airfoil the NACA 6-series is used as it's the one closest to meet the requirements choosing the different profiles from the Abbott catalog found on the tool.

The next figure shows the airfoil chosen, the NACA 63-210 which has a thickness similar to the one created in this project. The maximum lift coefficient has been settled to 1,6 according to Howe 2000 cited by Scholz [1], for subsonic flights and an angle for zero-lift of -3º according to airfoil tools.

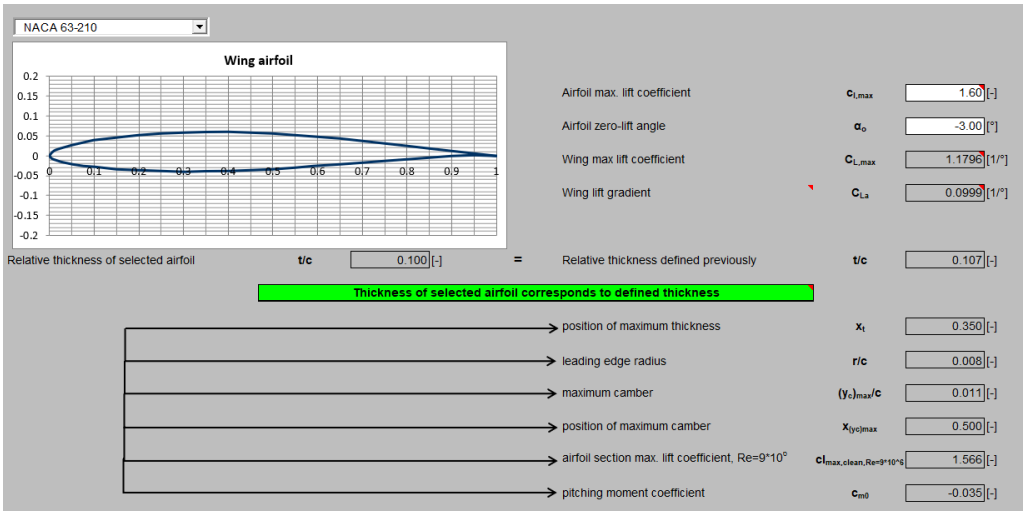

Figure 4.7: *Airfoil data on PreSTo*

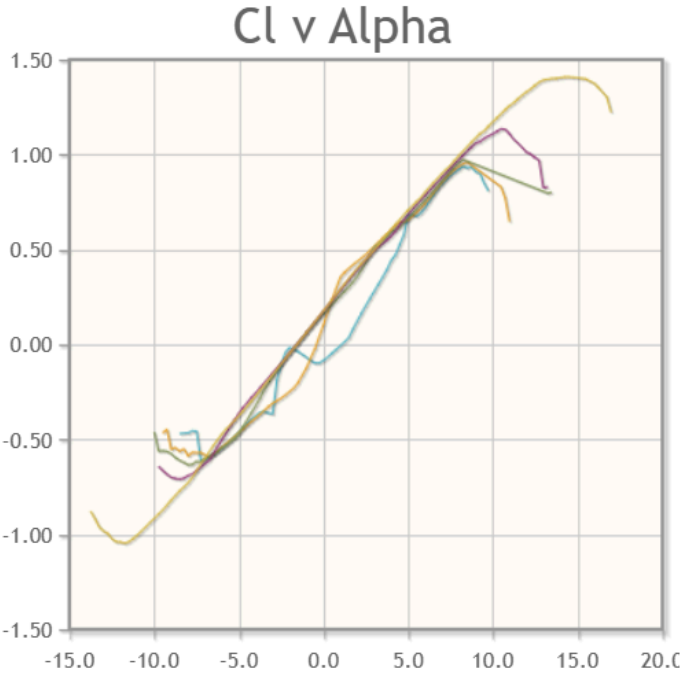

Figure 4.8: *Cl vs angle of attack plot of NACA 63-210 according to Airfoil Tools [9]*

4.4 Dihedral and incidence angle

A moment is caused around the longitudinal axis of the aircraft as the fuselage carries most of the weight, making the wing tips to level upwards with an angle called dihedral leading to positive stability.

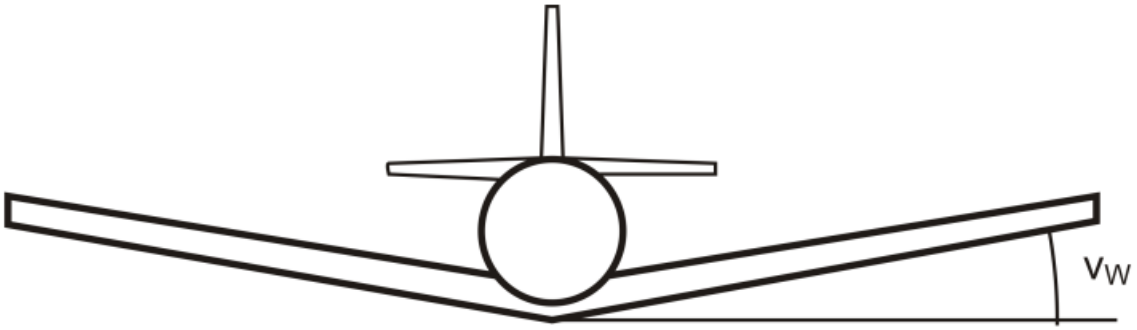

Figure 4.9: *Front view of an airplane showing the dihedral angle v_w by Scholz [1]*

From definition, the incidence angle is chosen to reduce drag during flight, being the relation of the chord line and the axis along the fuselage.

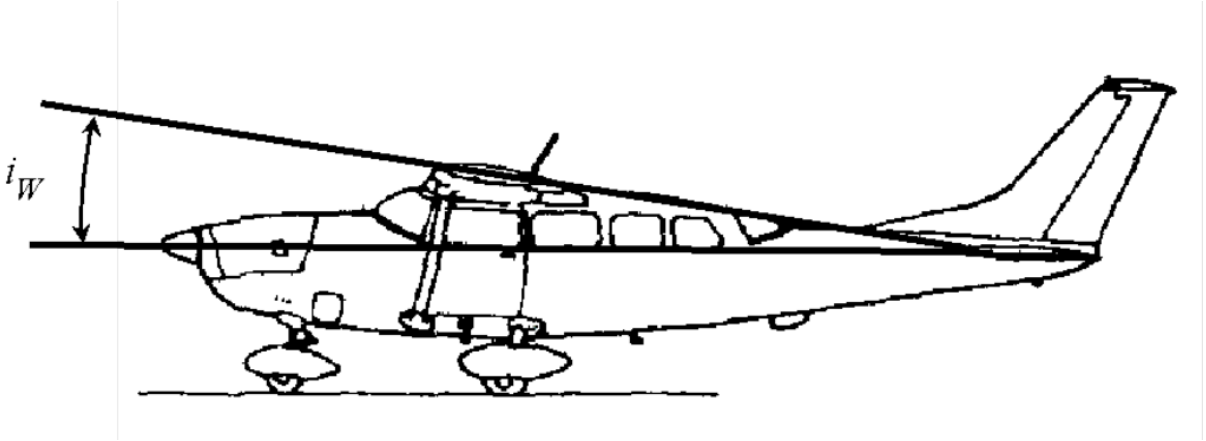

Figure 4.10: *Side view of an airplane showing the incidence angle i_w by Scholz [1]*

$$i_w = \frac{C_{L,CR}}{C_{L_\alpha}} + \alpha_0 + 0,4 \cdot \varepsilon_t \tag{4.17}$$

$C_{L,CR}$: lift coefficient on cruise flight, defined in the preliminary sizing as 0,447.

C_{L_α}: curve slope of the lift coefficient, with a value of 0,0999 1/º according to figure 4.7.

α_0: angle of attack for zero-lift, -3 º according to figure 4.7.

ε_t: twist angle, helps reduce incidence angle when it's negative, -3 º according to Raymer 2006 [].

Finally, $i_w = 2,67º$.

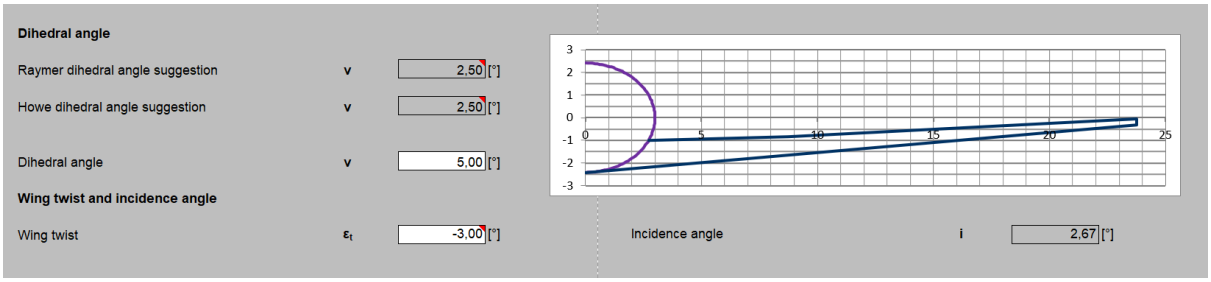

Figure 4.11: *Data used on PreSTo*

4.5 Volume of the tank and MAC calculation

The volume of the tank is calculated according to Torenbeek 1998, cited by Scholz [1]:

$$V_{Tank} = 0,54 \cdot S_W^{1,5} \cdot \left(\frac{t}{c}\right)_r \cdot \frac{1}{\sqrt{A}} \cdot \frac{1+\lambda \cdot \sqrt{\tau}+\lambda^2 \cdot \tau}{(1+\tau)^2} \quad (4.18)$$

The volume of fuel will be installed on the outer and inner wing as well as on the inboard tank, the total volume $V_{Tank} = 108,37\ m^3$ is splitted as it is shown in **Figure 4.12**.

Fuel mass, required	$m_{F,req}$	83521 [kg]				
Fuel density	ρ_F	800 [kg/m³]		Fuel volume, required	$V_{F,req}$	104.40 [m³]
Select: Fuel tank installation						
☑ Outer wing fuel tank	→			Outer wing fuel tank volume	V_{Fo}	37.60 [m³]
☑ Inner wing fuel tank	→			Inner wing fuel tank volume	V_{Fi}	42.34 [m³]
☑ Inboard fuel tank	→			Volume of inboard fuel tank(s)	V_{FF}	28.43 [m³]
				Total fuel volume	V_F	108.37 [m³]
				Total calculated fuel mass	M_{FC}	86693 [kg]
Check: Fuel volume						
Available fuel volume	V_F	108.37 [-]	>	Fuel volume, required	$V_{F,req}$	104.40 [m³]

Figure 4.12: *Volume of the tank used on PreSTo*

The available volume is more than the required volume computed on preliminary sizing.

The MAC (Mean Aerodynamic Chord) is defined as an average chord length of the wing, which will help represent the center of gravity. The different MAC values are stated.

Table 4.1: *MAC calculated on PreSTo*

Areas calculated	Data computed
Fuselage MAC ($c_{MAC,f}$)	10,549 m
Fuselage MAC span ($Y_{MAC,f}$)	1,479 m
Inner wing MAC ($c_{MAC,i}$)	9,185 m
Inner wing MAC semi-span ($Y_{MAC,f}$)	5,698 m
Outer wing MAC ($c_{MAC,o}$)	5,591 m
Outer wing MAC semi-span ($Y_{MAC,o}$)	15,064 m

Wing MAC (c_{MAC})	7,716 m
Wing MAC semi-span (Y_{MAC})	9,4 m

4.6 Geometry of ailerons

Ailerons are defined as simple flaps that are mounted close to the wing tips permitting the pilot to roll around the longitudinal axis of the aircraft. Looking at images of the L-1011 wing, an approximation of the sizes has been created on PreSTo, knowing that usually the chord of the ailerons is between 20-40% of the wing chord.

The L-1011-100 wing has ailerons located on the tip wings very close to the edges, defined on the next figures below.

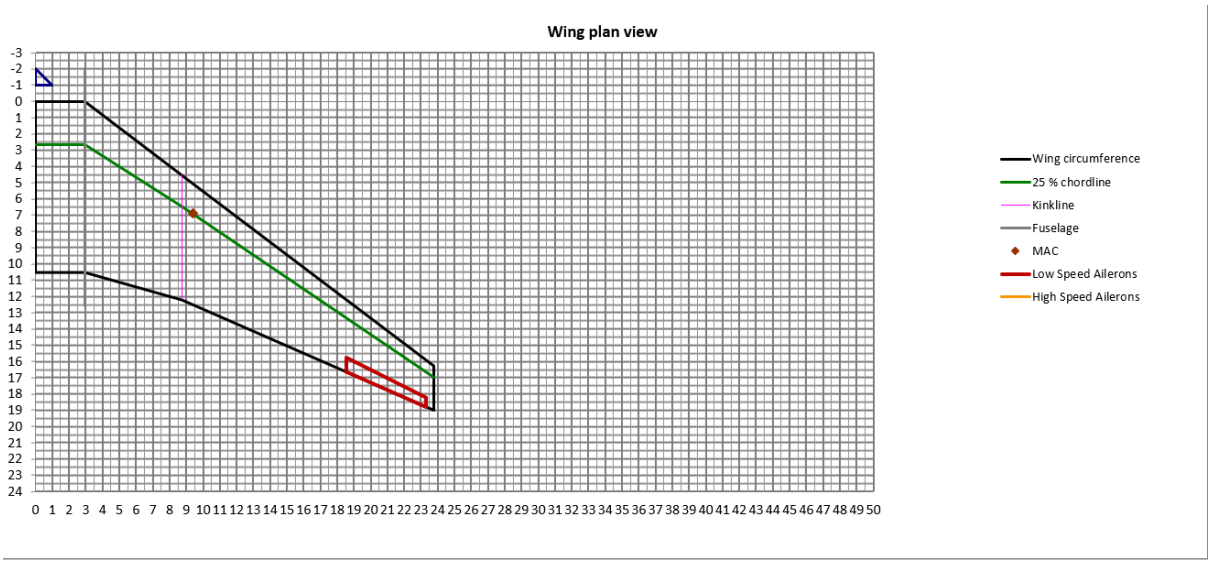

Figure 4.13: *Wing view created on PreSTo*

Aileron midpoint span						
Howe: Aileron midpoint span suggestion	$Y_{A,M}/b$	0.420 [-]				
Aileron midpoint span for constant V_A	$Y_{A,M}/b$	0.650 [-]	**Results**			
Aileron midpoint span	$Y_{A,M}/b$	0.440 [-]	Aileron outer span	$Y_{t,A}/b$	0.490	[m]
Total aileron span an chordwise distribution			Aileron midpoint span	$Y_{A,M}$	20.91	[m]
Total aileron span			Total aileron span	b_A	9.50	[m]
Howe: Total aileron span suggestion	b_A/b	0.210 [-]	Aileron root span	$Y_{r,A}$	18.53	[m]
Total aileron span for constant S_A	b_A/b	0.200 [-]	Aileron tip span	$Y_{t,A}$	23.28	[m]
Total aileron span	b_A/b	0.200 [-]	**Check**			
Chordwise distribution			Selected total aileron area	S_A	6.97	[m²]
Howe: Chordwise distribution suggestion	c_A/c	0.290 [-]				
Chordwise distribution for constant S_A	c_A/c	0.200 [-]				
Chordwise distribution	c_A/c	0.200 [-]				

Figure 4.14: *Aileron sizes on PreSTo*

As **Figure 4.14** shows the chord of the aileron is 20% of the total chord of the wing and the aileron outer span is close to 0,5 m, meaning that the aileron is almost on the tip of the wing, just as the models of the L-1011 aircraft.
The spoilers manage to slow the aircraft causing a yawing movement in the direction of the turn. In this case PreSTo couldn't define the geometry of the spoilers which are situated above the middle flaps defined in the next chapter.

The geometry of the L-1011 spoilers are defined for this project.

Table 8.7c) Jet Transports: Vert. Tail Volume, Rudder, Aileron and Spoiler Data

Type	Outb'd Ail. Span in/out fr.b/2	Outb'd Ail. Chord in/out fr.c_w	Inb'd Spoiler Span Loc. in/out fr.b/2	Inb'd Spoiler Chord in/out fr.c_w	Inb'd Spoiler Hinge Loc. in/out fr.c_w	Outb'd Spoiler Span Loc. in/out fr.c_w	Outb'd Spoiler Chord in/out fr.c_w	Outb'd Spoiler Hinge Loc. in/out fr.c_w
BOEING								
727-200	.76/.93	.23/.30	.14/.37	.09/.14	.79/.69	.48/.72	.16/.20	.65/.63
737-100	.74/.94	.20/.28	.40/.66	.14/.18	.66/.67	none	none	none
737-300	.72/.91	.23/.30	.38/.64	0.14	.64/.70	none	none	none
747-200B	.70/.95	.11/.17	.46/.67	.12/.16	0.71	none	none	none
747-SP	.70/.95	.11/.17	.46/.67	.12/.16	0.71	none	none	none
757-200	.76/.97	.22/.36	.41/.74	.12/.13	.73/.69	none	none	none
767-200	.76/.98	.16/.15	.16/.31	.09/.11	.85/.78	.44/.67	.12/.17	.74/.71
McDONNELL-DOUGLAS								
DC-9 S80	.64/.85	.31/.36	.35/.60	.10/.08	.69/.65	none	none	none
DC-9-50	.78/.95	.30/.35	.35/.60	.10/.08	.69/.65	none	none	none
DC-10-30	.75/.93	.29/.27	.17/.30	.05/.06	.78/.74	.43/.72	.11/.16	.75/.70
AIRBUS								
A300-B4	.83/.99	.32/.30	.57/.79	.16/.22	.73/.72	none	none	none
A310	none	none	.62/.83	.16/.22	.69/.66	none	none	none
Lockheed L1011								
-500	.77/.98	.26/.22	.13/.39	.05/.12	.82/.73	.50/.74	.14/.14	.67/.67
Fokker F-28								
-4000	.66/.91	.29/.28	no lateral control spoilers					
Rombac/British Aerospace								
1-11 495	.72/.92	0.26	.37/.68	.06/.11	.68/.63	none	none	none
British Aerospace								
146-200	.78/1.0	.33/.31	.14/.70	.23/.27	.76/.68	none	none	none
Tu-154	.76/.98	.34/.27	.43/.70	.14/.20	.62/.60	none	none	none

Figure 4.15: *Spoilers geometry according to Roskam II, cited by Scholz [1]*

Table 4.2 defines the relative sizes of **Figure 4.15** being the inboard spoiler the one closest to the fuselage and the outboard closest to wing tip, all in terms of fraction of semi-span ($b/2$) and of mean wing chord $\bar{c}_W$.

Table 4.2: *Relative sizes of spoilers for L-1011*

Spoiler data	Values
Inboard spoiler span (% $b/2$)	0,39
Inboard spoiler chord (% $\bar{c}_W$)	0,08
Inboard Spoiler Hinge Location (% $\bar{c}_W$)	0,12

Outboard Spoiler Span (% $b/2$)	0,5
Outboard Spoiler Chord (% $\bar{c}_w$)	0,14
Outboard Spoiler Hinge Location (% $\bar{c}_w$)	0,14

5 Wing high-lift systems

In order to perform the analysis of the high-lift devices installed on the wing, different graphs computed by PreSTo are used as it helps to understand why the data was chosen.

5.1 Maximum lift coefficient

First, the leading sharpness parameter (Δy) needs to be studied as the maximum lift coefficient depends on this parameter and it also follows **Equation 5.1** according to DATCOM 1978 [].

$$c_{L,max,clean} = (c_{L,max})_{base} + \Delta_1 c_{L,max} + \Delta_2 c_{L,max} + \Delta_3 c_{L,max} \quad (5.1)$$

$(c_{L,max})_{base}$: maximum lift coefficient for non cambered airfoil.

$\Delta_1 c_{L,max}$: term that corrects taking into account the airfoil camber and the position of maximum camber at 0,3.

$\Delta_2 c_{L,max}$: correction term for taking into account a position of maximum thickness different to 0,3.

$\Delta_3 c_{L,max}$: term that corrects including Reynolds number different to $9 \cdot 10^6$.

Table 5.1: *Leading sharpness parameter according to DATCOM 1978, cited on Scholz [1]*

Profile type	Δy
NACA 4 digit	$26 \cdot (\frac{t}{c})$
NACA 63 series	$22 \cdot (\frac{t}{c})$
NACA 64 series	$21{,}3 \cdot (\frac{t}{c})$
NACA 65 series	$19{,}3 \cdot (\frac{t}{c})$
NACA 66 series	$18{,}3 \cdot (\frac{t}{c})$

$$\Delta y = 22 \cdot (\frac{t}{c}) \tag{5.2}$$

The final value for a NACA 63 series profile airfoil selected is Δy=2,2%.

Using data provided on **Figure 4.7** the position for maximum thickness of the airfoil is $\frac{x_t}{c} = 0,35$.

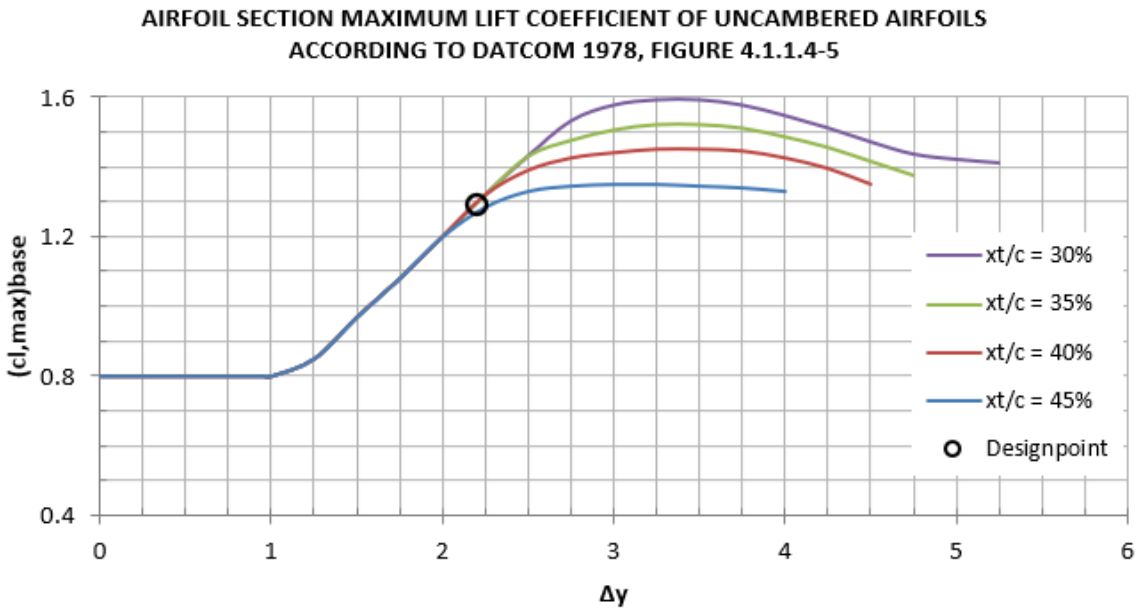

Figure 5.1: *First correction for non cambered airfoils according to DATCOM*

$(c_{L,max})_{base} = 1,295$.

The maximum camber and it's position is also found on **Figure 4.7**, being $\frac{(y_c)_{max}}{c} = 0,01$ and $x_{(yc)max} = 0,5$ respectively.

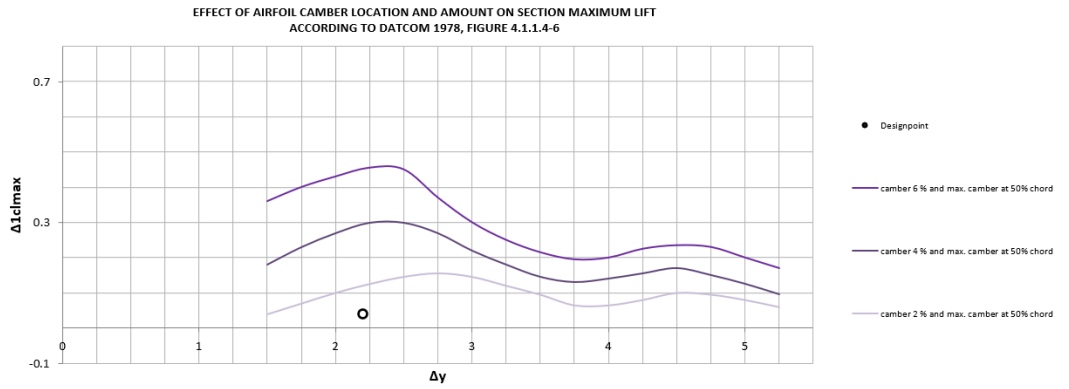

Figure 5.2: *First airfoil maximum lift coefficient correction according to DATCOM*

$\Delta_1 c_{L,max} = 0,041.$

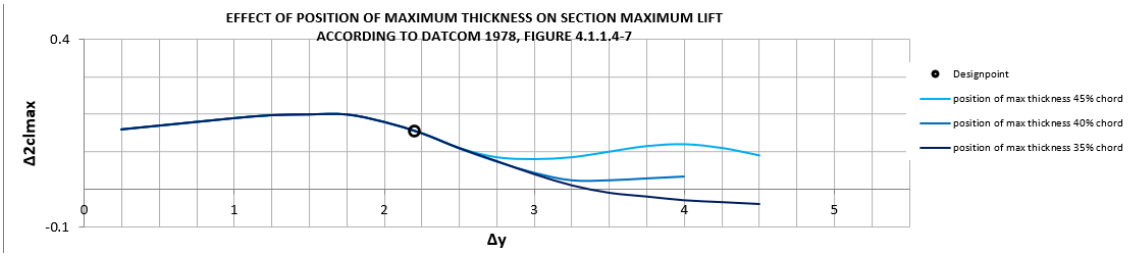

Figure 5.3: *Second airfoil maximum lift coefficient correction according to DATCOM*

$\Delta_2 c_{L,max} = 0,1546.$

The Reynolds number:

$$Re = \frac{\rho_0 \cdot c_{MAC} \cdot V_{APP}}{\mu} \tag{5.3}$$

ρ_0: density at ground level with a value of $1,255\ kg/m^3$.

μ: dynamic viscosity of $17,89 \cdot 10^{-6}\ kg/m \cdot s$.

$Re = 38,82 \cdot 10^6$.

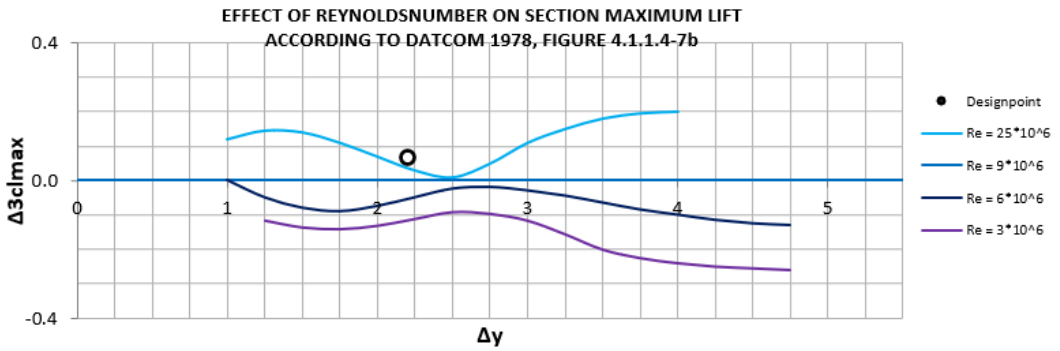

Figure 5.4: *Third airfoil maximum lift coefficient correction according to DATCOM*

$\Delta_3 c_{L,max} = 0,067.$

Being $c_{L,max,clean} = 1,633.$

An extra correction can be made for the Mach number, using **Equation 5.4** with the maximum lift coefficient calculated ($c_{L,max,clean}$) on 5.1:

$$C_{L,max,clean} = \left(\frac{C_{L,max}}{c_{l,max}}\right) \cdot c_{L,max,clean} + \Delta c_{L,max} \tag{5.4}$$

$\frac{C_{L,max}}{c_{l,max}}$: relation between maximum lift coefficient of the wing and a section of the wing.

$\Delta c_{L,max}$: Mach number correction.

From the next figures the data is extracted.

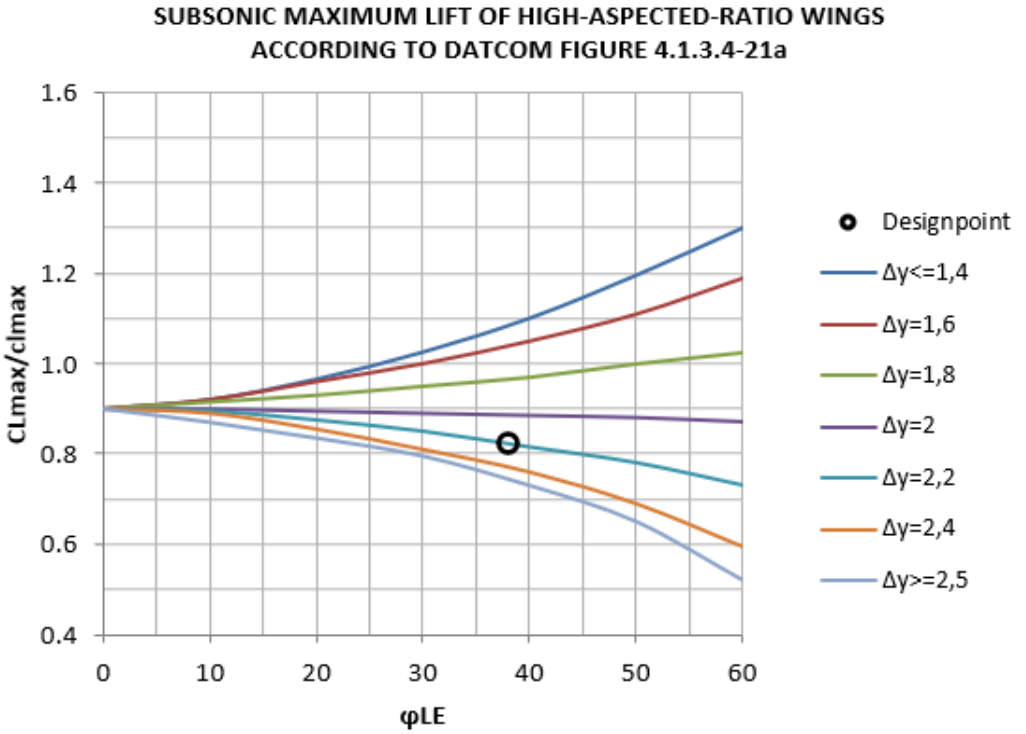

Figure 5.5: *Relation between airfoil maximum lift coefficients according to DATCOM*

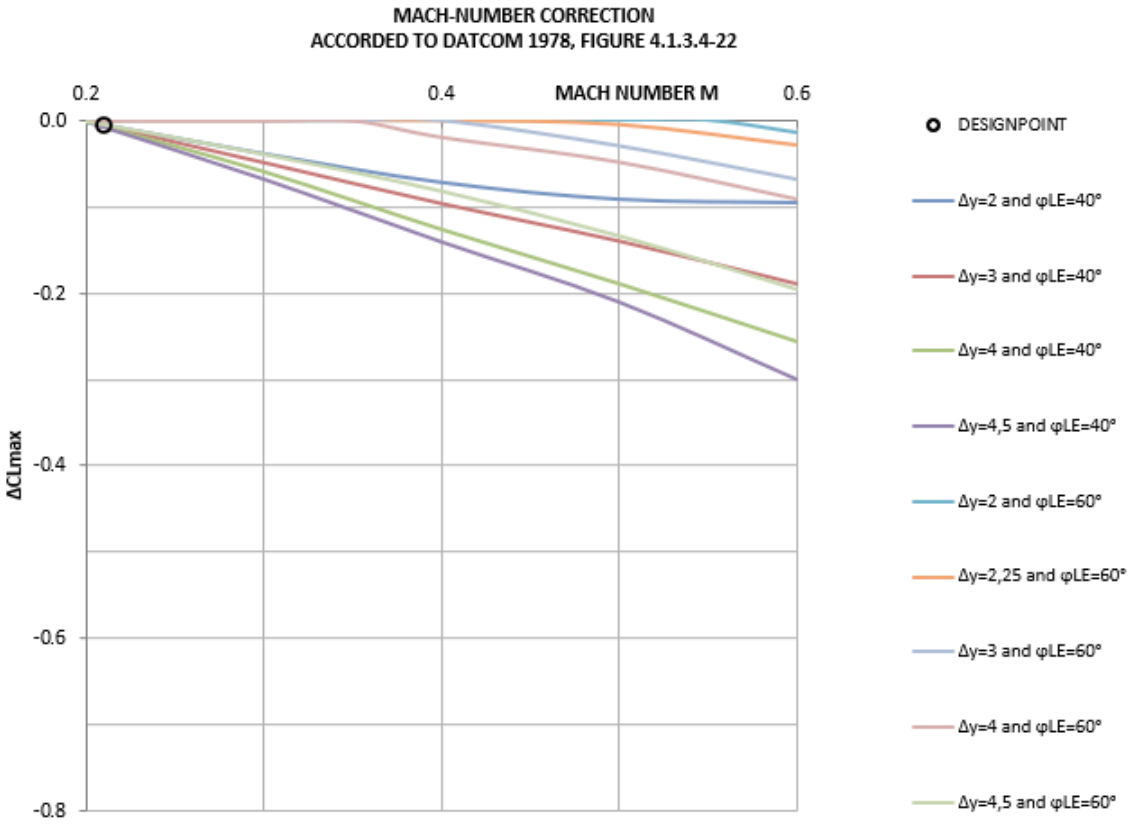

Figure 5.6: *Mach number correction for the airfoil maximum lift coefficient by DATCOM*

In **Figure 5.5** the leading edge sweep angle used on the X-axis is calculated with PreSTo.

Outer wing leading edge sweep angle	$\varphi_{LE,o}$	38.04	[°]
Outer wing sweep angle at 50 % chord	$\varphi_{50,o}$	31.72	[°]
Outer wing trailing edge sweep angle	$\varphi_{TE,o}$	24.40	[°]
Inner wing leading edge sweep angle	$\varphi_{LE,i}$	38.04	[°]
Inner wing sweep angle at 50 % chord	$\varphi_{50,i}$	28.08	[°]
Inner wing trailing edge sweep angle	$\varphi_{TE,i}$	15.89	[°]

Figure 5.7: *Sweep angles calculated with PreSTo*

Being $\varphi_{LE} = 38,04$ º the selected value to find $\frac{C_{L,max}}{c_{l,max}} = 0,823$.

From **Figure 5.6** the approach Mach number used was calculated with **Equation 5.5**:

$$M_{APP} = \frac{V_{APP}}{a} \tag{5.5}$$

$a = 340,29\ m/s$: speed of sound.

$M_{APP} = 0,21$.

$\Delta c_{L,max} = -\ 0,004$.

With all the variables calculated, the clean maximum lift coefficient of the wing is $C_{L,max,clean} = 1,341$ which gives an accurate approximation of the real value.

By using this method it is confirmed that $A > \frac{8}{3 \cdot cos\varphi_{25}}$ according to DATCOM 1978, cited in Scholz [1] as $6,97 > 3,3$.

5.2 Flaps and slats system

According to Elsevier [4] the L-1011 used fowler type flaps which have a slot between the wing and the device. When extended, the wing area is increased and with that also the lift becomes greater being very useful for take-off procedures.

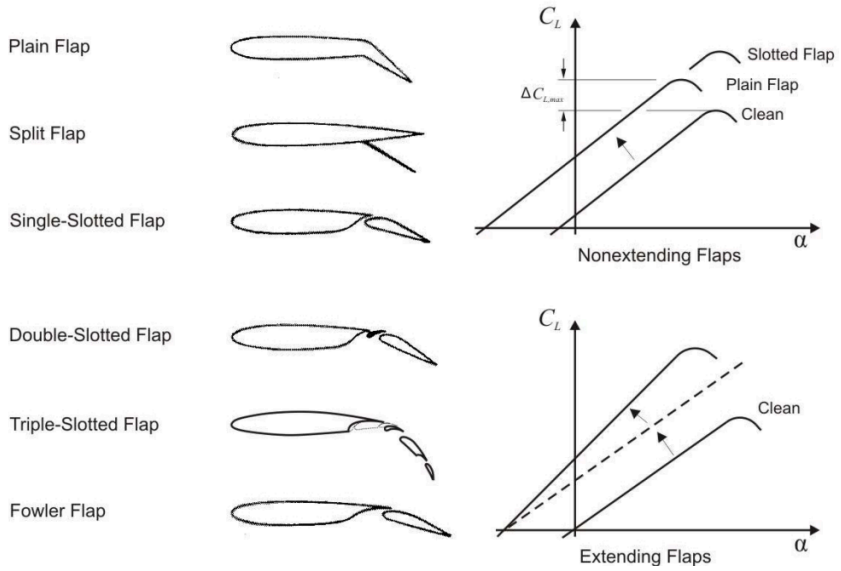

Figure 5.8: *Trailing edge flaps provided by DATCOM 1978, cited in Scholz [1]*

The configuration of the leading edge flaps (SLATS) of the wing stands as it follows, providing as well as the flaps an increase on camber and wing area :

minimum root span		0.1245 [-]				
relative slat root span	$\eta_{r,LED/b}$	0.14 [-]	→	slat root span	$Y_{r,LED}$	3.33 [m]
relative slat tip span	$\eta_{t,LED/b}$	0.98 [-]	→	slat tip span	$Y_{t,LED}$	23.28 [m]
leading edge device to chord ratio	$c_{LED/c}$	0.25 [-]	→	inner wing hinge line sweep angle	$\varphi_{HL,LED,i}$	33.34 [°]
			→	outer wing hinge line sweep angle	$\varphi_{HL,LED,o}$	35.00 [°]
					Sw,S,i	89.35 [m²]
					Sw,S,o	153.51 [m²]
				affected area	Sw,S	242.86 [m²]

Figure 5.9: *SLAT configuration on PreSTo.*

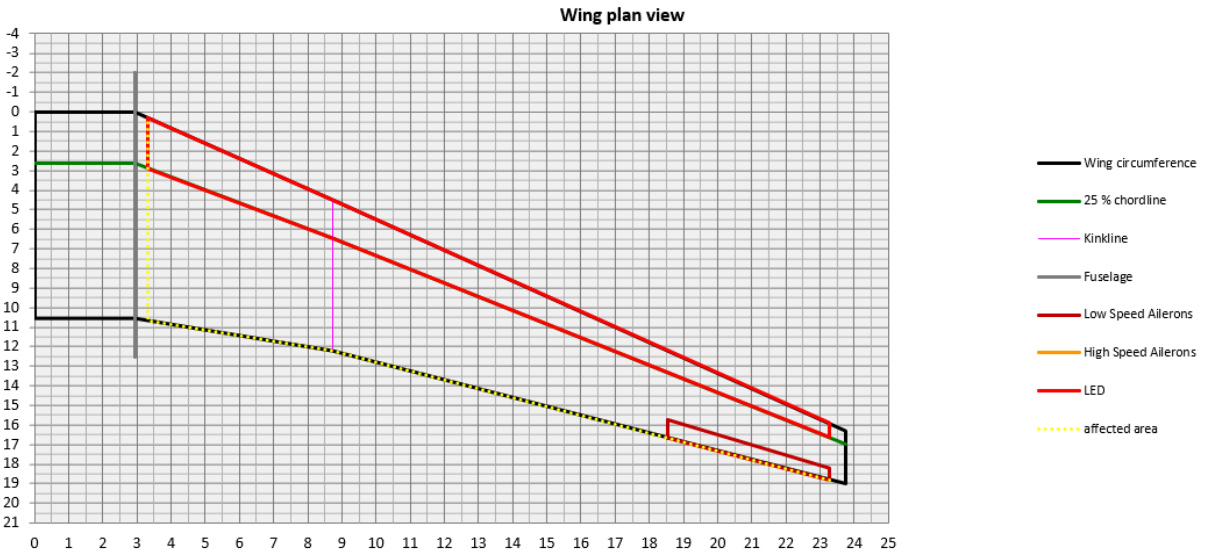

Figure 5.10: *Wing view with SLATS installed on PreSTo*

The geometry of the flaps has been sized to maximize the lift coefficient in order to meet the requirements.

inner Wing						
minimum relative root span		0.1245 [-]				
relative flap root span inner Wing	$\eta_{r,flap,i/b}$	0.15 [-]	→	flap root span inner Wing	$Y_{r,flap,i}$	3.56 [m]
maximum relative tip span		0.0000 [-]				
relative flap tip span inner Wing	$\eta_{t,flap,i/b}$	0.3 [-]	→	flap tip span inner Wing	$Y_{t,flap,i}$	7.13 [m]
mid Wing						
minimum relative root span		0.0000 [-]				
relative flap root span mid Wing	$\eta_{r,flap,m/b}$	0.3 [-]	→	flap root span mid Wing	$Y_{r,flap,m}$	7.13 [m]
maximum relative tip span		0.7800 [-]				
relative flap tip span mid Wing	$\eta_{r,flap,m/b}$	0.78 [-]	→	flap tip span mid Wing	$Y_{r,flap,m}$	18.53 [m]
outer Wing						
minimum relative root span		0.9800 [-]				
relative flap root span outer Wing	$\eta_{r,flap,o/b}$	0 [-]	→	flap root span outer Wing	$Y_{r,flap,o}$	0.00 [m]
relative flap tip span outer Wing	$\eta_{t,flap,o/b}$	0 [-]	→	flap tip span outer Wing	$Y_{t,flap,o}$	0.00 [m]
flap-chord	$c_{flap/c}$	0.3 [-]	→	inner wing hinge line sweep angle	$\Phi_{HL,flap,i}$	23.46 [°]
			→	outer wing hinge line sweep angle	$\Phi_{HL,flap,o}$	28.91 [°]
					Sw,f,i	84.09 [m²]
					Sw,f,o	118.64 [m²]
				area affected by trailing edge device	Sw,f	202.73 [m²]

Figure 5.11: *Configuration of the wing flaps determined on PreSTo*

According to images of the L-1011, the dimensions of the slats and flaps are very similar in terms of span and chord distribution to the real ones.

Figure 5.12: *Wing flaps geometry computed on PreSTo*

The increase on the available lift due to high-lift devices is concreted in order to know if it's bigger than the required lift coefficient.

$$\Delta C_{L,max,High-lift} = 0,95 \cdot \Delta C_{L,max,f} + \Delta C_{L,max,s} \tag{5.6}$$

$\Delta C_{L,max,f}$: increase on lift coefficient due to flaps devices

$$\Delta c_{L,max,f} = k_1 \cdot k_2 \cdot k_3 \cdot (\Delta c_{l,max})_{base} \tag{5.7}$$

k_1: flap chord correction factor.

k_2: flap angle correction factor.

k_3: flap-motion correction factor.

$(\Delta c_{l,max})_{base}$: increase of airfoil section maximum lift coefficient due to a trailing edge device with 25 % of chord and reference deflection.

$\Delta C_{L,max,s}$: increase in lift coefficient due to slats devices.

$$\Delta c_{L,max,s} = c_{l,\delta,max} \cdot \eta_{max} \cdot \eta_{\delta} \cdot \delta_{f,LED} \cdot \frac{c'}{c} \tag{5.8}$$

$c_{l,\delta,max}$: theoretical maximum lifting effectiveness of LED (Leading Edge Device).

η_{max}: empirical factor regarding leading edge radius divided by thickness ratio (r/t).

η_{δ}: empirical factor regarding deflection angle.

$\delta_{f,LED}$: deflection angle between chord line and half of the extended chord due to LED.

$\frac{c'}{c}$: ratio of area enlargement due to slats extension.

Usually, the chord of the flap extends till the 30% of the wing's chord, and for this project the same methodology was established, giving the flap chord correction.

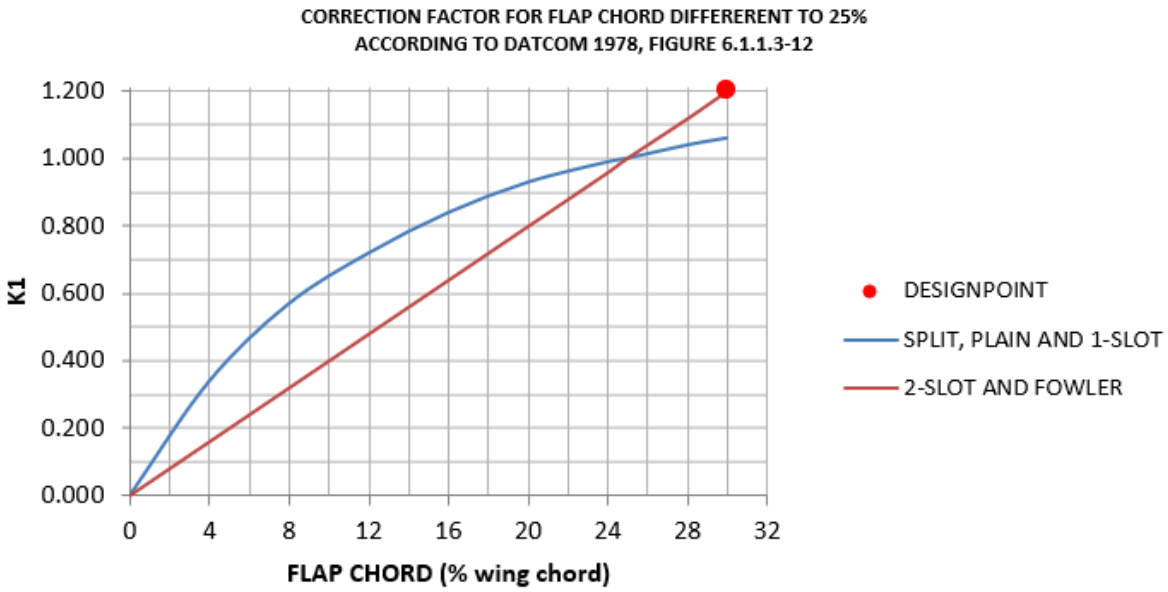

Figure 5.13: *K1 correction computed on PreSTo*

$k_1 = 1,201.$

$\frac{c_{flap}}{c} = 0,3.$

In order to find K_2 and k_3, the maximum possible deflection angle has been chosen with fowler flaps selected.

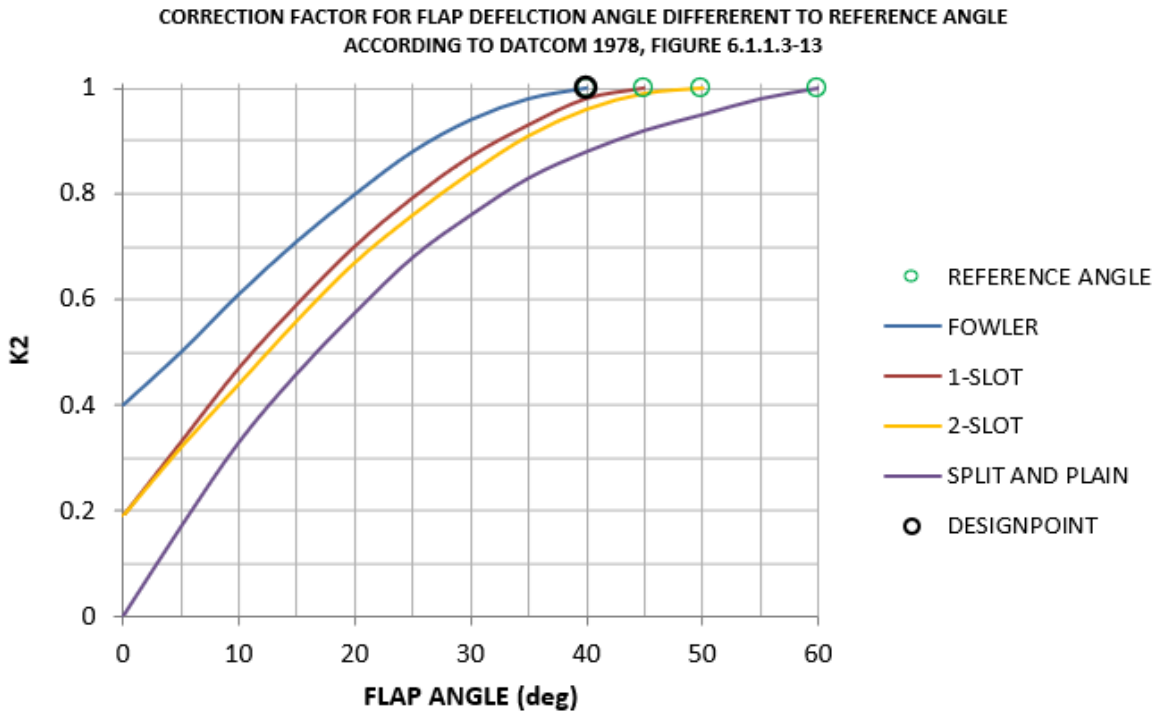

Figure 5.14: *K2 correction computed on PreSTo*

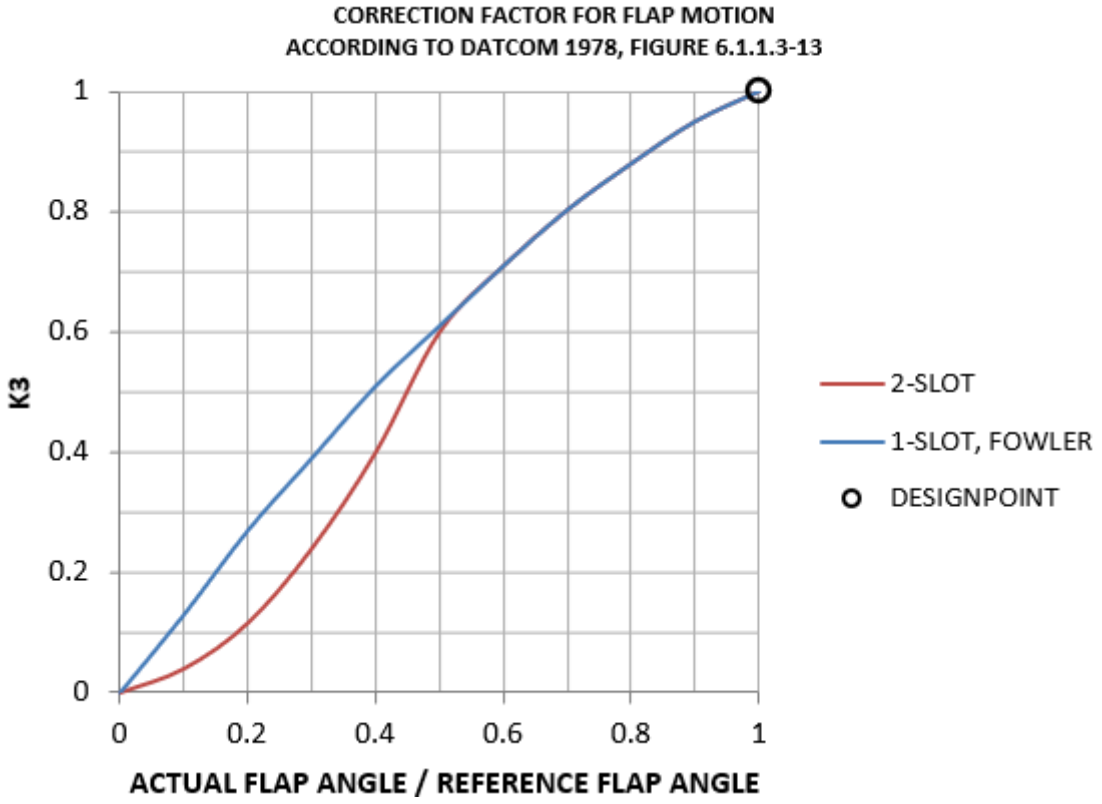

Figure 5.15: *K3 correction computed on PreSTo*

$k_2 = 1,0.$

$\delta_f = 40$ º.

$k_3 = 1,0.$

Actual flap angle (δ_f)/Reference flap angle (δ_{ref}) $= 1,0.$

Extracting the data form the airfoil on **Figure 4.7**, the thickness was stated to a value of 10% which helps to extract $(\Delta c_{l,max})_{base}$.

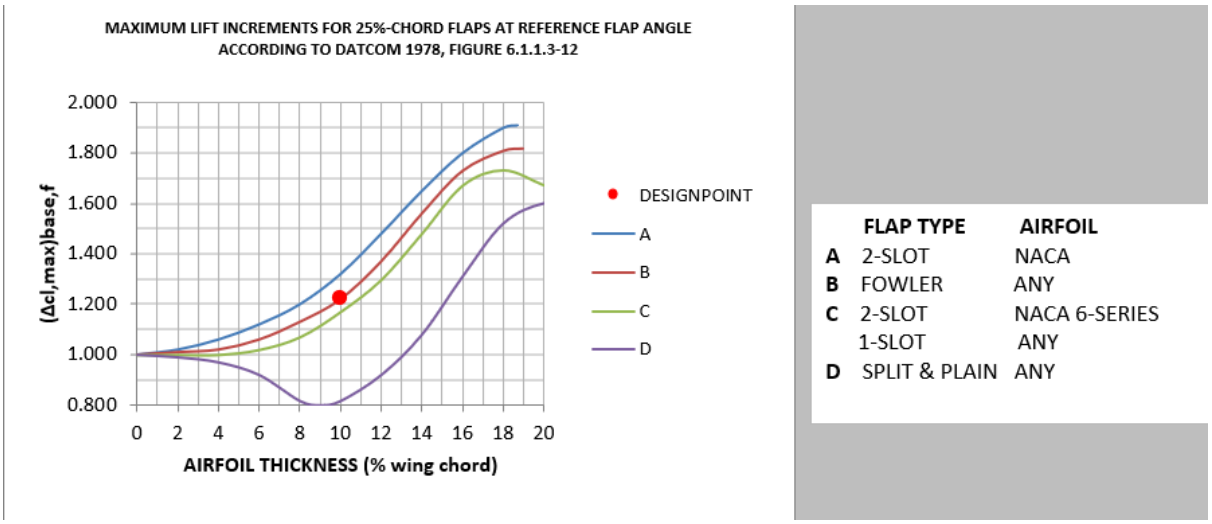

Figure 5.16: $(\Delta c_{l,max})_{base}$ *calculation computed on PreSTo*

$(\Delta c_{l,max})_{base} = 1,224.$

Another factor is taking into account according to Raymer 1992, cited in Scholz [1]:

$$\Delta C_{L,max,s} = \Delta c_{l,max,s} \cdot \frac{S_{W,s,i}}{S_{W,s,o}} \cdot cos(\varphi_{H.L}) \tag{5.9}$$

$\frac{S_{W,s,i}}{S_{W,s,o}}$: relation between affected areas of the wing from **Figure 5.9** with value of 0,56.

$\varphi_{H.L}$: Hingeline sweep angle, from **Figure 5.9.**

In case of the high-lift increase for the slats regarding **Equation 5.8**:

To find the maximum lift effectiveness ($c_{l,\delta,max}$), LED chord to wing chord ratio was computed on **Figure 5.9** following the geometry of real L-1011 wings.

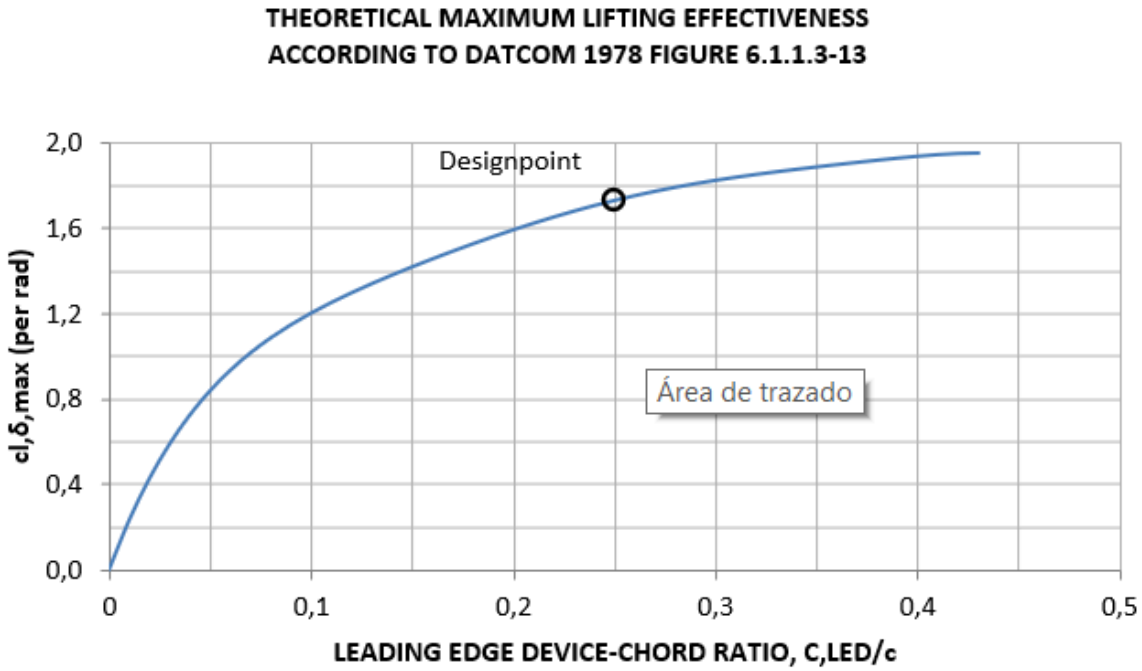

Figure 5.17: *$c_{l,\delta,max}$ computation on PreSTo*

$cl_{\delta,\,max} = 1,736\ 1/rad.$

$c_f/c = 0,25.$

The empirical factors (η_{max}, η_δ) are found knowing the leading edge radius over thickness ratio (r/t) and the deflection angle $\delta_{f,LED}$ (accordingly a value of 20º leads to a high increase in lift coefficient respect to other values).

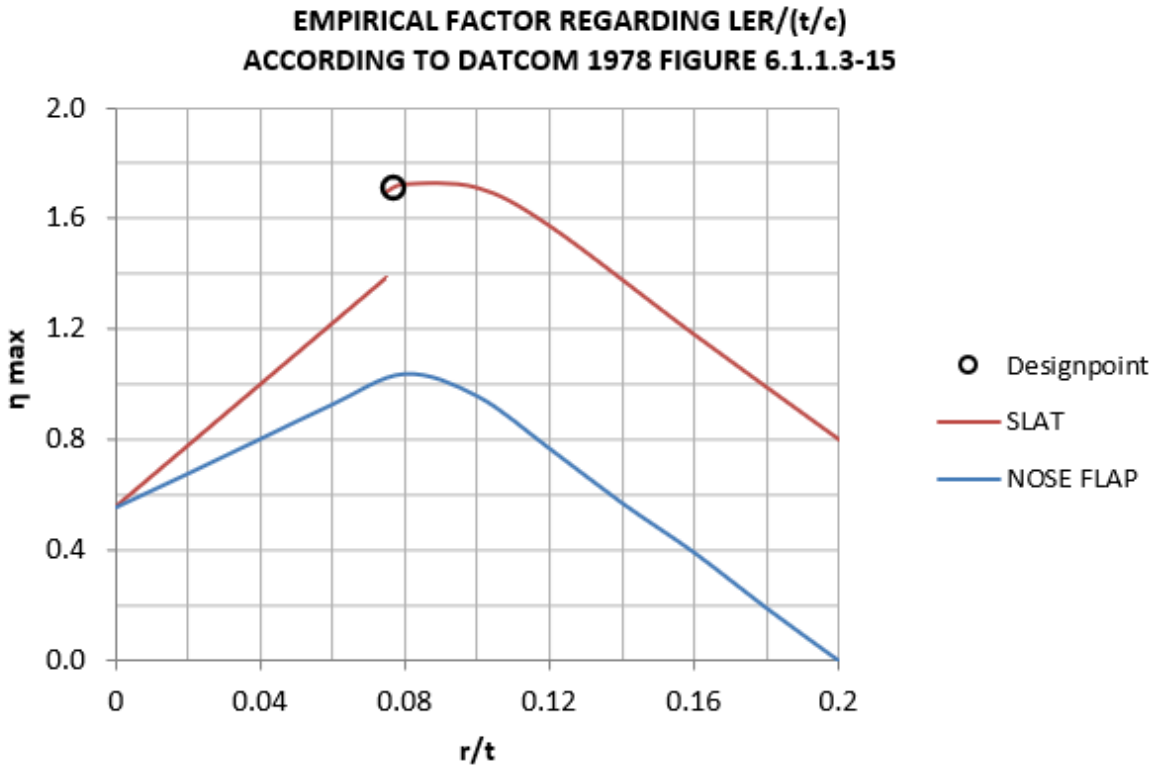

Figure 5.18: η_{max} *computation on PreSTo*

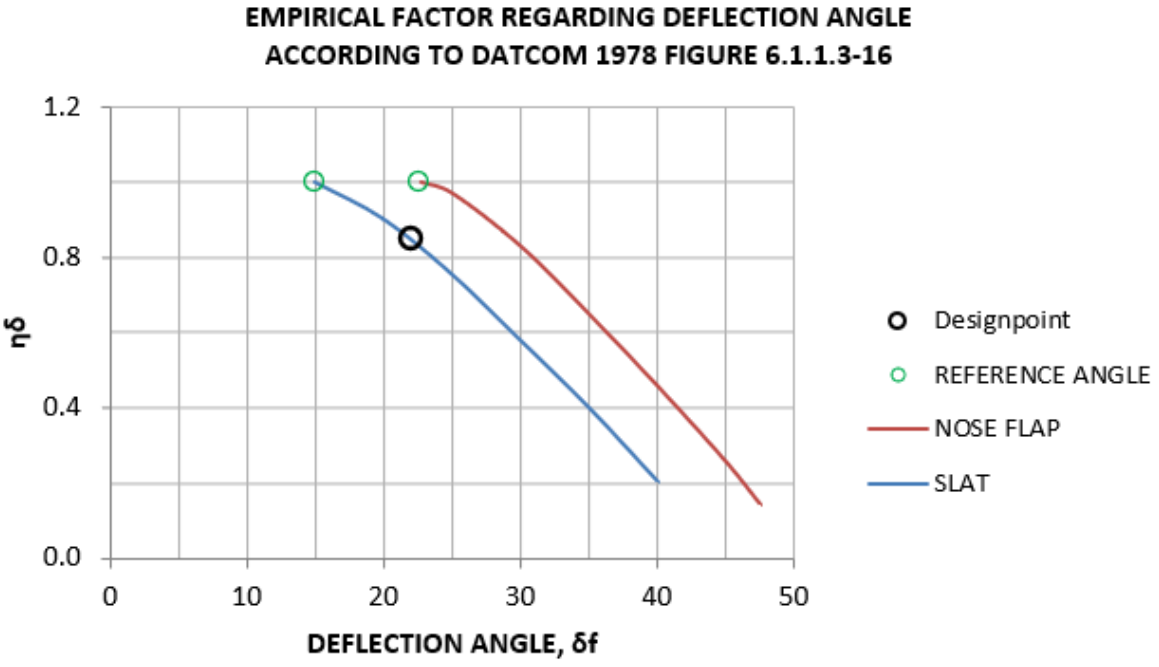

Figure 5.19: η_{δ} *computation on PreSTo*

$\eta_{max} =$ 1, 708 with an r/t= 0, 077 according to the data of the airfoil.

$\eta_{\delta} = 0,848$ with $\delta_{f,LED} = 22º$.
The final enlargement do to the usage of slats is computed using PreSTo [] following the data of the airfoil, with a value of $\frac{c'}{c} = 1,1$ extending the chord.

As well as for the slats, the **Equation 5.10** is used to have a more detailed approach of the flaps increasing on the lift coefficient:

$$\Delta C_{L,max,f} = \Delta c_{l,max,f} \cdot \frac{S_{W,f}}{S_W} \cdot K_{\Lambda} \tag{5.10}$$

$\frac{S_{W,f}}{S_W}$: From **Figure 5.11** the affected area is divided in the inner and outer parts, with a summed value of 0,6257.

K_{Λ}: Sweep angle correction computed on PreSTo[] with values of 0,825 for the inner part and 0,815 for the outer part using the sweep angles at 25% of the chord.

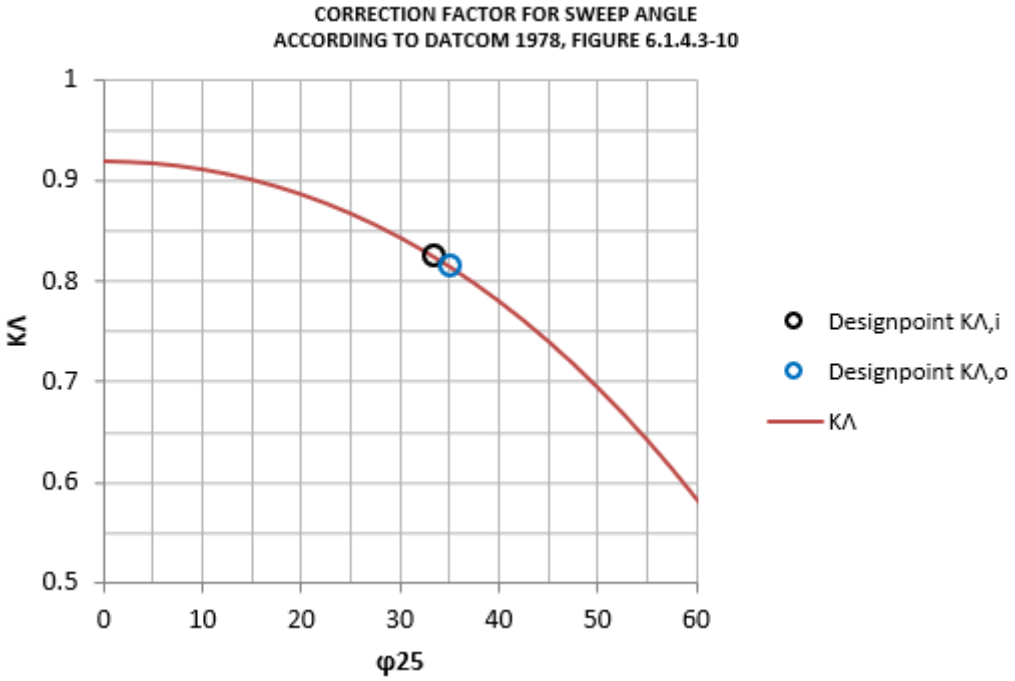

Figure 5.20: *K_{Λ} determination computed on PreSTo*

Finally, the increase due to high-lift devices is:

$\Delta c_{l,max,s} = 1,065.$

$\Delta c_{l,max,f} = 1,47.$

After corrections from DATCOM 1978 and Raymer:

$\Delta C_{L,max,f} = 0,933.$

$\Delta C_{L,max,s} = 0,8013.$

Being $\Delta C_{L,max,High-lift} = 1,688$, and the required increase of lift coefficient is calculated using an increase of maximum coefficient in landing knowing it's the biggest demand for the aircraft and taking out the clean maximum lift coefficient as is the lift only provoked by the wing with flaps retracted.

$$\Delta C_{L,max,required} = 1,1 \cdot C_{L,max,L} - C_{L,max,clean} \tag{5.11}$$

Computing all the values, $\Delta C_{L,max,High-lift} > \Delta C_{L,max,required}$ as $1,688 > 1,684$ meeting the requirements.

The final view of the wing computed and the one drawn on the technical profile is compared on the next figure, knowing that the program extends the slats to the chord line, so with more detailed measures the slats could be of the same size on the inner board and on the outer.

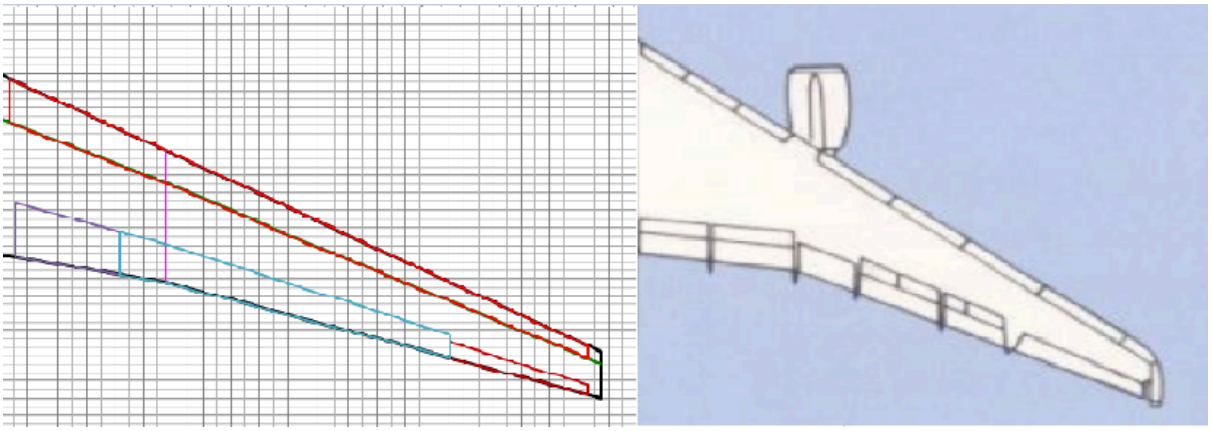

Figure 5.21: *Final wing comparison.*

6 Tail design I

There are two components to the tail assembly design (Tail Design I & II). The so-called tail assembly volume is used to estimate the tail assembly dimensions. The aircraft's mass and center of gravity can be determined using this initial tail assembly size estimate. Following the determination of the mass and center of gravity of the separate aircraft parts the possible relative eros can be estimated in order to detail the design.
Since tail assembly essentially works similarly to (small) wings, many of the relationships that govern wing design also apply to tail assembly. The aircraft's stability, controllability, and trim are all aided and an extended center of gravity range is achievable with the use of a THS (trimmable horizontal stabilizer) computed on PreSTo .

The L-1011 had a particularity different from the aircrafts of that age, the tail is all-moving meaning that the incidence angle can be changed during flight being more effective but also heavier. The main function is to create a moment around the lateral axis, different from the wing ailerons which create a roll moment around the longitudinal axis.

6.1 Horizontal tail geometry

The tailplane has a conventional configuration with a lever arm (l_H) of 17,7 meters according to Elsevier [4] which is the distance between the aerodynamic center of the wing and horizontal tailplane.

Type	Horizontal Tailplane		Vertical Tailplane	
	A	λ	A	λ
Conventional Tail	3.00 ... 5.00	0.3 ... 0.6	1.3 ... 2.0	0.3 ... 0.6
T-Tail	as Conventional Tail	as Conventional Tail	0.7 ... 1.2	0.6 ... 1.0

Figure 6.1: *Typical values for aspect and taper ratios according to Raymer 1989, cited in Scholz [1]*

Type	Dihedral Angle Γ [°]	Incidence Angle i_h [°]	Aspect Ratio A_h [-]	Sweep Angle φ [°]	Taper Ratio λ_h [-]
Business Jets	- 4 ... 9	-3.5 fixed	3.2 ... 6.3	0 ... 35	0.32 ... 0.57
Transport Jets	0 ... 11	variable	3.4 ... 6.1	18 ... 37	0.27 ... 0.62
Fighters	-23 ... 5	0 fixed or variable	2.3 ... 5.8	0 ... 55	0.16 ... 1.00
Supersonic Civil Transport	-15 ... 0	0 fixed or variable	1.8 ... 2.6	32 ... 60	0.14 ... 0.39

Figure 6.2: *Typical values according to Roskam II, cited in Scholz [1]*

The surface of the horizontal tail can be computed according to Scholz [1]:

$$C_H = \frac{S_H \cdot l_H}{S_W \cdot c_{MAC}} \tag{6.1}$$

S_H: Horizontal tail surface

From PreSTo tool, the value for the horizontal tail volume coefficient (C_H) is settled to 0,875 which is a normal value for general transport jets.

$S_H = 123,58\ m^2$

From Elsevier [4] the aspect ratio chosen (A_H) is 4,03 and the sweep angle at 25% of the chord is $\varphi_{25} = 35$ º as the wing angle. The taper ratio (λ_H) is set to 0,31 with a dihedral and incidence angles of 8 º and $-$ 2 º respectively, according to **Figure 6.1** and **Figure 6.2** the values are inside the range for transport jets.

Following PreSTo 4.3.2 simulations the relative thickness of the horizontal tail is $(\frac{t}{c})_H = 0,095$.

The span of the horizontal tail:

$$b_H = \sqrt{A_H \cdot S_H} \tag{6.2}$$

$b_H = 23,11\ m$

Following the same methodology as for the wing, the same airfoil has been chosen (NACA 63-210 series) knowing that its relative thickness is 0, 1 being very similar to the one calculated with simulations.

6.2 Elevator

One of the most important control surfaces on an aircraft's horizontal tail, or horizontal stabilizer, is the elevator. It permits the nose to move up or down by regulating the aircraft's pitch. The elevator deflects upward when the pilot pulls back on the stick or control yoke, which causes the tail to experience a downward aerodynamic force. The airplane climbs as a result of this force raising the nose.

During flight, the elevator is essential for preserving and modifying the aircraft's altitude.

Looking at examples of L-1011 tails and knowing that typically the elevator covers till the tip with a chord of 25%-40% of the tail, with deflections of maximum 25 º downwards and 35 º upwards. The sketch of the tailplane shows the elevator installed on the horizontal tail (red area) together with the 25 % chord line (yellow) and the MAC span point (red dot).

Figure 6.3: *Horizontal tail and elevator by PreSTo*

6.3 Vertical tail

The upright surface at the back of an airplane (located just in the middle of the rear engine) that stabilizes the yaw axis, which governs side-to-side motion, is known as the vertical tail or vertical stabilizer. Maintaining the aircraft's alignment with its flight path and avoiding unintended side sliding are its primary duties. The vertical tail helps the aircraft retain directional stability which helps for controlled flying, particularly during turns.

Following the horizontal stabilizer analysis, the vertical tail surface and important data has been selected taking data from Elsevier [4] with an elevator arm of 20,6 meters.

$$C_V = \frac{S_V \cdot l_V}{S_W \cdot b} \tag{6.3}$$

$C_V = 0,079$ contrasted with data from PreSTo and typical values.

$S_V = 59,04\ m^2$ with a span of $b_V = 10,65\ m$ using 6.2 for vertical tail

The aspect ratio (A_V) and sweep angle ($\varphi_{25,V}$) are 1,92 and 35 º.

Taper ratio is 0, 29, while dihedral angle is 90 º and incidence angle is null, according to **Figure 6.4**.

Type	Dihedral Angle v [°]	Incidence Angle i_h [°]	Aspect Ratio A_h [-]	Sweep Angle φ [°]	Taper Tratio λ_h [-]
Business Jets	90	0	0.8 … 1.6	28 … 55	0.30 … 0.74
Transport Jets	90	0	0.7 … 2.0	33 … 53	0.26 … 0.73
Fighters	75 … 90	0	0.4 … 2.0	9 … 60	0.19 … 0.57
Supersonic Cruise Airplanes	75 … 90	0	0.5 … 1.8	37 … 65	0.20 … 0.43

Figure 6.4: *Vertical tail data from Roskam II, cited in Scholz [1]*

After checking that all data is inside the range, the airfoil selected again is NACA 63-210 following the same results as for the horizontal tail.

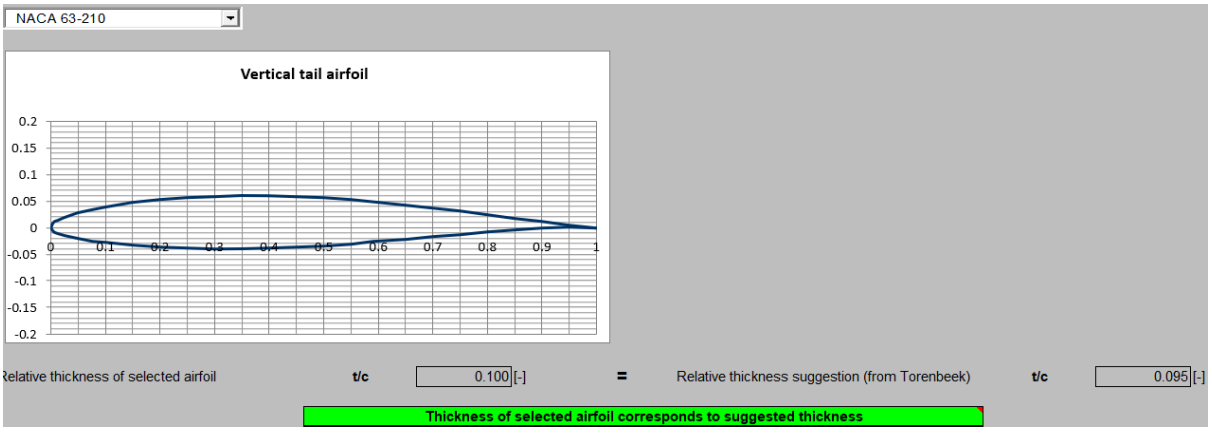

Figure 6.5: *Airfoil for vertical tail computed on PreSTo*

6.4 Rudder

A movable control surface that is fastened to an aircraft's vertical tail is called a rudder. It regulates the aircraft's nose's side-to-side movement, or yaw motion. The nose turns when the rudder deflects to the left or right, producing a horizontal aerodynamic force that pulls the tail in the opposite direction. The rudder is used by

pilots to coordinate turns, adjust for adverse yaw, and maintain directional control, particularly when taking off and landing in crosswinds or when aircraft are experiencing asymmetric thrust.
Typically the rudder covers 90 % of the total vertical tail with a maximum deflection of 35 º and a chord of 30 % respect to the chord of tail. The modelage and resulting geometry was used with this data.

Chordwise distribution			
Raymer: Chordwise distribution suggestion	c_R/c	All-moving	[-]
Chordwise distribution	c_R/c	0.30	[-]
Root chord span			
Raymer: Root chord span suggestion		All-moving	[-]
Root chord span	$Y_{r.R}/b_V$	0.05	[-]
Tip chord span			
Raymer: Tip chord span suggestion		All-moving	[-]
Tip chord span	$Y_{t.R}/b_V$	0.95	[-]

Figure 6.6: *Geometry of rudder for vertical tail computed on PreSTo*

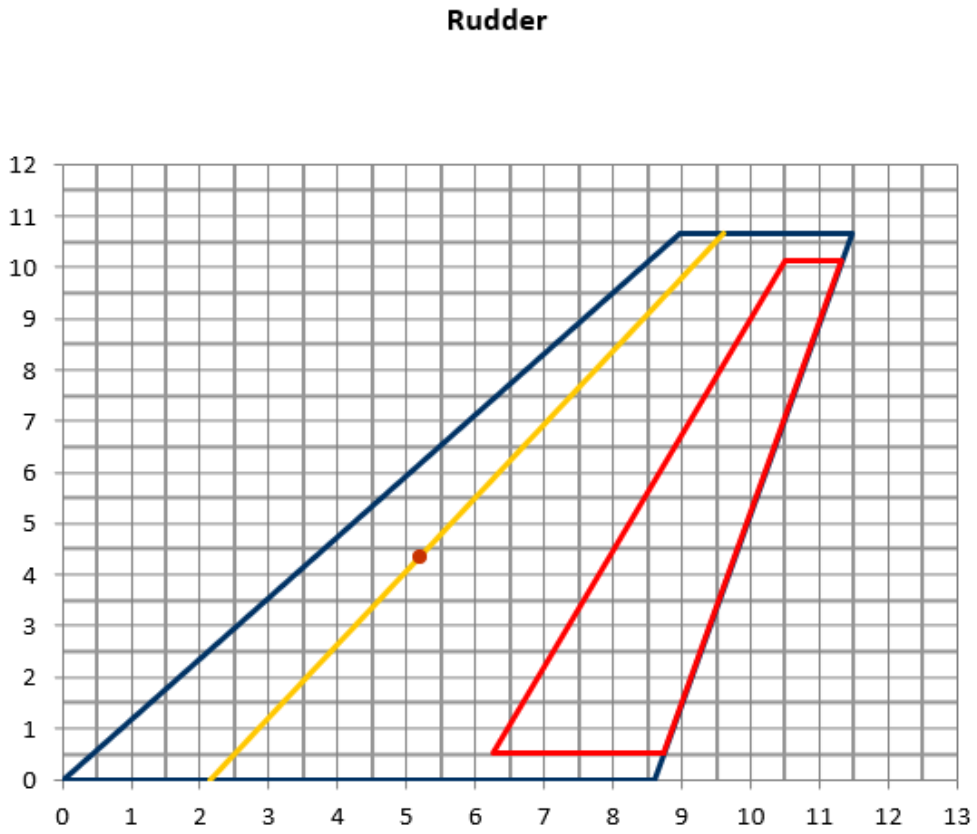

Figure 6.7: *Rudder for vertical tail drawn on PreSTo*

In order to prevent an event of stalling or spinning, the tail is crucial to make the aircraft recover from such situations where there pilots lose control and limits are surpassed. A simulation has been created on PreSTo showing the distances from root chords to tail positions showing that the vertical position is at a considerable distance from the fuselage as the diameter of the engine is considered.

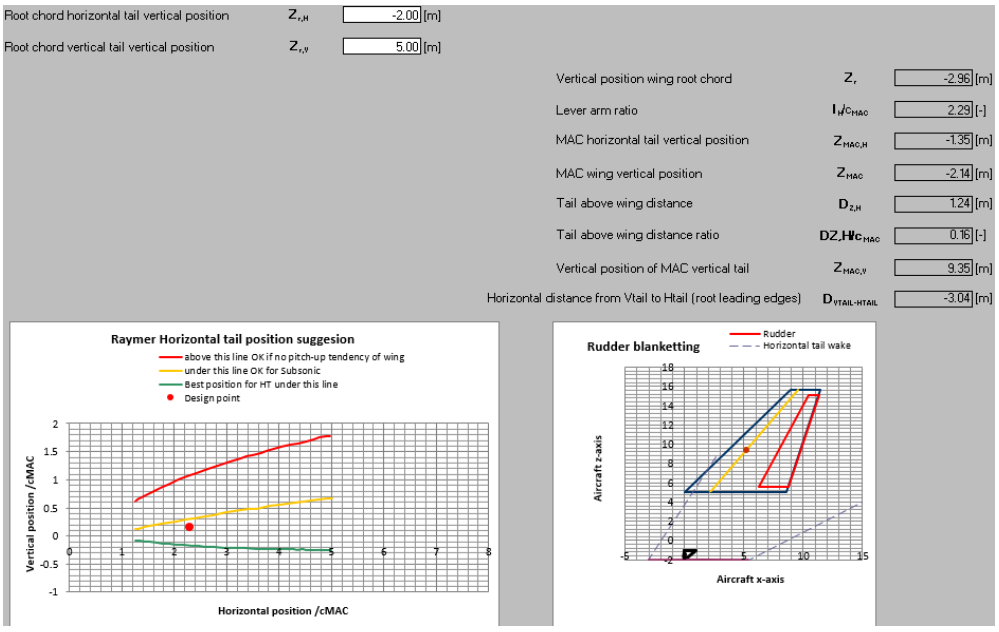

Figure 6.8: *Stall and spin recovery calculated and drawn on PreSTo*

7 Mass and center of gravity

In this section a further analysis of the masses and the definition of the CG (center of gravity) is realized using three different methods, being the first one the less accurate and the last one a Class II measurement which will be used for the last sections making this a top-priority configuration in the aeronautic industry.

7.1 Class I: Roskam V

This method provides a forecast of the mass breakdown according to Roskam V, cited by Scholz [1], the required input is the operating empty mass (m_{OE}) computed on the preliminary sizing and a model of an aircraft that is similar to the L-1011 in terms of dimensions and certifications.

The aircraft with more similar characteristics is as mentioned in previous sections the McDonnell Douglas DC-10, which is used by PreSTo 4.3.2 to compute the relative mass breakdowns that compound the operating empty mass in order to find the different masses of the aircraft.

Table 7.1 shows the relative mass breakdown from each component of the aircraft used from Appendix A of Roskam V used to calculate the masses in **Figure 7.1**.

The final operating empty mass (m_{OE}) has been calculated summing all the masses which are multiplied by the relative mass breakdowns (r_{group}) of the model aircraft used as an example with the operating empty mass of the preliminary sizing of the L-1011.

Table 7.1: *Class I calculations of mass groups*

Relative mass groups	Values	Final weights ($r_{group} \cdot m_{OE}$)
Wing (r_W)	0,18459	20812 kg
Fuselage (r_F)	0,21864	24652 kg
Tail (r_T)	0,05197	5860 kg
Landing gear (r_{LG})	0,07168	8083 kg
Nacelle (r_N)	0,02688	3031 kg

Structure (r_S)	0,55556	62639 kg
Power plant (r_{PP})	0,15233	17175 kg
Fixed equipment (r_{FE})	0,29391	33138 kg

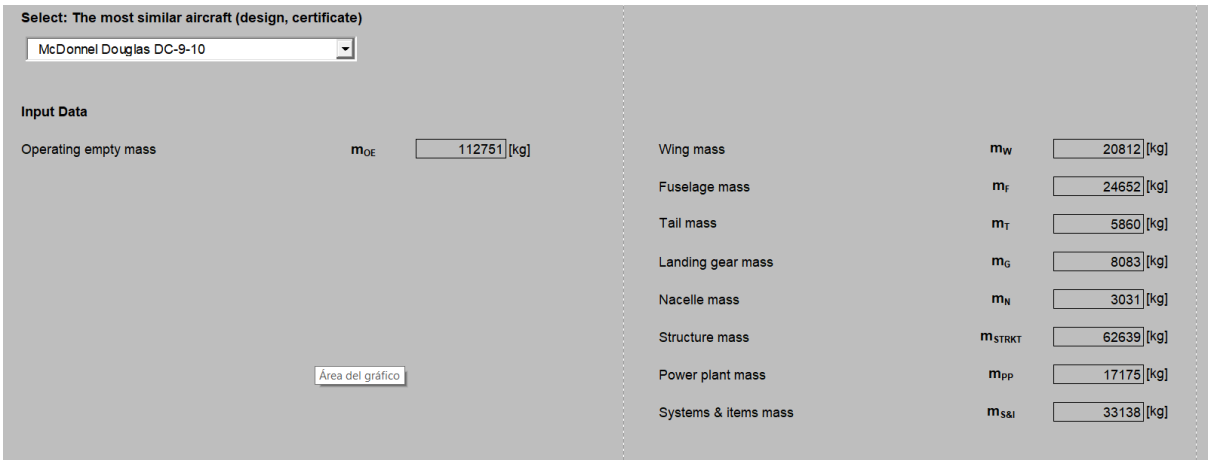

Figure 7.1: *Mass breakdown Class I used on PreSTo*

Summing all values the maximum operating empty mass is $m_{OE} = 175390\ kg$.

The final maximum take-off mass calculated with this method, using the payload and fuel mass calculated in the preliminary sizing:

$$m_{TO} = m_{OE} + m_{PL} + m_F \tag{7.1}$$

$m_{TO} = 275417\ kg$.

As the method is not precise, another Class I analysis is performed to analyze the data.

7.2 Class I: RAYMER 89

This method is also based on the usage of different factors to calculate mass groups, but in this case data is provided directly from RAYMER 89, cited by Scholz [1]..

The wetted and exposed surfaces of the aircraft will be calculated as they are the ones in contact with the airflow and will be multiplied by the factors to find the weights of the aircraft.

	Factors		Selected:		
	Transport	Business	Transport		
k1	74.61	34.53	74.61	kg/m²	wing
k2	20.27	11.5	20.27	kg/m²	fuselage
k3	43.45	17.03	43.45	kg/m²	horizontal tail
k4	31.42	12.52	31.42	kg/m²	vertical tail
k5	0.006	0.006	0.006	-	nose gear
k6	0.033	0.029	0.033	-	main gear
k7	1.45	1.32	1.45	-	power plan
k8	0.161	0.19	0.161	-	systems
kx	1.143	1.0923	1.143	-	operational empty

Figure 7.2: *Factors used on Class I computed for PreSTo*

The exposed area of the wing is simply calculated extracting the fuselage from the total wing area:

$$S_{exp,W} = S_W - S_F \tag{7.2}$$

$S_{exp,W} = 261,59\ m^2$.

According to Scholz [1] the following wetted areas are calculated:

$$S_{wet,W} = 2 \cdot S_{exp,W} \cdot (1 + 0,25 \cdot (\frac{t}{c})_r \cdot \frac{1+\tau \cdot \lambda}{1+\lambda}) \tag{7.3}$$

$S_{wet,W} = 537,36\ m^2$.

$$S_{wet,F} = \pi \cdot d_f \cdot l_f \cdot (1 - \frac{2}{\lambda_f})^{2/3} \cdot (1 + \frac{1}{\lambda_f^{\,2}}) \tag{7.3}$$

$\lambda_f = 8,125$: fuselage fineness ratio, dividing the length and diameter of the fuselage.

$S_{wet,F} = 751,77\ m^2$.

Accordingly, $S_{exp,H} = 0,8 \cdot S_H = 98,86\ m^2$ and $S_{exp,V} = S_V = 59,04\ m^2$.

Following DataHammami [5], the weight of the engines is set to $4449,74\ kg$ each one, corresponding to a mass of $m_E = 3 \cdot 4449,74 = 13349,22\ kg$.

As for the previous phase, **Figure 7.3** shows the final mass of the groups calculated showing the operating empty mas (m_{OE}) calculated with this method multiplying the factor with the preliminar maximum take-off mass (m_{TO}) computed on preliminary sizing.

Wing exposed area	$S_{exp,W}$	261.59 [m²]	Wing mass	m_W	19517 [kg]
Fuselage outer diameter	$d_{f,o}$	5.92 [m]			
Fuselage length	$l_{Fuselage}$	48.10 [m]	Fuselage wetted area	$S_{wet,F}$	751.77 [m²]
			Fuselage mass	m_F	15238 [kg]
Exposed area, horizontal tail	$S_{exp,H}$	98.86 [m²]	Horizontal tail mass	m_{HT}	4296 [kg]
Exposed area, vertical tail	$S_{exp,V}$	59.04 [m²]	Vertical tail mass	m_{VT}	1855 [kg]
Max. take-off mass	m_{MTO}	211375 [kg]	Nose gear mass	m_{GN}	1268 [kg]
			Main gear mass	m_{GM}	6975 [kg]
			Nacelle mass	m_N	0 [kg]
			Structure mass	m_{STRKT}	49150 [kg]
Engine mass suggestion	m_E	22715 [kg]			
Engine mass	m_E	13349 [kg]	Power plant mass	m_{PP}	19356 [kg]
			Systems & items mass	$m_{S\&I}$	34031 [kg]
			Operation Empty Weight	m_{OE}	117201 [kg]

Figure 7.3: *Final weights of Class I (Raymer) computed for PreSTo*

Using **Equation 7.1**, $m_{TO} = 217228\ kg$ being a value more exact than the one computed on the first method comparing weights with preliminary sizing.

7.3 Class II: Torenbeek 88

This method is the most precise, as an iteration will be carried at the end in order to have a relative error for the maximum take-off mass of less than 0,5 %. First, the weights of the mass groups such as wing, fuselage, horizontal stabilizer, vertical stabilizer, landing gear, engine nacelle, installed engines, and systems are estimated using experimental formulas and the input value for the maximum takeoff mass from the preliminary sizing.

Following the equations provided by Scholz [1], every mass will be calculated precisely till the maximum operating empty mass is calculated summing all weights and therefore, the maximum take-off mass.

The structural span:

$$b_s = \frac{b}{cos\varphi_{50,o}} \tag{7.4}$$

$\varphi_{50,0} = 31,72$ º: outer wing sweep angle at 50 % chord according to PreSTo 4.3.2.

Outer wing leading edge sweep angle	$\varphi_{LE,o}$	38.04	[°]
Outer wing sweep angle at 50 % chord	$\varphi_{50,o}$	31.72	[°]
Outer wing trailing edge sweep angle	$\varphi_{TE,o}$	24.40	[°]
Inner wing leading edge sweep angle	$\varphi_{LE,i}$	38.04	[°]
Inner wing sweep angle at 50 % chord	$\varphi_{50,i}$	28.08	[°]
Inner wing trailing edge sweep angle	$\varphi_{TE,i}$	15.89	[°]

Figure 7.4: *Sweep angles computed on PreSTo*

$b_s = 55,86\ m.$

The ultimate load factor:

$$n_{ult} = 1,5 \cdot n_{lim} \tag{7.5}$$

n_{lim}: limit load factor, according to Scholz [1] is set to $2,5$.

$n_{ult} = 3,75.$

The wing mass for aircraft with $m_{TO} \geq 5700\ kg$:

$$\frac{m_w}{m_{ZF}} = 6,67 \cdot 10^{-3} \cdot b_S^{\,0,75} \cdot \left(1 + \sqrt{\frac{b_{ref}}{b_s}}\right) \cdot n_{ult}^{\,0,55} \cdot \left(\frac{b_s/t_r}{m_{ZF}/S_W}\right)^{0,3} \tag{7.6}$$

b_{ref}: reference value set to $1,905\ m$.

b_s/t_r: cantilever ratio set to 40.

The wing mass divided by maximum take-off mass is then $\frac{m_W}{m_{ZF}} = 0,156$.

Therefore multiplying by m_{ZF} the wing mass is found, $m_W = 22789,42\ kg$.

The fuselage mass:

$$m_F = 0,23 \cdot \sqrt{V_D \cdot \frac{I_H}{w_F + h_F}} \cdot S_{wet,F}^{1,2} \tag{7.7}$$

V_D: Dive speed calculated multiplying speed of sound and dive Mach (0,05 higher than M_{CR}) being the final value 268,78 m/s.

w_F: width of fuselage, $6,0\ m$.

h_F: height of the fuselage, $4,83\ m$.

$m_f = 13627,01\ kg$.

For the case of the tail:

$$m_H = k_H \cdot S_H \cdot \left(62 \cdot \frac{S_H^{0,2} \cdot V_D}{1000 \cdot \sqrt{cos\varphi_{H,50}}} - 2,5\right) \tag{7.8}$$

$$m_H = k_V \cdot S_V \cdot \left(62 \cdot \frac{S_V^{0,2} \cdot V_D}{1000 \cdot \sqrt{cos\varphi_{V,50}}} - 2,5\right) \tag{7.9}$$

k_H: horizontal tail constant set to 1,1 for trimmable tails.

$\varphi_{H,50}$: horizontal tail sweep angle for 50 % chord.

$\varphi_{H,50}$:vertical tail sweep angle for 50 % chord.

According to PreSTo 3.4.2:

Figure 7.5: *PreSTo 3.4.2 calculation of sweep angles for the tail at 50 % chord*

$$k_V = 1 + 0,15 \cdot \frac{S_H \cdot z_H}{S_V \cdot b_V} \tag{7.9}$$

z_H: distance from root of vertical airplane to where horizontal and vertical tails are attached with a null value.

$k_V = 1.$

$m_H = 5194\ kg.$

$m_V = 1911\ kg.$

The nose and main retractable landing gears:

$$m_{LG} = k_{LG} \cdot (A_{LG} + B_{LG} \cdot m_{TO}^{3/4} + C_{LG} \cdot m_{TO} + D_{LG} \cdot m_{TO}^{3/2}) \tag{7.10}$$

k_{LG}: constant, for low wing aircrafts is set to 1.

airplane type	gear type	gear component	A_{LG}	B_{LG}	C_{LG}	D_{LG}
jet trainers and business jets	retractable gear	main gear	15.0	0.033	0.0210	-
		nose gear	5.4	0.049	-	-
other civil types	fixed gear	main gear	9.1	0.082	0.0190	-
		nose gear	11.3	-	0.0024	-
		tail gear	4.1	-	0.0024	-
	retractable gear	main gear	18.1	0.131	0.0190	$2.23 \cdot 10^{-5}$
		nose gear	9.1	0.082	-	$2.97 \cdot 10^{-6}$
		tail gear	2.3	-	0.0031	-

Figure 7.6: *Constants for landing gear provided by Torenbeek 88, cited by Scholz [1]*

The constants chosen are for other types of aircrafts and with retractable gear, being $A_{LG,N} = 9,1,\ B_{LG,N} = 0,082,\ D_{LG,N} = 2,97 \cdot 10^{-6},\ A_{LG,M} = 18,1,\ B_{LG,M} = 0,131,\ C_{LG,M} = 0,019$ and $D_{LG,M} = 2,23 \cdot 10^{-5}$.

$m_{LG,N} = 1115\ kg.$

$m_{LG,M} = 7562\ kg.$

Summing both the landing gear mass is $m_{LG} = 8676\ kg.$

For turbo fans, the mass of the nacelle:

$$m_N = \frac{0{,}065 \cdot T_{TO}}{g} \tag{7.11}$$

$m_N = 3311\ kg.$

The mass of the engines:

$$m_{E,inst} = k_E \cdot k_{thr} \cdot n_E \cdot m_E \tag{7.12}$$

k_E: constant set to 1,15 for passenger aircrafts with nacelles.

k_{thr}: 1,18 for reverse thrust engines.

n_E: number of engines seto to 3 for the L-1011.

m_E: mass for one engine set to $4449,74\ kg$.

$m_{E,inst} = 18114,89\ kg.$

Mass of the systems:

$$m_{SYS} = k_{EQUIP} \cdot m_{TO} + 0,768 \cdot k_{F/C} \cdot m_{TO}^{2/3} \tag{7.13}$$

k_{EQUIP}: 0,11 for transport aircraft.

$k_{F/C}$: for transport aircraft with primary surface controls is set to 0, 88.

$m_{SYS} = 25856,9\ kg.$

The operating empty mass is calculated summing all values stated before:

$$m_{OE} = m_W + m_F + m_H + m_V + m_{LG} + m_N + m_{E,insi} \tag{7.14}$$

$m_{OE} = 99480,22\ kg.$

And with that, the $m_{TO} = 199507,22\ kg$ and if the relative error is calculated, that gives a difference of $10,48$ %. Therefore, an iteration must be carried out, changing the values of the maximum take-off mass at the very start to compute all mass groups again.

Table 7.2 shows the iterations and the relative error at the end.

Table 7.2: *Class II iterations for calculating maximum take-off mass*

Iteration number	m_{TO}	relative error(Δ%)
0	213140 kg	0 %
1	199507,22 kg	6,4 %
2	194920,94 kg	2,3 %
3	193616,12 kg	0,66 %
4	193246,75 kg	0,19 %

The maximum take-off mass selected is $m_{TO} = 193246,75\ kg$ giving a deviation of less than $0,5\%$ together with an operating empty mass of $m_{OE} = 93220\ kg$ and a zero fuel mass of $m_{ZF} = 112358\ kg$.

7.4 Center of gravity

The center of gravity (CG) of an aircraft is the place at which its complete weight is assumed to act, independent of orientation. It indicates the aircraft's balance point, which is critical for stability and control. If the CG is set too far front or aft, the aircraft may become unstable or uncontrolled. Designers ensure that the CG remains

within precise limitations throughout the flight, particularly when fuel burns and payload fluctuates.

The calculations are made dividing the fuselage from the wing to two different groups.

The center of gravity of the fuselage has been determined using PreSTo[] suggestion using a mean value between the minimum and maximum, which is between 20,2 and 21,65 meters respectively, at $X_{CG,f} = 20,92\,m$. For the systems of the aircraft the center is usually located at 40 %-50 % of the fuselage's length and for this case it will be located at 45 %, at $X_{CG,SYS} = 21,65\,m$.

The landing gear located on the nose has been calculated using sizes provided on **Figure 3.13** and adapted for the longitudinal length of this model, being $X_{CG,LG,N} = 8,01\,m$. Therefore, taking the wheelbase (distance from nose to main landing gears) provided by Elsevier [4] adapted to this aircraft (21,33 meters) and adding the distance from nose to landing gear already calculated before, $X_{CG,LG,M} = 29,34\,m$.

The installed engines on the wing were computed with distance settled to $X_{CG,E,INST} = 20,20\,m$ according to Scholz [1], using a 42 % distance of the total fuselage, as the distance from nose to edge of nacelle is $\Delta LE_E = 18,124\,m$.

The center of gravity for the nacelle has been determined as it's located at 40 % of the length of the engine (5,19 meters according to Wikipedia [10]), and knowing the spanwise location (43,6 % of fuselage length) according to Elsevier [4], $X_{CG,N} = 19,24\,m$.

To find the center of gravity for the wing and tail, the LEMAC (Leading Edge of MAC) has to be defined in order to compute the values on PreSTo.

Firstly, an initial LEMAC is set to $X_{LEMAC} = 23,7\,m$ as it will help find the distance to the wing with PreSTo.

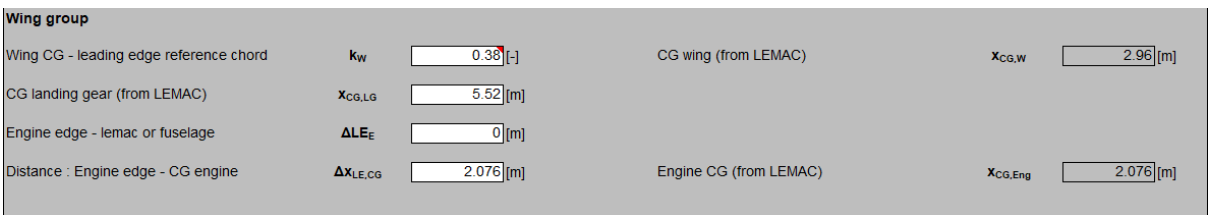

Figure 7.7: *Wing distances compute on PreSTo*

Therefore the center of gravity of the wing is:

$$X_{WG} = X_{LEMAC} - X_{WG,LEMAC} \tag{7.15}$$

$X_{WG} = 20,74\ m.$

From the requirements, the distance from the center of gravity to LEMAC is found at 25 % of the MAC chord.

$$\Delta x_{CG,LEMAC} = 0,25 \cdot c_{MAC} \tag{7.16}$$

$X_{CG,LEMAC} = 1,9289\ m.$

Knowing this, the calculation of the LEMAC is performed.

$$X_{LEMAC} = X_{FG} - X_{CG,LEMAC} + \frac{m_{WG}}{m_{FG}} \cdot (X_{WGG,LEMAC} - X_{CG,LEMAC}) \tag{7.17}$$

X_{FG}: center of gravity of the total fuselage group set to $24,55\ m$.

$X_{WGG,LEMAC}$: distance from center of gravity of wing group to LEMAC, set to $2,71\ m$.

$X_{LEMAC} = 24,25\ m.$

Accordingly, the center of gravity of the wing is $X_{WG} = 27,21\ m$ and the distance to the tail is calculated on PreSTo.

CG Tail	$x_{CG,T}$	46.6671141 [m]				
For Raymer89 and Torenbeek 88 method						
Lemac Vtail	$LEMAC_{VT}$	43.8013424 [m]	CG Vtail	$x_{CG,VT}$	44.44 [m]	
Lemac Htail	$LEMAC_{HT}$	40.76008 [m]	CG Htail	$x_{CG,HT}$	43.14 [m]	

Figure 7.8: *Tail distances compute on PreSTo*

Two tables have been created showing the values of the different mass groups of 4th iteration calculated before (used from now on for the next steps), the center of gravity of the different sections, splitting the fuselage and wing group.

Table 7.3: *Fuselage group masses and center of gravity*

Fuselage group	m	X_{CG}	$m \cdot X_{CG}$
m_f	13627,01 kg	20,9235 m	285124,74 $kg \cdot m^2$
m_{SYS}	23560 kg	21,645 m	509956,2 $kg \cdot m^2$
m_H	5194 kg	43,14 m	224069,16 $kg \cdot m^2$
m_V	1911 kg	44,44 m	84924,84 $kg \cdot m^2$
$m_{LG,N}$	1019 kg	8,01 m	8162,19 $kg \cdot m^2$
m_{FG}	45311,01 kg	24,55 m	1112251 $kg \cdot m^2$

Table 7.4: *Wing group masses and center of gravity*

Wing group	m	X_{CG}	$m \cdot X_{CG}$
m_W	36803,60 kg	26,71 m	983024,16 $kg \cdot m^2$
$m_{LG,M}$	8080 kg	29,34 m	237067,2 $kg \cdot m^2$
m_N	3311 kg	19,24 m	63703,64 $kg \cdot m^2$
$m_{E,inst}$	20753,96 kg	20,202 m	419271,5 $kg \cdot m^2$
m_{WG}	68948,56 kg	24,32 m	1703066,5 $kg \cdot m^2$

The final $X_{CG,PLANE}$ is computed:

Results

Distance CG - LEMAC	$\Delta x_{CG,LEMAC}$	1.92888568 [m]	CG Fuselage section	$x_{CG,Fs}$	24.56 [m]
			CG wing section (from LEMAC)	$x_{CG,Ws}$	3.00 [m]
			Position of LEMAC	x_{LEMAC}	24.25 [m]
			Wing group mass	$m_{w,group}$	68949 [kg]
			Fuselage group mass	$m_{F,group}$	45311 [kg]
			CG Plane	$x_{CG,Moe}$	26.18 [m]

Figure 7.9: *Results on PreSTo*

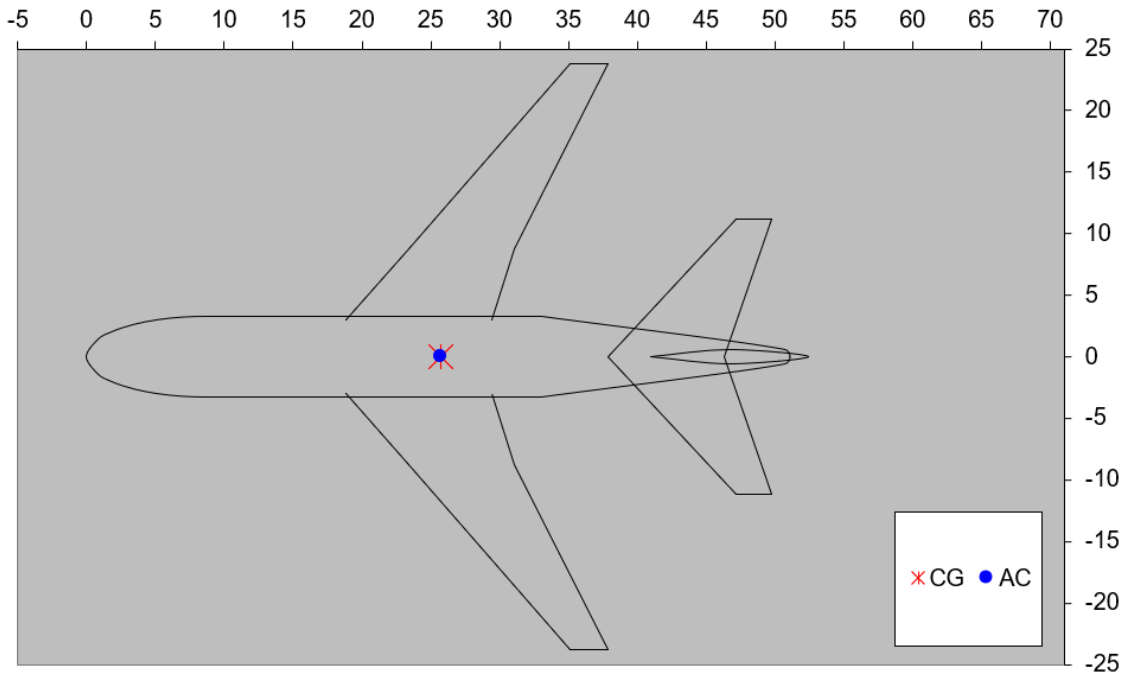

Figure 7.10: *Sketch of the aircraft on PreSTo*

8 Tail design II

After the analysis of masses and the preliminar empennage designing a new detailed examination of the tails is done calculating again the surface areas of both horizontal and vertical tail using the PreSTo tool.

8.1 Horizontal tail

In order to maintain the stability of the aircraft, the next values are computed using the tool.

			Wing lift gradient (landing condition)	$C_{L,\alpha,W}$	4.25 [1/rad]
			HTP lift gradient (landing condition)	$C_{L,\alpha,H}$	3.63 [1/rad]
Aspect ratio coefficient	k_A	0.11 [-]			
Taper ratio coefficient	k_λ	1.32 [-]			
HTP location coeficient	k_h	1.07 [-]			
Wing lift gradient (M=0)	$C_{L,\alpha,W}$	4.20 [1/rad]	Downwash gradient	$\delta\varepsilon/\delta\alpha$	0.43 [-]
			Gradient of natural stability curve	a	0.9875 [-]

Figure 8.1: *HT data computed on PreSTo*

The control of the aircraft also depends on the horizontal tail, and using the V-diagram performance will help to give a value for the horizontal tail surface. The permissible center of gravity ranges are located between the straight lines representing the controllability (red) and stability requirements, with the minimum stability also included (pink).

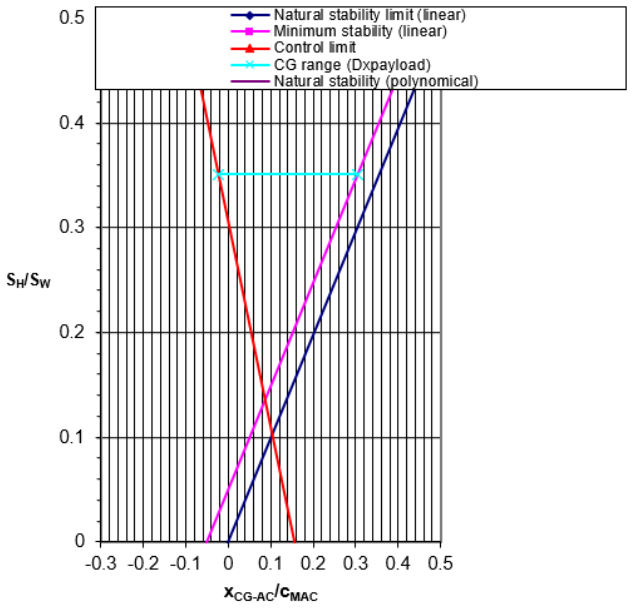

Figure 8.2: *V diagram computed on PreSTo*

As it can be extracted from the graph, the ratio between the horizontal tailplane area and the wing area is 0,35 which gives **Equation 8.1**.

$$\frac{S_H}{S_W} = \frac{C_L}{C_{L,H} \cdot \eta_H \cdot \frac{l_H}{c_{MAC}}} \cdot \overline{x_{CG-AC}} + \frac{C_{M,W} + C_{M,E}}{C_{L,H} \cdot \eta_H \cdot \frac{l_H}{c_{MAC}}} \tag{8.1}$$

The data left to define is found on 8.1 is computed on PreSTo[], with $\overline{x_{CG-AC}}$ being the slope of the V diagram.

Lift coefficent aircraft (landing condition)	C_L	2,03	[-]
Lift coefficent HTP	$C_{L,H}$	-0,5	[-]
Dynamic pressure ratio	η_H	0,9	[-]
Gradient of control limit curve	**a**	-1,9647	[-]

Figure 8.3: *HTP data computed on PreSTo*

The final horizontal surface is $S_H = 113,74\ m^2$ and comparing with the first $S_H = 123,58\ m^2$ the deviation is less than 10% (7, 96 %) meeting the requirements.

The sizes and geometry computed on the first tail design is again calculated with the new surface area.

$I_H = 19,23\ m.$

$b_H = 21,41\ m.$

Sweep, leading edge	$\varphi_{LE,V}$	40.15	[°]
Sweep, 50 % chord line	$\varphi_{50,V}$	22.47	[°]
Sweep, trailing edge	$\varphi_{TE,V}$	15.12	[°]
Effective drag divergence Mach number (VT)	$M_{DDeff,V}$	0.824	[-]

Figure 8.4: *HTP sweep angles and drag computed on PreSTo*

8.2 Vertical tail

In the case of the vertical tail, the same methodology is used and also applying some different corrections in order to select between two different new vertical tails, meeting the requirements.

Drag due to active engine	N_E	1349.19 [kN.m]				
Gap between engine and center line	y_E	8.10 [m]				
Drag due to inactive engine	N_D	337.30 [kN.m]	Total drag due to engines (active&inactive)	N_V	1686.49 [kN.m]	
			Dynamic pressure at minimum flying speed	q_{mc}	2000.53 [kg/(m*s²]	
			VTP rudder throw	δ_r	25.00 [°]	
			Empirical correction for lift effectiveness of plain f	$c_{L,\delta}/(c_{L,\delta})_{theory}$	0.88 [-]	
			Theoretical Lift effectiveness of plain flaps	$(c_{L,\delta})_{theory}$	4.45 [-]	
			Empirical correction factor for effectiveness of plain flaps @δ_r=25	K'	0.70 [-]	
			Taper ratio correction factor	K_λ	0.81 [-]	
			VTP area	S_V	41.99 [m²]	

Figure 8.5: *VTP area for control requirements computed on PreSTo*

			Yawing moment coefficient due to sideslip	$C_{N,\beta}$	0.0571 [1/rad]	
Parameter for wing-fuselage interference	k_N	0.0016 [-]				
Parameter for Reynolds number function of fusela	$k_{R,l}$	2.07 [-]				
Reynolds number	Re	2.11E+08 [-]	Fuselage yawing moment coefficient due to sides	$C_{N,\beta,F}$	-0.1670 [1/rad]	
VTP lift gradient (landing condition)	$C_{L,\alpha,H}$	2.48 [1/rad]	VTP side force coefficient due to sideslip	$C_{y,\beta,V}$	-2.48 [1/rad]	
			Wing yawing moment coefficient due to sideslip	$C_{N,\beta,W}$	0.0235 [1/rad]	
			Ratio between VTP area and wing area	S_V/S_W	0.1863 [-]	
			VTP area	S_V	60.36 [m²]	

Figure 8.6: *VTP area for stability requirements with corrections computed on PreSTo*

The new area has an error of 2, 24 % which is acceptable, with a new lever arm of $l_V = 20, 15\ m$ and span of $b_V = 10, 77\ m$.

The final elevator and rudder are updated with the new sizes.

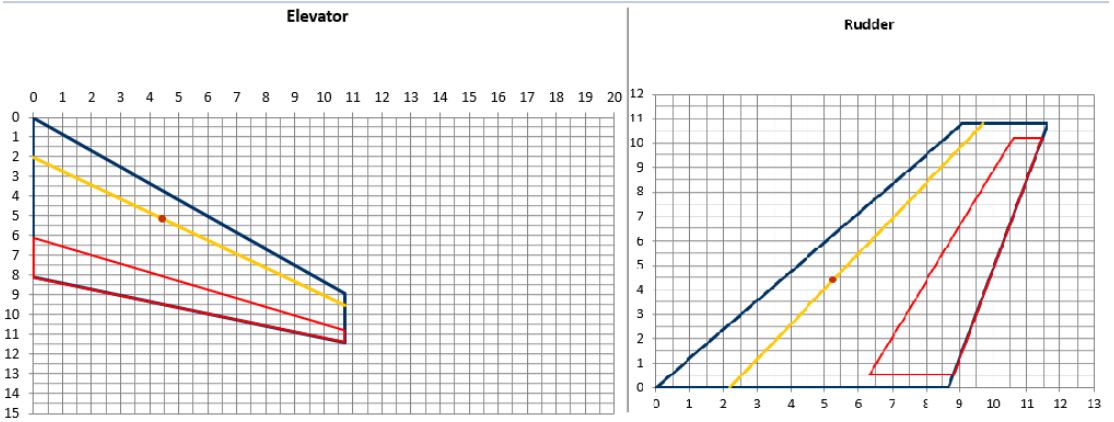

Figure 8.7: *New elevator and rudder drawn on PreSTo*

9 Landing gear

The aircraft will have a nose and main landing gear, with two legs under the wings. The position and length of the landing gear legs must be determined using a variety of parameters. Using the reference aircraft, all landing gear legs' number, length, and position are calculated with the PreSTo 3.4.2 tool.

9.1 Landing gear position

The position of the nose and main landing gears is computed first respecting the wheelbase distance and knowing that the distance from nose to nose gear is $8,01\ m$ as calculated in previous sections. Dividing this value with the external diameter of the fuselage gives a value of $1,35$ which is bigger as expected than other smaller aircrafts as the A330 or A320.

The position of the main landing gear according to MAC has a relation of 66 %, bigger than usual statistics ($52\ \% - 58\ \%$) which makes sense as the longitudinal lengths are considerably bigger than typical aircrafts.

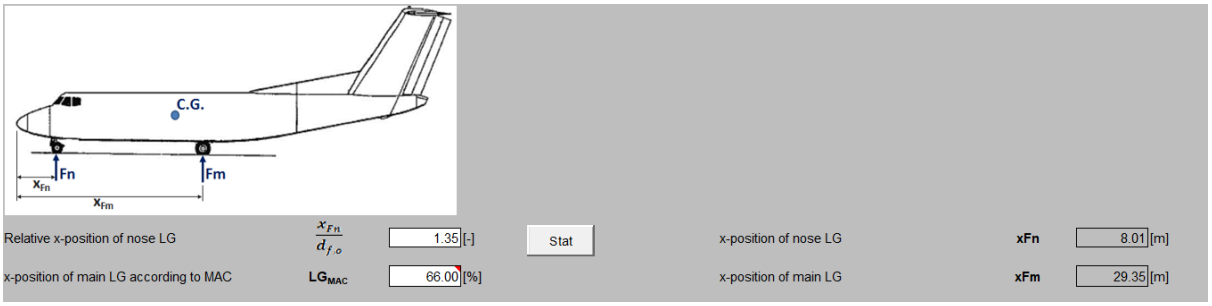

Figure 9.1: *Landing gear position on PreSTo*

9.2 Longitudinal and lateral tip stability

In order to maintain stability the tip-over angles are needed, firstly calculating the aft and forward distances from the center of gravity (jet transport according to ROSKAM II (cited by Scholz [1]) and selecting a mean value) as well as the distance from ground to fuselage.

$$X_{CG,fwd} = X_{CG} - 0,5 \cdot 0,22 \cdot c_{MAC} \tag{9.1}$$

$$X_{CG,aft} = X_{CG} + 0,5 \cdot 0,22 \cdot c_{MAC} \tag{9.2}$$

Type	C.G. Range fr.$\bar{c}_w$	Type	C.G. Range fr.$\bar{c}_w$
Homebuilts	0.10	Military Trainers	0.10
Single Engine Prop. Driven	0.06-0.27	Fighters	0.20
Twin Engine Prop. Driven	0.12-0.22	Mil.Patr. Bomb and Transp.	0.30
Ag. Airpl.	0.10	Fl.Boats, Amph. and Float	0.25
Business Jets	0.10-0.21	Amph. and	
Regional TBP	0.14-0.27	Supersonic Cruise	0.30
Jet Transp.	0.12-0.32		

Figure 9.2: *Center of gravity range of ROSKAM II, cited by Scholz [1]*

$X_{CG,fwd} = 25,33\ m$

$X_{CG,aft} = 27,02\ m$

According to the technical profile [6] adjusted for the sizes of this model, the height from ground to fuselage bottom is $H = 1,64\ m$ which is similar to other aircrafts with the same size.

$$\psi_L = arctan\left(\frac{X_{Fm} - X_{CG,aft}}{\Delta z_{cg} + H}\right) \tag{9.3}$$

The longitudinal tip stability angle should be at least 15 º to prevent the aircraft from tipping over during turns on ground. **Figure 9.3** shows that the angle is bigger than the minimum.

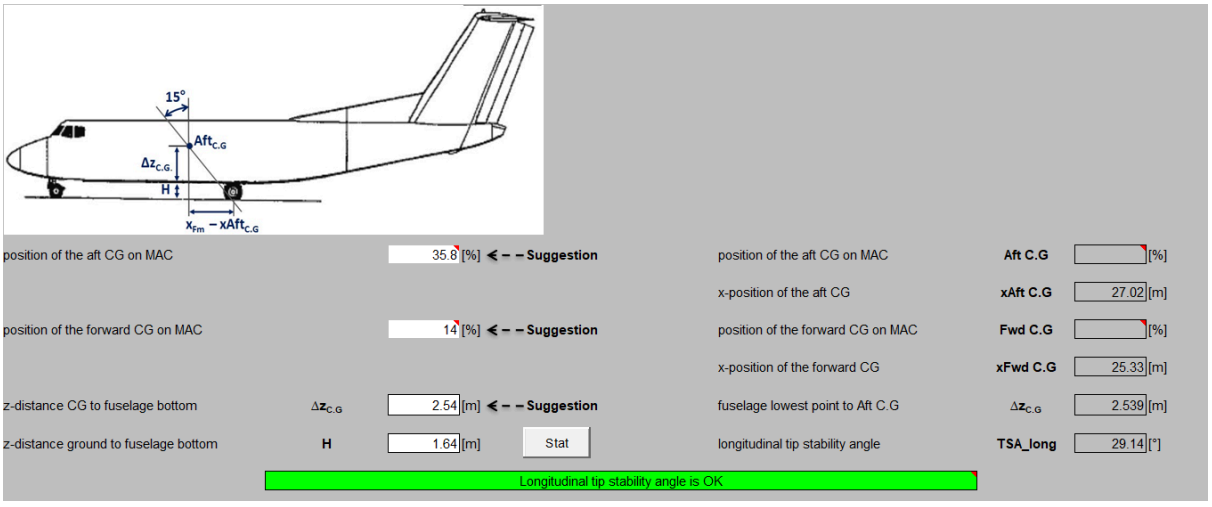

Figure 9.3: *Longitudinal stability on PreSTo*

$\phi_{tip-over,L} = 29,14$ º.

In case of the lateral stability:

$$\psi_Q = arctan\left(\frac{\Delta z_{cg} + H}{\frac{y_{track} \cdot (X_{CG,aft} - X_{CG,LG,N})}{2 \cdot X_{CG,LG,N-LG,M}}}\right) \quad (9.4)$$

$X_{CG,LG,N-LG,M}$: wheelbase distance.

y_{track}: lateral distance of the main gears set to 10, 9 m using **Figure 3.13** adapted to this aircraft.

The lateral tip-over angle should be maximum 55 º, and according to the data the requirement is met, $\psi_Q = 38,29$ º.

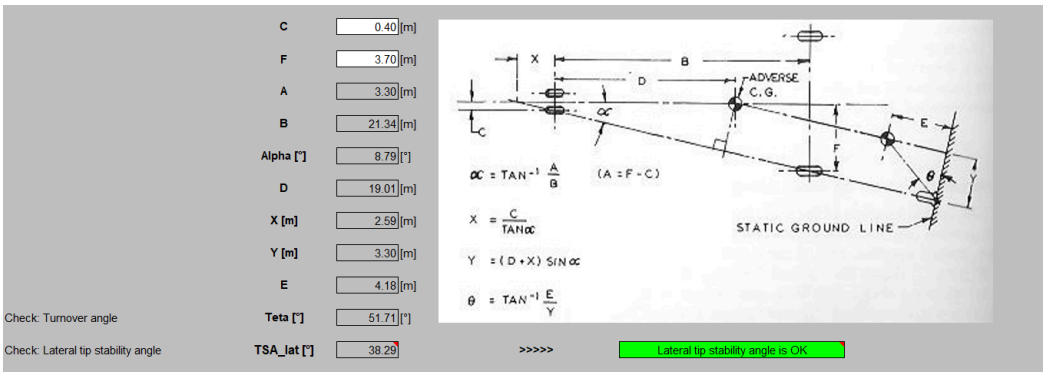

Figure 9.4: *Lateral stability on PreSTo 4.3.2*

9.3 Longitudinal and lateral clearance, retraction check

The track width and length of the main landing gear legs must be chosen so that the wings or engines do not come into contact with the ground while rotating.

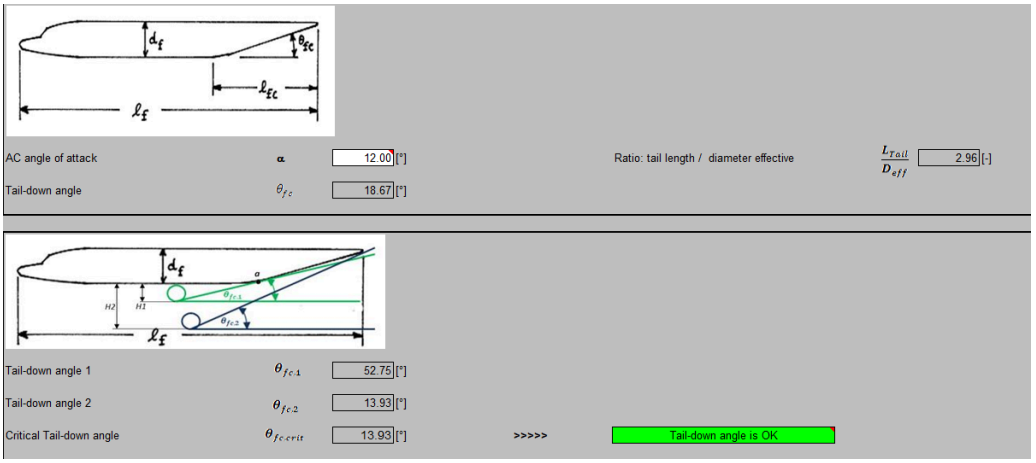

Figure 9.5: *Longitudinal clearance on PreSTo*

For the lateral clearance the engine and wing dimensions are taken into account being the bank angle bigger than $7,5$ º as a requirement. The engine diameter is $2,19\ m$ according to Wikipedia [10] and the symmetry to pylon (distance from center of fuselage to the engine) has been taken using **Figure 3.13** and adapting the distances to the width of this aircraft.

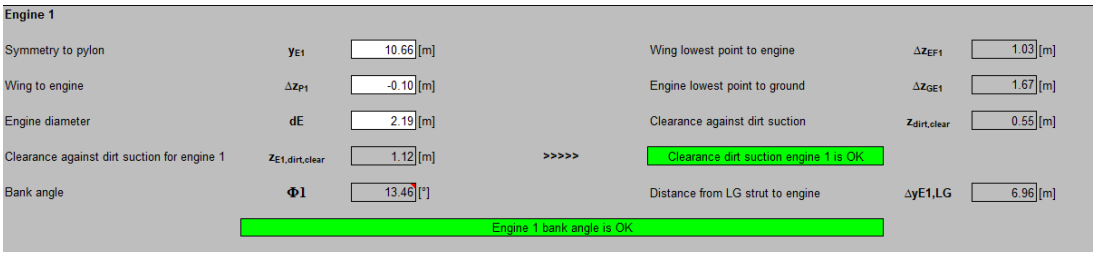

Figure 9.6: *Lateral clearance of the engine on PreSTo*

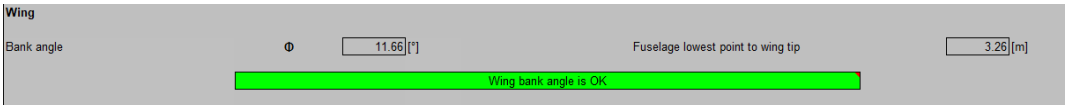

Figure 9.7: *Longitudinal clearance of the wing on PreSTo*

The retraction of the wheels is also checked as the retracting clearance is bigger than zero.

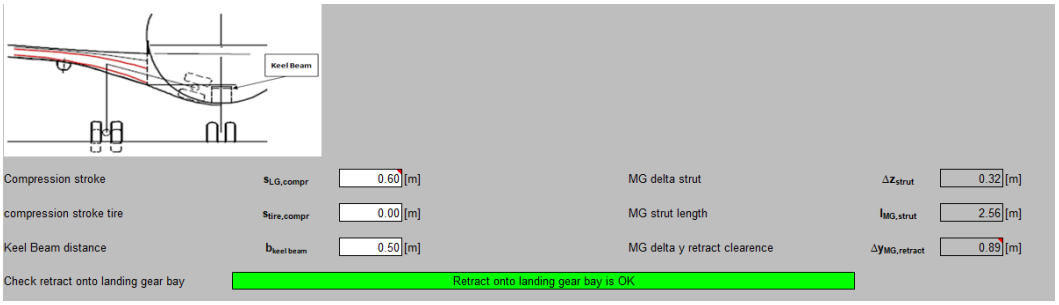

Figure 9.8: Retract clearance of the landing gears on PreSTo

9.4 Load classification number (LCN) and ACR

Firstly, the number of tires and how they are distributed is computed together with their loads according to the model of the aircraft.

Number of weels on MG	$n_{W,MG}$	8 [-]
Number of Main Gear struts	$n_{S,MG}$	2 [-]
Number of wells on Main Gear per strut	$n_{W,MG/S}$	4 [-]
Number of Center Gear struts	$n_{S,CG}$	0 [-]
Number of wells on Center Gear	$n_{W,CG}$	0 [-]
Number of Nose Gear struts	$n_{S,NG}$	1 [-]
Number of wells on Nose Gear	$n_{W,NG}$	2 [-]

Figure 9.9: *Landing gear configuration on PreSTo*

Basic loads

Max. static MG load	$load_{(stat,MG)max}$	172142.28 [kg]			F	21.34 [m]
Max. static MG load [%MTOW]	$load_{(stat,MG)max}$	89.08 [%]			M	2.33 [m]
Max. static NG load	$load_{(stat,NG)max}$	36338.82 [kg]			N	19.01 [m]
Min. static NG load	$load_{(stat,NG)min}$	21104.47 [kg]			L	17.32 [m]
Max. brake load NG	$load_{NG,brake}$	48060.10 [kg]			J	4.18 [m]
Max. static NG load [%MTOW]	$load_{(stat,NG)max}$	18.80 [%]	>>>>>	Max static NG load is OK		
Min. static NG load [%MTOW]	$load_{(stat,NG)min}$	10.92 [%]	>>>>>	Min. static NG load is OK		

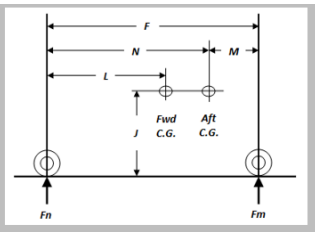

Safety margins on basic loads

General safety margin	S1	7 [%]	Max static MG load [kg]	$load_{(stat,MG)max}$ 227227.81 [kg]
Margin for AC growth potential	S2	25 [%]	Max static NG load [kg]	$load_{(stat,NG)max}$ 47967.25 [kg]
			Min static NG load [kg]	$load_{(stat,NG)min}$ 27857.90 [kg]
			Max brake load NG	$load_{NG,brake}$ 63439.33 [kg]

Figure 9.10: *Landing gear loads on PreSTo*

Torenbeek, cited by Scholz [1] states that the tire pressure and the equivalent single wheel load (ESWL) are used to determine the Load Classification Number. The ESWL is a load that has the same impact on the runway as the real landing gear when viewed as a single tire.

$$ESWL = \frac{load\ on\ one\ assembly}{reduction\ factor} \tag{9.5}$$

The maximum load on one undercarriage assembly (main gear) is found:

$$L_{LG,M,Max} = \frac{m_{TO} \cdot (X_{CG,aft} - X_{CG,LG,N})}{2 \cdot X_{CG,LG,M-LG,N}} \tag{9.6}$$

$L_{LG,M,Max} = 86073,7\ kg = 189760,06\ lb$, with $X_{CG,LG,M-LG,N} = 21,33\ m$ using m_{TO} computed on the mass analysis.

To determine the reduction factor, the area where tires make contact needs to be computed.

$$A_C = \frac{L_{LG,M,Max}}{Tire\ pressure} \tag{9.7}$$

Using the PreSTo tool the tire pressure is selected from a catalogue.

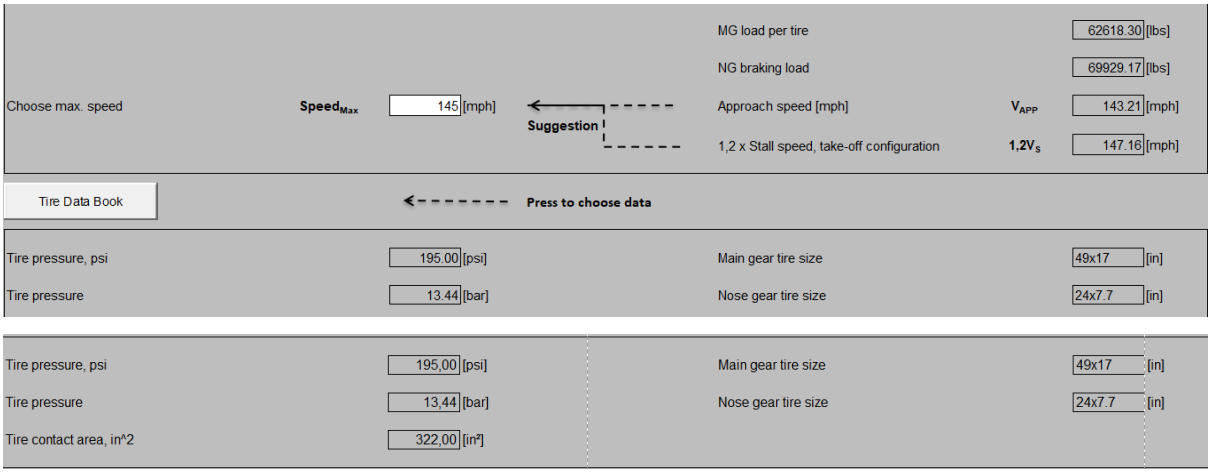

Figure 9.11: *Tire data selected on PreSTo*

$A_C = 973,16\ in^2$

The distance between the wheels on a main landing gear legs is set to $s_T = 59,06\ in$ while the condition of the subsoil is $L = 45\ in$ making the ratios $s_T/L = 1,3124$ and $A_C/L^2 = 0,48$, by using **Figure 9.12** and **Figure 9.13** the ESWL is found.

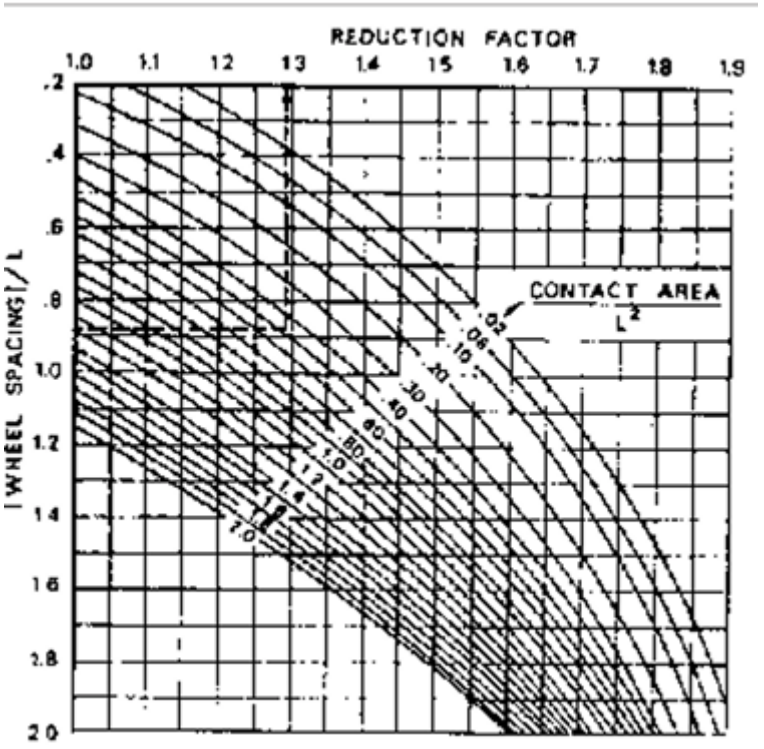

Figure 9.12: *Wheel spacing by Scholz [1]*

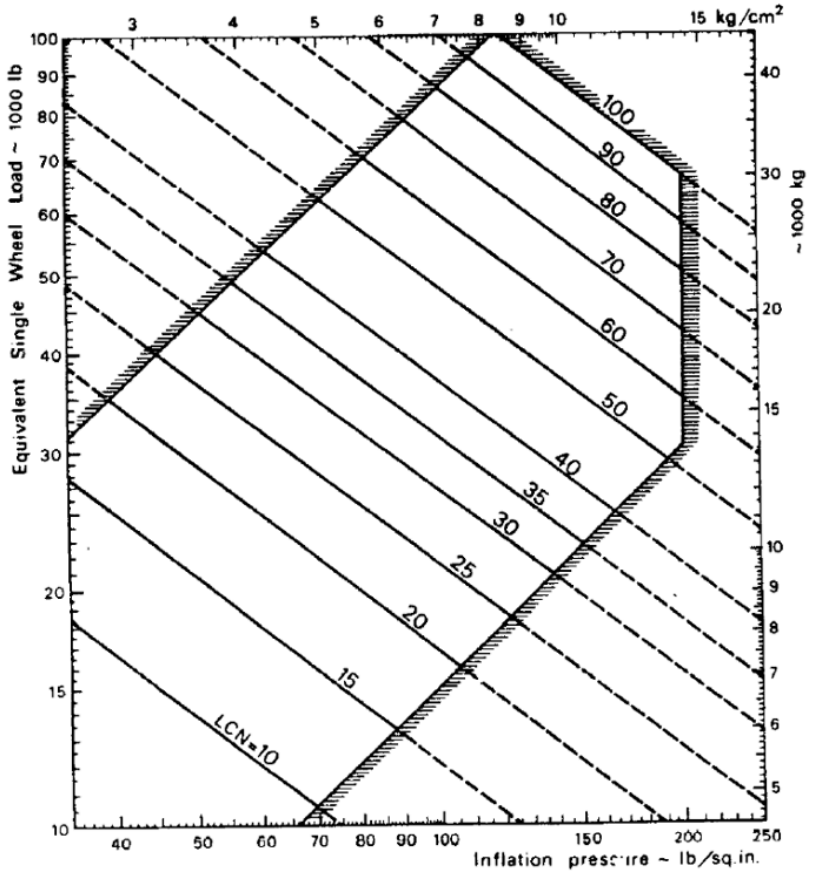

Figure 9.13: *ESWL by Scholz [1]*

The reduction factor is 1,51, giving an ESWL= $125668,91\ lb$ with a tire pressure of $194,3\ lb/in^2$ giving this a LCN of 100.

In addition, The ACR (Aircraft Classification Rating) system was created by the International Civil Aviation Organization (ICAO). It captures the effects of better qualities of new pavement materials and advanced landing gear arrangements, resulting in more accurate findings. It is a classification of the aircraft and its flight surfaces that determines whether damage will occur to the flight surfaces or the aircraft's landing gear during landing.

The ACR number is calculated with the ICAO-ACR 1. 4 [11] program. The L-1011 is already included in the ICAO-ACR software database, thus only the aircraft type needs to be selected. Next figures show the ACR numbers and required covering thicknesses for the various subfloor categories of rigid and flexible airport floor coverings.

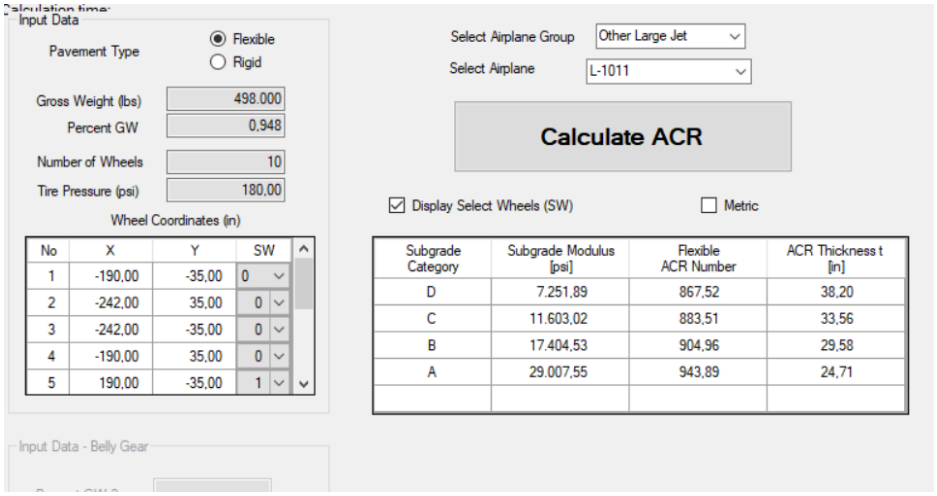

Figure 9.14: *Data extracted from ICAO-ACR program for flexible pavement*

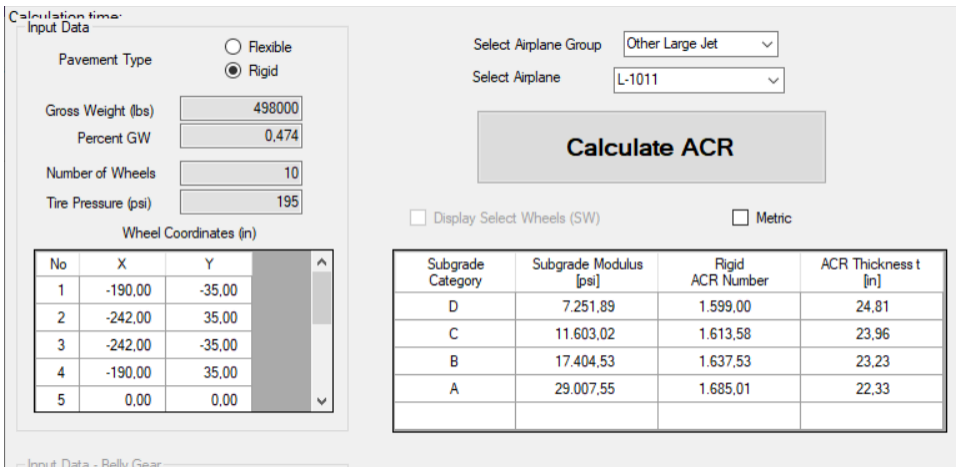

Figure 9.15: *Data extracted from ICAO-ACR program for rigid pavement*

10 Drag analysis

At the completion of the design phase, the final design's flight performance must be verified.
The drag calculation is performed by two phases with the zero-lift part and the codependent to lift drag.

The aircraft's weight determines the needed lift during cruise flight calculated in previous sections.

$$C_D = C_{D0} + \Delta C_{D_{WAVE}} + \frac{C_L^{\,2}}{\Pi \cdot A \cdot e} \tag{10.1}$$

The zero drag coefficient is described summing all the components of the aircraft that influence directly to this value, according to Scholz[1]:

$$C_{D0} = \sum_{c=1}^{n} C_{f,c} \cdot FF_c \cdot Q_c \cdot \frac{S_{wet}}{S_{ref}} \tag{10.2}$$

$C_{f,c}$: coefficient of frictional drag.

FF_c: factor for form drag.

Q_c: interference drag relative to the fuselage.

$\frac{S_{wet}}{S_{ref}}$: ratio of area affected by flow and actual reference area for every section.

A distinction has to be made between laminar and turbulent flow for further detailed analysis of the drag including also the Reynolds number (ratio of inertial forces to viscous forces) in a fluid flow which is compared to its limit ($Re_{cut-off}$) .

$$C_{f,laminar} = 1,328/\sqrt{Re} \tag{10.3}$$

$$C_{f,turbulent} = \frac{0,455}{(log\ Re)^{2,58} \cdot (1+0,144 \cdot M^2)^{0,65}} \tag{10.4}$$

$$Re = \frac{V_{CR} \cdot l}{v} \tag{10.5}$$

v: kinematic viscosity.

$$Re_{cut-off} = 38,21 \cdot \left(\frac{l}{k}\right)^{1,053} \tag{10.6}$$

$\frac{l}{k}$: ratio of length of the section studied divided by roughness, being this last one $k = 6,35 \cdot 10^{-6}\ m$ according to DATCOM, cited by Scholz [1].

The analysis will be performed following this requirement:

For $\frac{V \cdot l}{\nu} > Re_{cut-off}$ $C_{f,turbulent}$ is calculated with $Re = Re_{cut-off}$,

for $\frac{V \cdot l}{\nu} \leq Re_{cut-off}$ $C_{f,turbulent}$ is calculated with $Re = \frac{V \cdot l}{\nu}$.

Figure 10.1: Requirement for analysis of drag coefficients

The flow along the aircraft is assumed to be 20% laminar ($k_{laminar} = 20\ \%$). The average frictional drag can be estimated as follows.

$$C_f = k_{laminar} \cdot C_{f,laminar} + (1 - k_{laminar}) \cdot C_{f,turbulent} \tag{10.7}$$

10.1 Fuselage drag

The fuselage has length of $l_f = 48,1\ m$ and diameter of $d_{f,E} = 5,92\ m$, yet the form drag factor:

$$FF_F = 1 + \frac{60}{(l_f/d_{f,E})^3} + \frac{(l_f/d_{f,E})}{400} \tag{10.8}$$

$FF_F = 1,132$.

The Reynolds number is set with a cruise velocity $V_{CR} = 254\ m/s$ and a kinematic viscosity $v = 5,4603 \cdot 10^{-5}\ m^2/s$ with a value of $Re = 2,237 \cdot 10^8$ being minor to the one for cut-off ($Re_{cut-off} = 6,7 \cdot 10^8$).

The friction drag component is $C_{f,Fuselage} = 1,44 \cdot 10^{-3}$ as $C_{f,laminar} = 8,88 \cdot 10^{-5}$, $C_{f,turbulent} = 1,78 \cdot 10^{-3}$.

The interference drag $Q_F = 1,0$ according to Scholz [1].

Table 13.4 Interference factor Q

Interference factor with respect to ...	Property	Interference factor Q
nacelle	engine mounted directly on the wing or fuselage	1.5
	distance of engine to wing respectively fuselage is *smaller* than engine diameter d_N	1.3
	distance of engine to wing respectively fuselage is *greater* than engine diameter d_N	1.0
wing	high-wing, mid-wing or low-wing position *with* aerodynamically optimized wing-fuselage fairing	1..0
	low-wing position *without* aerodynamically optimized wing-fuselage fairing	1.10 ... 1.40
fuselage	-	1.0
horizontal or vertical tailplane	conventional empenage	1.04
	H-tail	1.08
	V-tail	1.03

Figure 10.2: *Interference factor Q by Scholz [1]*

The zero-lift coefficient drag of the fuselage according to **Equation 10.2**:
$C_{D0,F} = 3,67 \cdot 10^{-3}$.

10.2 Wing drag

The wing has a length of $c_{MAC} = 7,716\ m$ and the form drag factor:

$$FF_W = \left[1 + \frac{0,6}{x_t} \cdot \left(\frac{t}{c}\right) + 100 \cdot \left(\frac{t}{c}\right)^4\right] \cdot \left[1,34 \cdot M_{CR}^{0,18} \cdot (cos\varphi_m)^{0,} \right. \tag{10.8}$$

$FF_W = 1,56$ with a position of maximum thickness $x_t = 0,35$ and arrow angle $\varphi_m = \varphi_{35} = 33,68$ º.

$$tan\varphi_{35} = tan\varphi_{W,25} - \frac{4}{A} \cdot \left(\frac{10}{100} \cdot \frac{1-\lambda}{1+\lambda}\right) \tag{10.9}$$

The Reynolds number is set with a value of $Re = 3,59{\cdot}10^{7}$ being minor to the one for cut-off ($Re_{cut-off} = 9,76{\cdot}10^{7}$).

The friction drag component is $C_{f,Fuselage} = 1,89{\cdot}10^{-3}$ as $C_{f,laminar} = 2,22{\cdot}10^{-4}$, $C_{f,turbulent} = 2,307{\cdot}10^{-3}$.

The interference drag $Q_F = 1,0$ according to **Figure 10.2** and the relation of wetted area and reference area is $\frac{S_{wet,W}}{S_{ref}} = 1,659$ and finally, $CD_{0,W} = 3,40{\cdot}10^{-3}$.

10.3 Horizontal tail drag

The horizontal tailplane has a length of $c_{MAC,H} = 5,8\ m$ and the form drag factor:

$$FF_W = \left[1 + \frac{0,6}{x_{t-H}}\cdot\left(\frac{t}{c}\right)_H + 100\cdot\left(\frac{t}{c}\right)_H^{4}\right]\cdot\left[1,34\cdot M_{CR}^{0,18}\cdot(cos\varphi_m)^{0,28}\right] \qquad (10.10)$$

$FF_H = 1,3$ with a position of maximum thickness $x_t = 0,35$ and arrow angle $\varphi_{m,H} = \varphi_{35,H} = 33,98$ º.

$$tan\varphi_{35,h} = tan\varphi_{H,25} - \frac{4}{A_H}\cdot\left(\frac{10}{100}\cdot\frac{1-\lambda_H}{1+\lambda_H}\right) \qquad (10.11)$$

The Reynolds number is set with a value of $Re = 2,69{\cdot}10^{7}$ being minor to the one for cut-off ($Re_{cut-off} = 7,21{\cdot}10^{7}$).

The friction drag component is $C_{f,Fuselage} = 1,98{\cdot}10^{-3}$ as $C_{f,laminar} = 2,56{\cdot}10^{-4}$, $C_{f,turbulent} = 2,82{\cdot}10^{-3}$.

The wetted area for the horizontal tailplane is calculated with **Equation 7.3** adapted to the tail, $S_{wet,H} = 231,35\ m^2$.

The interference drag is $Q_H = 1,04$ according to **Figure 10.2** and the relation of wetted area and reference area is $\frac{S_{wet,H}}{S_{ref}} = 2,03$ and finally, $CD_{0,H} = 7,74{\cdot}10^{-3}$.

10.4 Vertical tail drag

The vertical tailplane has a length of $c_{MAC,V} = 6,17\ m$ and the form drag factor:

$$FF_V = \left[1 + \frac{0,6}{x_{tV}}\cdot\left(\frac{t}{c}\right)_V + 100\cdot\left(\frac{t}{c}\right)_V^4\right]\cdot\left[1,34\cdot M_{CR}^{0,18}\cdot(cos\varphi_m)^{0,28}\right] \quad (10.12)$$

$FF_V = 1,31$ with a position of maximum thickness $x_t = 0,35$ and arrow angle $\varphi_{m,V} = \varphi_{35,V} = 32,74$ º.

$$tan\varphi_{35,V} = tan\varphi_{V,25} - \frac{4}{A_V}\cdot\left(\frac{10}{100}\cdot\frac{1-\lambda_V}{1+\lambda_V}\right) \quad (10.13)$$

The Reynolds number is set with a value of $Re = 2,74{\cdot}10^7$ being minor to the one for cut-off ($Re_{cut-off} = 7,33{\cdot}10^7$).

The friction drag component is $C_{f,Fuselage} = 1,48{\cdot}10^{-3}$ as $C_{f,laminar} = 2,67{\cdot}10^{-4}$, $C_{f,turbulent} = 1,78{\cdot}10^{-3}$.

The wetted area for the horizontal tailplane is calculated with **Equation 7.3** adapted to the tail, $S_{wet,V} = 112,25\ m^2$.

The interference drag is $Q_H = 1,04$ according to **Figure 10.2** and the relation of wetted area and reference area is $\frac{S_{wet,V}}{Sref} = 1,86$ and finally, $CD_{0,V} = 3,75{\cdot}10^{-3}$.

10.5 Nacelle drag

The nacelle has a length of $l_n = 5,19\ m$ according to Wikipedia[] and the form drag factor:

$$FF_N = 1 + \frac{0,35}{(l_n/d_n)} \tag{10.14}$$

$FF_V = 1,15.$

The Reynolds number is set with a value of $Re = 2,41{\cdot}10^7$ being minor to the one for cut-off ($Re_{cut-off} = 6,4{\cdot}10^7$).

The friction drag component is $C_{f,Fuselage} = 2,01{\cdot}10^{-3}$ as $C_{f,laminar} = 2,7{\cdot}10^{-4}$, $C_{f,turbulent} = 2,45{\cdot}10^{-3}$.

The wetted area for the horizontal tailplane is calculated.

$$S_{wet,N} = S_{wet,fan\ cowl.} + S_{wet,gas\ gen.} + S_{wet,plug} \tag{10.15}$$

$$S_{wet,fan\ cowl.} = l_n{\cdot}d_n{\cdot}\left[2 + 0,35{\cdot}\frac{l_1}{l_n} + 0,8{\cdot}\frac{l_1{\cdot}d_{hl}}{l_n{\cdot}d_n} + 1,15{\cdot}(1 - \frac{l_1}{l_n}){\cdot}\frac{d_{ef}}{d_n}\right] \tag{10.16}$$

$$S_{wet,gas\ gen.} = \pi{\cdot}l_g{\cdot}d_g{\cdot}\left[1 - \frac{1}{3}{\cdot}(1 - \frac{d_{eg}}{d_g}){\cdot}(1 - 0,18{\cdot}(\frac{d_g}{l_g})^{5/3}\right] \tag{10.17}$$

$$S_{wet,plug} = 0,7{\cdot}\pi{\cdot}l_p{\cdot}d_p \tag{10.18}$$

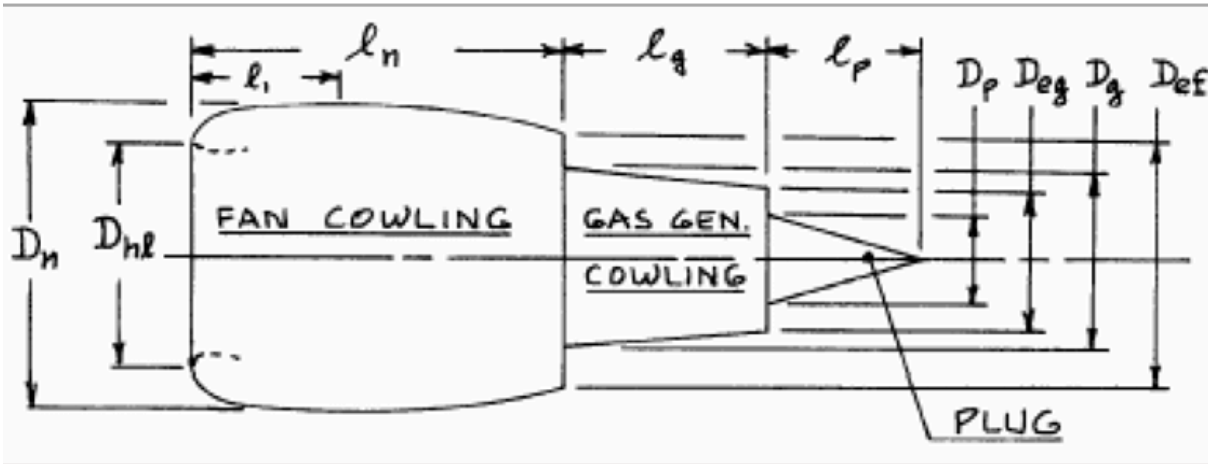

Figure 10.3: *Engine sizes by Scholz [1]*

The values used are sized, using values of similar engines if no information is available for the ones installed on the L-1011.

Table 10.1: *Dimensions of the engine*

Sizes of the engine	Values
d_h	$2,19\ m$
d_{hl}	$1,8\ m$
l_1	$1,7\ m$
l_n	$0,8\ m$
l_g	$1,5\ m$
l_p	$1\ m$
d_p	$0,5\ m$
d_{eg}	$0,7\ m$
d_g	$1,6\ m$
d_{ef}	$2,15\ m$

$$S_{wet,fan\ cowl.} = 20,57\ m^2$$

$S_{wet,gas\ gen.} = 7,41\ m^2$

$S_{wet,plug} = 1,32\ m^2$

$S_{wet,N} = 29,3\ m^2$

The interference drag is $Q_H = 1,3$ according to **Figure 10.2** and the relation of wetted area and reference area is $\frac{S_{wet,N}}{S_{ref}} = 0,812$ being $S_{ref} = 31,6\ m^2$ according to typical values for nacelles and, $CD_{0,N} = 3{\cdot}2,44{\cdot}10^{-3} = 7,32{\cdot}10^{-3}$ for two engines on the wing plus one on the back.

10.6 Total drag coefficient, wave drag and Oswald factor correction

Summing all values, the total zero-lift drag coefficient is $C_{DO} = 2,588{\cdot}10^{-2}$.

The wave drag is also considered affecting in case of shock waves. Using the plot provided by Scholz [1] the wave drag is calculated.

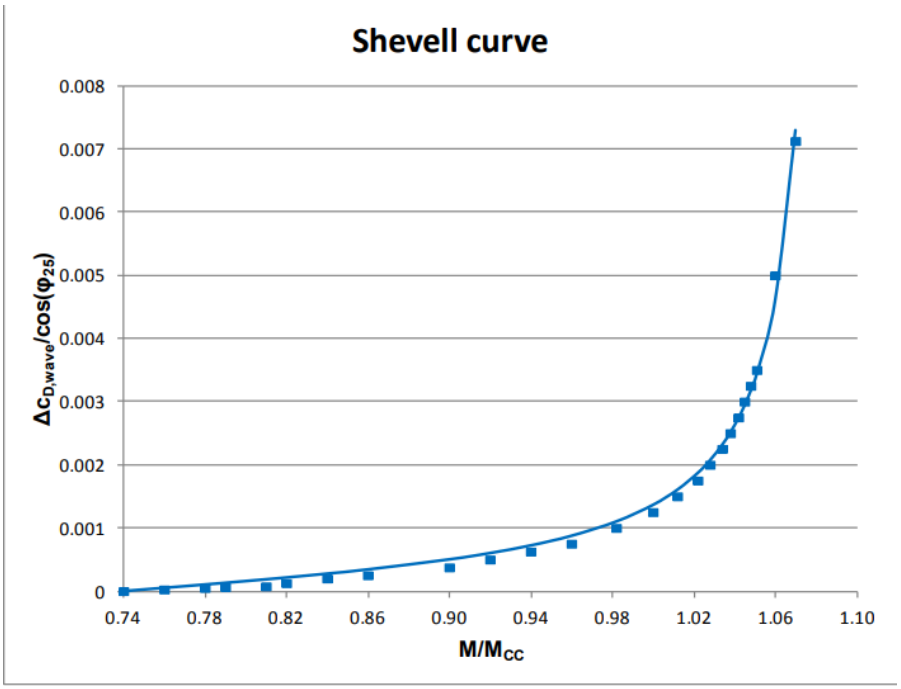

Figure 10.4: *Wave drag plot by Scholz [1]*

$\frac{M_{CR}}{M_{crit}} = 0,98$ with $M_{crit} = 0,88$.

From **Figure 10.4**, $\Delta C_{D,wave}/cos(\varphi_{25}) = 0,001$ and $\Delta C_{D,wave} = 8,19 \cdot 10^{-4}$

The resulting total drag coefficient is found as the following expression from **Equation 10.1** being $C_D = 2,67 \cdot 10^{-2} + 5,37 \cdot 10^{-2} \cdot C_L^{\ 2}$ and for cruise level, $C_D = 3,37 \cdot 10^{-2}$.

The Oswald factor is corrected with **Equation 10.19** from Scholz [1]:

$$e = \frac{1}{(1+0,12 \cdot M_{CR}^{\ 6}) \cdot (1+\frac{0,142+f(\lambda) \cdot A \cdot (10t/c)^{0,33}}{(cos\varphi_{25})^2} + \frac{0,1 \cdot (3 \cdot N_e + 1)}{(4+A)^{0,8}})} \quad (10.19)$$

$f(\lambda) = 0,005 \cdot (1 + 1,5 \cdot (\lambda - 0,6)^2)$: equation used for the Oswald factor, by Scholz [1]

The Oswald factor $e = 0,693$, and with that the new drag coefficient for cruise level is $C_D = 3,987 \cdot 10^{-2}$.

11 Direct Operating Costs (DOC)

The DOC for long-haul aircraft is computed using the Association of European Airlines' (AEA) 1989b approach. PreSTo 4.3.2 calculates the overall direct running costs of an airplane by adding various cost items such as depreciation, interest, insurance, fuel, maintenance, crew, and fees calculating everything using half of the range assigned for the L-1011 model.

$$C_{DOC} = C_{DEP} + C_{INT} + C_{INS} + C_F + C_M + C_C + C_{FEE} \tag{11.1}$$

11.1 Depreciation costs

Depreciation C_{DEP} measures the decline in value of an item over its useful service life.

$$C_{DEP} = \frac{P_{TOTAL} - P_{RESIDUAL}}{n_{DEP}} = \frac{P_{TOTAL} \cdot (1 - P_{TOTAL}/P_{RESIDUAL})}{n_{DEP}} \tag{11.2}$$

$P_{TOTAL} - P_{RESIDUAL}$: purchase price of the aircraft taking out its residual value.

n_{DEP}: useful service life, chosen according to the PreSTo tool.

	AEA 1989a	AEA 1989b	AI 1989	ATA 1967	kker 1993	own	Chosen
n_{DEP}	14.00000	16.00000	15.00	12.00	15.00	Eingabe	16
$P_{residual}/P_{tot}$	0.10000	0.10000	0.10	-	0.10	Eingabe	0.1
$k_{S,AF}$	0.10000	0.10000	0.06	0.10	0.08	Eingabe	0.1
$k_{S,E}$	0.30000	0.30000	0.25	0.10	0.08	Eingabe	0.3
p	0.08000	0.08000					0.08
q = 1 + p	1.08000	1.08000					1.08
n_{PAY}	14.00000	16.00000					16
k_n/k_0	0.10000	0.10000					0.1
n_{DEP}	14.00000	16.00000					16
p_{av}	0.05290	0.05340					0.0534
k_{INS}	0.00500	0.00500					0.005
k_{LD}	0.00780	0.00590					0.0059
k_{NAV}	0.00414	0.00166					0.00166
k_{GND}	0.10000	0.11000					0.11
k_{U1}	3,750	4,800					4800
k_{U2}	0.75000	0.42000					0.42

Figure 11.1: *AEA 1989b data by PreSTo*

The total price of the aircraft is known by summing the price of spares which depends on the delivery price, the contribution to engine and airframe and their prices together with the delivery.

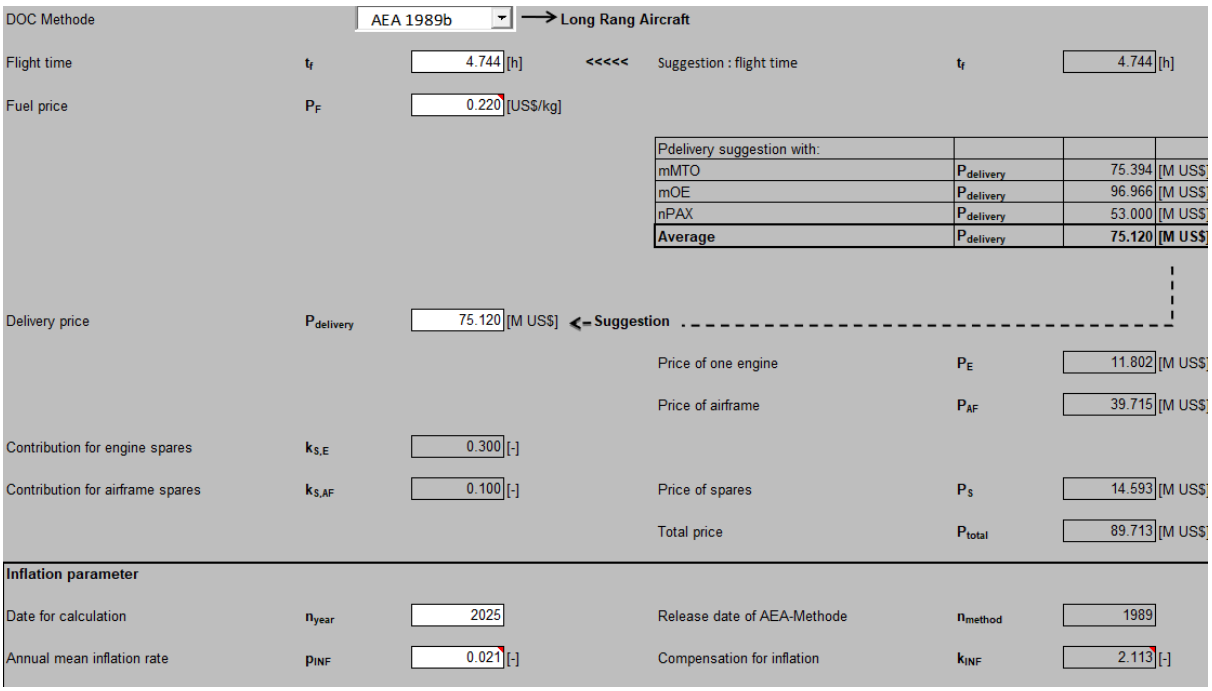

Figure 11.2: *Delivery and spares price by PreSTo*

Therefore $P_{TOTAL} = 89,713\ M\ US\$$.

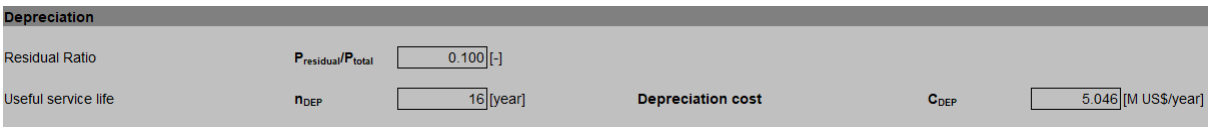

Figure 11.3: *Depreciation cost by PreSTo*

By knowing all the data, the depreciation cost is calculated with a value of $C_{DEP} = 5,046\ M\ US\$/year$.

11.2 Interest costs

The full price of the aircraft is invested and the interest paid to the investor is calculated.

$$C_{INT} = p_{av} \cdot P_{TOTAL} = p_{av} \cdot k_0 \tag{11.3}$$

p_{av}: average interest rate.

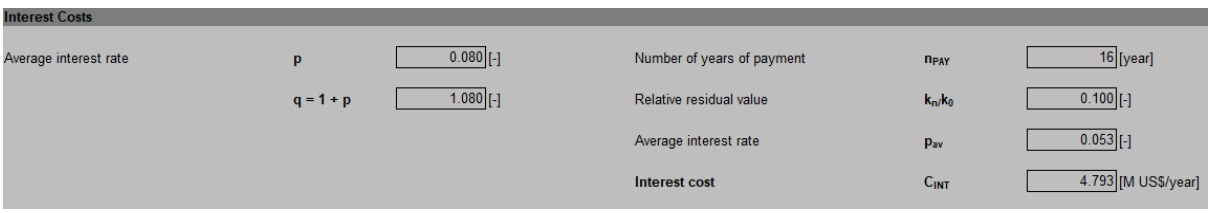

Figure 11.4: *Interest cost by PreSTo*

$C_{INT} = 4,793\ M\ US\$/year.$

11.3 Insurance cost

To make the calculation more robust an insurance payment must be carried on in case of damage to the fuselage.

$$C_{INT} = k_{INS} \cdot P_{delivery} \tag{11.4}$$

k_{INS}: parameter for insurance costs.

Figure 11.5: *Insurance cost by PreSTo*

$C_{INS} = 0,376\ M\ US\$/year$

11.4 Fuel costs

The fuel costs are calculated:

$$C_F = n_{t,a} \cdot P_F \cdot m_F \tag{11.5}$$

In this equation $n_{t,a}$ is the number of flights made per year, P_F is the fuel price and m_F is the mass of the fuel consumed calculated in previous sections.

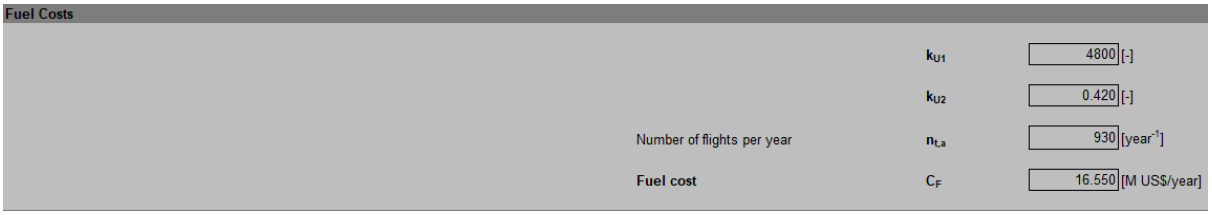

Figure 11.6: *Fuel cost by PreSTo*

The number of flights has been calculated using the time from **Figure 11.2** with half of the range for the aircraft and some constants in order to improve the accuracy.

$C_F = 16,55\ M\ US\$/year.$

11.5 Maintenance costs

Initially, maintenance expenses are computed per flight hour and then multiplied by the annual amount of flights.

$$C_M = ((t_{M,AF,f} + t_{M,E,f}) \cdot L_M + C_{M,M,AF,f} + C_{M,M,E,f}) \cdot t_f \cdot n_{t,a} \tag{11.6}$$

Where $t_{M,AF,f} + t_{M,E,f}$ is the airframe and engine maintenance hours and $C_{M,M,AF,f} + C_{M,M,E,f}$ is the airframe and engine maintenance costs, all per flight hour.

In addition, the Bypass ratio and the overall pressure ratio are computed together with the number of compressor stages and shafts extracted from the engine data.

Engine maintenance cost							
Bypass ratio	BPR	5.000 [-]	Stat Eng		k1	0.994	[-]
Overall pressure ratio	OAPR	21.800 [-]	Stat Eng		k2	0.847	[-]
Number of compressor stages	n_C	13 [-]	Stat Eng		k3	1.056	[-]
Number of shafts	n_S	3 [-]	Stat Eng		k4	0.640	[-]
				Mass of all engines (including nacelles)	$m_{E,inst}$	17175	[kg]
				Engine maintenance man hours per flight hour	$t_{M,E,f}$	4.042	[-]
				Engine maintenance cost per flight hour	$C_{M,M,E,f}$	600.32	[US$/h]
Airframe maintenance cost							
				Airframe maintenance cost per flight hour	$C_{M,M,AF,f}$	122.53	[US$/h]
				Airframe maintenance man hours per flight hour	$t_{M,AF,f}$	11.24	[-]

Figure 11.7: *Maintenance cost data by PreSTo*

The labor rate L_M is computed multiplying the inflation rate calculated for 2025 in **Figure 11.2** by 69 US $/h according to Scholz [1]

Results							
Labor rate	L_M	145.806 [US$/h]	<<<<<	Labor rate	L_M	145.81	[US$/h]
				Maintenance cost	C_M	13.023	[M US$/year]

Figure 11.8: *Maintenance cost by PreSTo*

$C_M = 13,02\ M\ US\$/year.$

11.6 Staff costs

The usage of cabin and cockpit crew is also included in the final formula.

$$C_C = (n_{CO} \cdot L_{CO} + n_{CA} \cdot L_{CA}) \cdot t_b \cdot n_{t,a} \tag{11.7}$$

Where n_{CO}, n_{CA} is the number of cabin and cockpit members already stated and L_{CO}, L_{CA} is the cost rate of cockpit and cabin crew per hour together with the block time t_b stated with the AEA 1989b information.

Crew Costs						
Number of cabin crew members	n_{CA}	8 [-]	<<<<<	Number of cabin crew members	n_{CA}	6 [-]
Number of cockpit crew members	n_{CO}	2 [-]		Block time	t_b	5.164 [h]
Cockpit crew hourly rate	L_{CO}	355.00 [US$/h]		Cockpit crew cost	$C_{C,CO}$	3.410 [M US$/year]
Cabin crew hourly rate	L_{CA}	90.00 [US$/h]		Cabin crew cost	$C_{C,CA}$	3.458 [M US$/year]
				Crew cost	C_C	6.868 [M US$/year]

Figure 11.9: *Staff cost by PreSTo*

$C_C = 6,868\ M\ US\$/year.$

11.7 Fees and charges costs

Landing, navigation and ground charges are included in the equation.

$$C_{FEE} = C_{FEE,LD} + C_{FEE,NAV} + C_{FEE,GND} \tag{11.8}$$

The charges of landing:

$$C_{FEE,LD} = k_{LD} \cdot m_{TO} \cdot n_{t,a} \cdot k_{INF} \tag{11.9}$$

Air Traffic Control (ATC) and navigation:

$$C_{FEE,NAV} = k_{NAV} \cdot R \cdot \sqrt{m_{TO}} \cdot n_{t,a} \cdot k_{INF} \tag{11.10}$$

The fees of ground handling:

$$C_{FEE,GND} = k_{GND} \cdot m_{PL} \cdot n_{t,a} \cdot k_{INF} \tag{11.11}$$

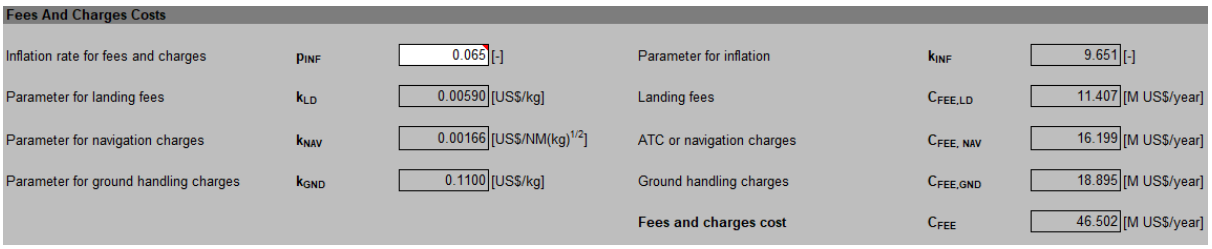

Fees And Charges Costs					
Inflation rate for fees and charges	p_{INF}	0.065 [-]	Parameter for inflation	k_{INF}	9.651 [-]
Parameter for landing fees	k_{LD}	0.00590 [US$/kg]	Landing fees	$C_{FEE,LD}$	11.407 [M US$/year]
Parameter for navigation charges	k_{NAV}	0.00166 [US$/NM(kg)$^{1/2}$]	ATC or navigation charges	$C_{FEE,\ NAV}$	16.199 [M US$/year]
Parameter for ground handling charges	k_{GND}	0.1100 [US$/kg]	Ground handling charges	$C_{FEE,GND}$	18.895 [M US$/year]
			Fees and charges cost	C_{FEE}	46.502 [M US$/year]

Figure 11.10: *Fees and charges cost by PreSTo*

$C_{FEE} = 46,50\ M\ US\$/year.$

11.8 Total DOC costs and pie chart

Finally, the total cost using **Equation 11.1** is $C_{DOC} = 93,157\ M\ US\$/year.$

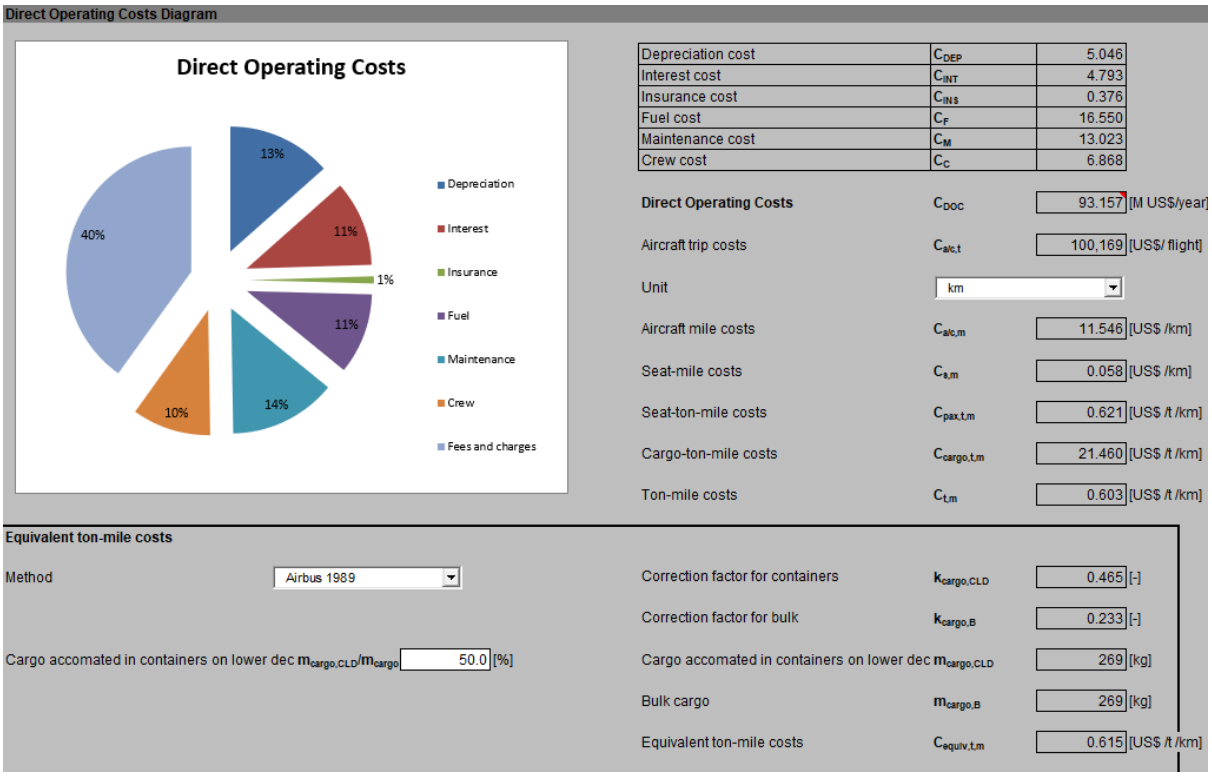

Figure 11.11: *Total DOC cost by PreSTo 3.4.2*

The distribution of the L-1011's operating costs is clearly shown in this pie chart of direct operating costs. Since the L-1011 is a huge tri-jet widebody aircraft with a reputation for using a lot more fuel than contemporary twin-engine jets, it is not surprising that fuel accounts for 40% of the total cost and that in in line with older aircraft needing greater maintenance the percentage is 11%, as insurance and charges are almost negligible.

12 3D MODELS

The Open VSP [2] 3D depiction of the redesign can be found in the next section. A double-trapezoidal wing was utilized to create the 3D model by computing general data of the different sections explained and determined in this project. These findings are displayed in **Figures 12.1–12.5**.

In order to have a better understanding and approach of the L-1011 geometry and dimensions a 3D movable is also included apart from the screenshots taken of the OpenVSP program.

Top:

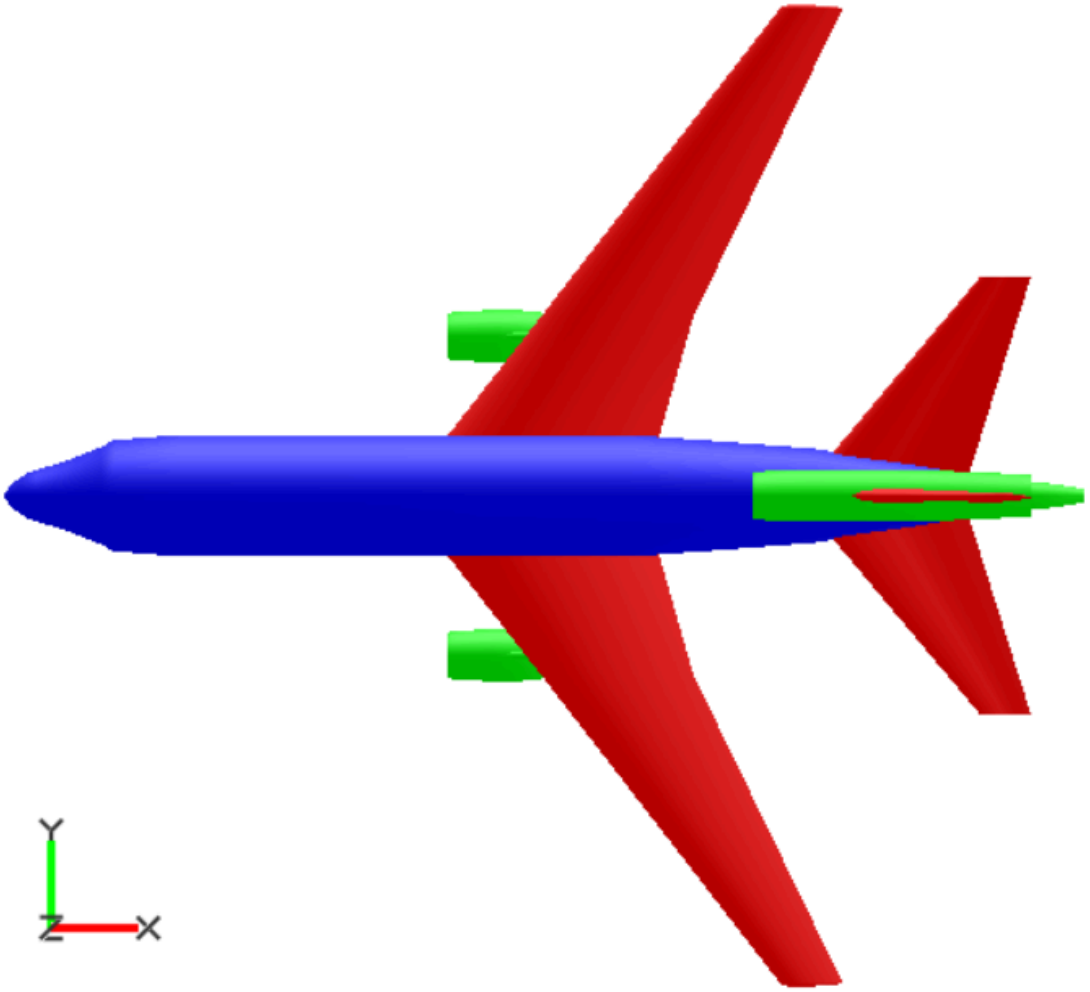

Figure 12.1: *L-1011 top view on OpenVSP [2]*

Front:

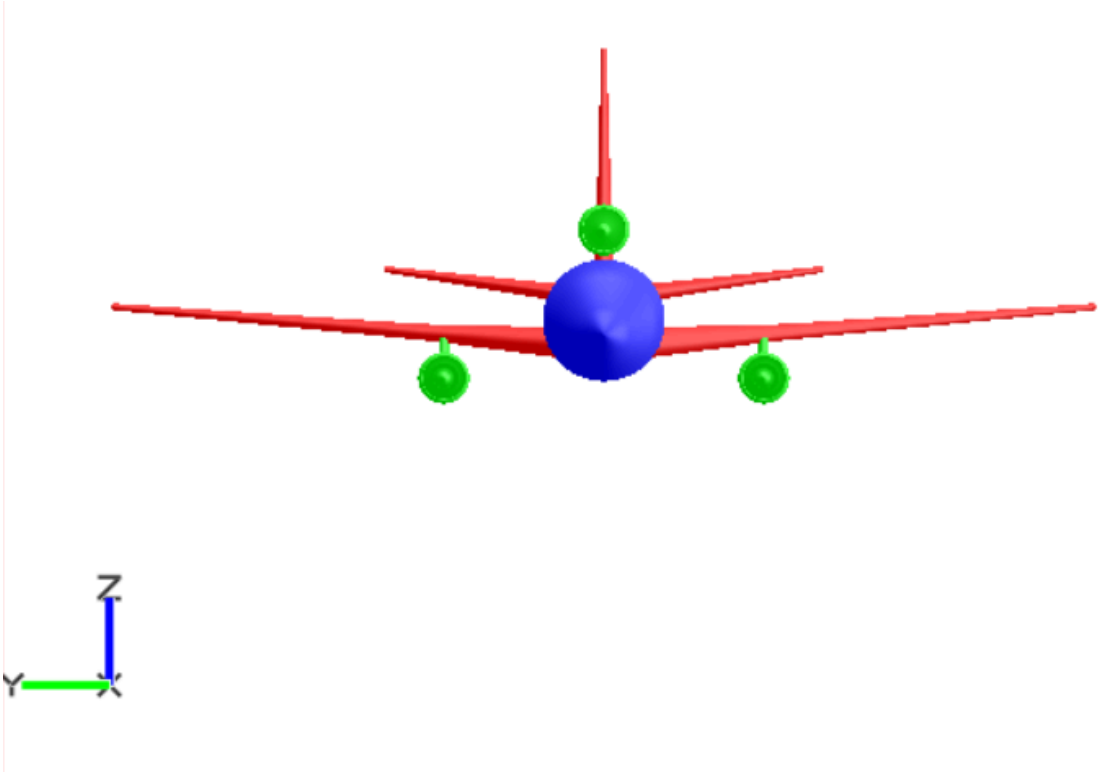

Figure 12.2: *L-1011 front view on OpenVSP [2]*

Side:

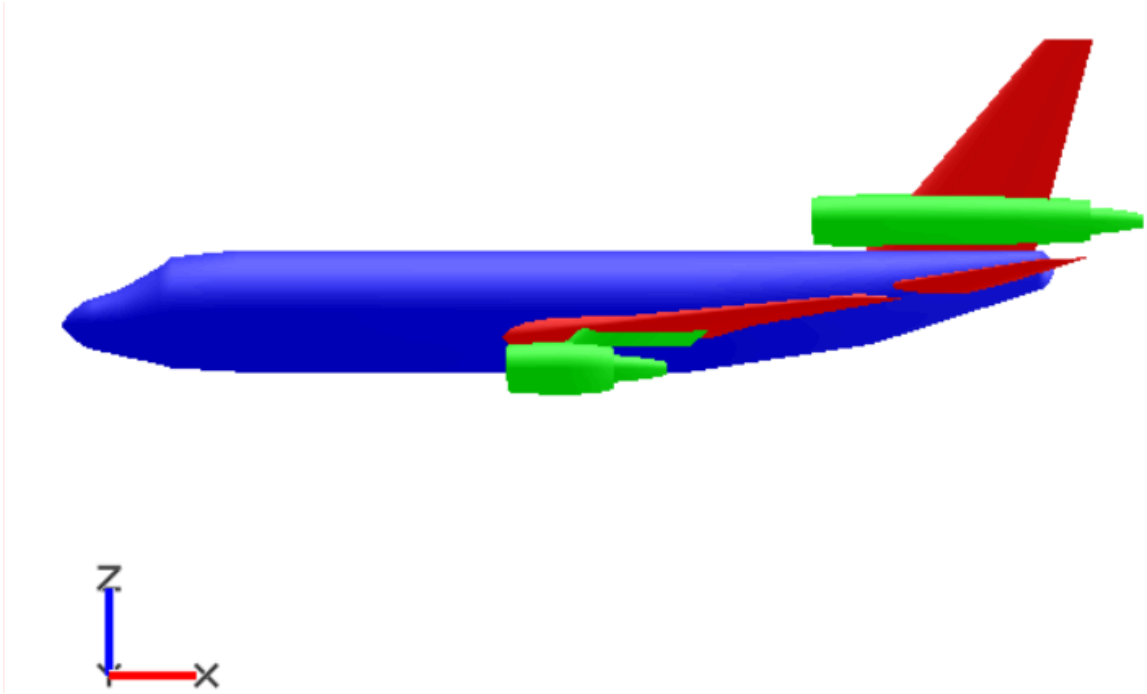

Figure 12.3: *L-1011 side view on OpenVSP [2]*

Iso-perspective:

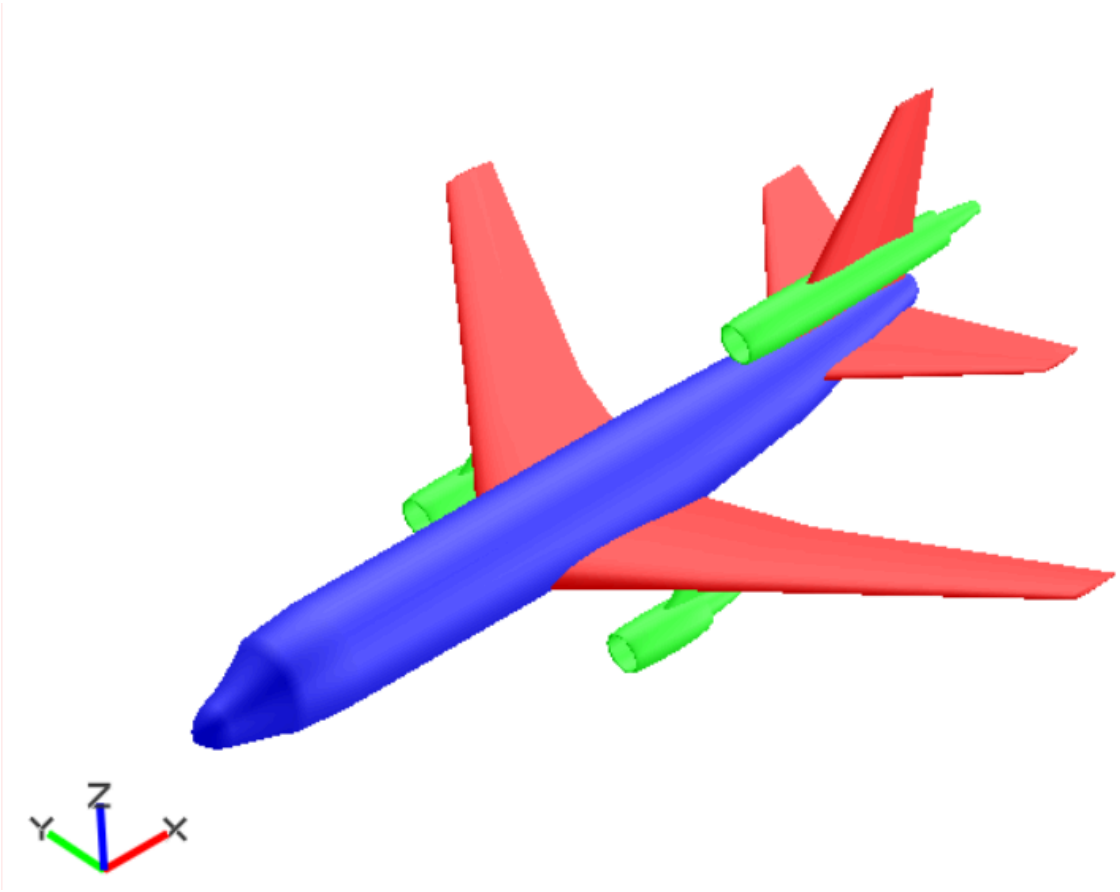

Figure 12.4: *L-1011 iso-perspective view on OpenVSP [2]*

Rear:

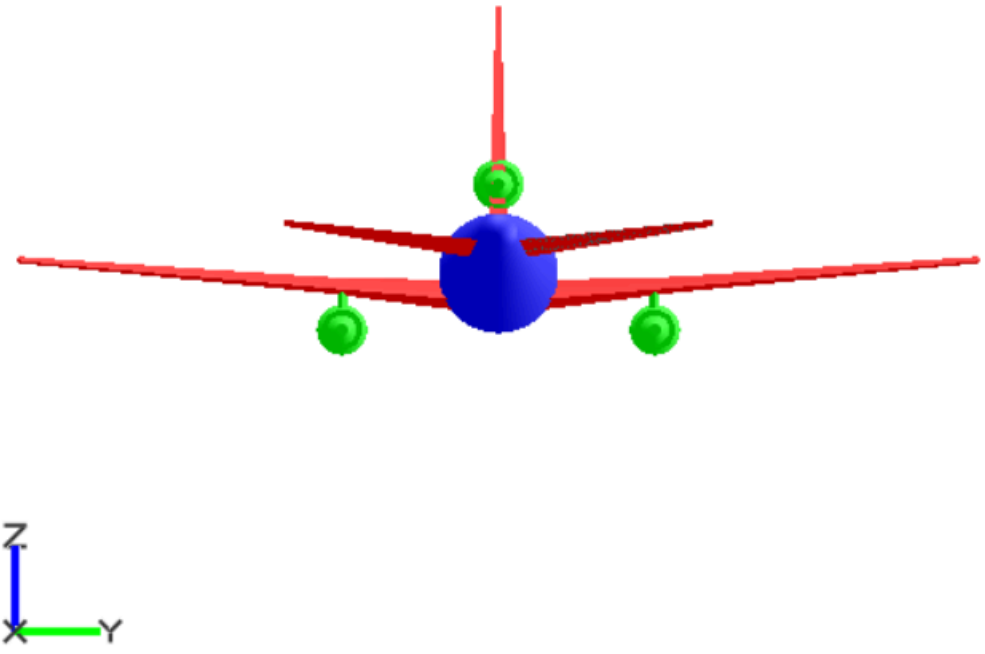

Figure 12.5: *L-1011 rear view on OpenVSP [2]*

Bibliography

[1] “Flugzeugentwurf, HAW Hamburg.” Accessed: Jul. 05, 2025. [Online]. Available: https://www.fzt.haw-hamburg.de/pers/Scholz/HOOU/index.html

[2] “OpenVSP.” Accessed: Jul. 05, 2025. [Online]. Available: https://openvsp.org/

[3] “Lockheed L1011-1 Tristar performance | aircraft investigation info | passenger aircraft.” Accessed: Jul. 05, 2025. [Online]. Available: https://aircraftinvestigation.info/airplanes/L1011-1.html

[4] “Butterworth-Heinemann - Civil Jet Aircraft Design - Aircraft Data File - Douglas, Boeing and Lockheed Aircraft.” Accessed: Jul. 05, 2025. [Online]. Available: https://booksite.elsevier.com/9780340741528/appendices/data-a/table-6/table.htm

[5] “fzt.haw-hamburg.de/pers/Scholz/arbeiten/DataHammami/DataHammami.html.” Accessed: Jul. 05, 2025. [Online]. Available: https://www.fzt.haw-hamburg.de/pers/Scholz/arbeiten/DataHammami/DataHammami.html

[6] Tristar 500, “L-1011-500 TRISTAR TECHNICAL PROFILE.” Accessed: Jul. 05, 2025. [Online]. Available: https://www.tristar500.net/library/technicalprofile.pdf

[7] “SeatGuru Seat Map United.” Accessed: Jul. 05, 2025. [Online]. Available: https://www.seatguru.com/airlines/United_Airlines/United_Airlines_Boeing_767_300_ER.php

[8] “Requiem For a Trijet Masterpiece – The Lockheed L-1011 : AirlineReporter.” Accessed: Jul. 05, 2025. [Online]. Available: https://www.airlinereporter.com/2015/09/requiem-trijet-masterpiece-lockheed-l-1011-trist ar/

[9] “NACA 63-210 AIRFOIL (n63210-il).” Accessed: Jul. 05, 2025. [Online]. Available: http://airfoiltools.com/airfoil/details?airfoil=n63210-il

[10] “Rolls-Royce RB211,” *Wikipedia*. Apr. 12, 2025. Accessed: Jul. 05, 2025. [Online]. Available: https://en.wikipedia.org/w/index.php?title=Rolls-Royce_RB211&oldid=1285200743

[11] “Airport Safety Detail.” Accessed: Jul. 05, 2025. [Online]. Available: https://www.airporttech.tc.faa.gov/Products/Airport-Safety-Papers-Publications/Airport-S afety-Detail

[12] “Loftin, L.K.: Subsonic Aircraft: Evolution and the Matching of size to Performance”, NASA Reference Publication, 1980

[13] “Raymer, D.P.: Aircraft Design: A Conceptual Approach”, AIAA Education Series, Washington D.C.: AIAA, 1989

[14] “Roskam, J. I: Airplane Design. Bd. 1 : Preliminary Sizing of Airplanes, Ottawa, Kansas,” Distribution: Analysis and Research Corporation, 120 East Ninth Street, Suite 2, Lawrence, Kansas, 66044, USA, 1989

[15] “Marckwardt”, K.: Unterlagen zur Vorlesung Flugzeugentwurf, Fachhochschule Hamburg, Fachbereich Fahrzeugtechnik, 1998

[16] “Torenbeek, E.”: Synthesis of Subsonic Airplane Design, Delft : Delft University Press, 1988

[17] “Schmitt, D.”: Luftfahrttechnik, Flugzeugentwurf, Technische Universität München, Lehrstuhl für Luftfahrttechnik, Skript zur Vorlesung, 1988

[18] “JOINT AVIATION AUTHORITIES”: Joint Aviation Requirements, JAR-25, Large Aeroplanes

[19] “U.S. DEPARTMENT FOR TRANSPORTATION, FEDERAL AVIATION ADMINISTRATION”: Federal Aviation Regulations, Part 25, Transport Category Airplanes

[20] “ROSKAM, J.: Airplane Design. Bd. 2” : Preliminary Configuration Design. and Integration of the Propulsion System, Ottawa, Kansas, 1989

[21] “ROSKAM, J.: Airplane Design. Bd. 3 : Layout Design of Cockpit, fuselage, Wing and Empennage: Cutaways and Inboard Profiles, Ottawa, Kansas, 1989

[22] “HOAK, D.E.: USAF Stability and Control Datcom, Wright-Patterson Air Force Base”, Air Force Flight Dynamics Laboratory, Flight Control Division, Ohio, 1978. - Vertrieb: NTIS

[23] “ABBOTT”, Ira H.; von DOENHOFF, Albert E.: "Theory of Wing Sections". New York : Dover, 1959